



**POLITECNICO**  
**MILANO 1863**

SCUOLA DI INGEGNERIA INDUSTRIALE  
E DELL'INFORMAZIONE

# Hybrid energy storage system for recovering regenerative braking energy of railway systems taking advantage of EVs battery

TESI DI LAUREA MAGISTRALE IN  
ENGINEERING-INGEGNERIA

**Author: Mostafa Golnargesi**

Student ID:	10756489
Advisor:	Dr. Hamed Jafari Kaleybar
Co-advisor:	Prof. Morris Brenna
Academic Year:	2022-23



## Abstract

In the last years, focusing on electric vehicles (EVs) is enhanced by nations due to the environmental reasons and the deficiency of fossil fuels. Meanwhile, supporting the required power of widespread EV charging infrastructures (EVCIs) would surcharge the power grid and cause some problems. Utilizing the inherent energy-saving method in electric railway systems (ERSs) known as regenerative braking energy (RBE) in strategic points, like parking areas close to railway stations or park-and-ride areas can help the grid to avoid overload situations and increase energy efficiency. In this research, a new collaborative charging method is proposed to charge EVs batteries by RBE of trains and taking advantage of batteries energy to auxiliary supply the trains during acceleration mode towards peak shaving purposes. In addition, the hybrid energy storage system (HESS) is also able to provide power to the grid through vehicle to grid (V2G) technology and mitigate the power demand from the grid and increase the efficiency. The optimization of the HESS sizing is performed by considering different driving scenarios and power demands. The results show that the HESS can significantly improve the energy efficiency of the railway system while reducing the overall energy consumption and cost. The simulation results are provided to validate the effectiveness of the proposed method with 24 hours' train traffic considering the EV population number with different global charging/discharging rates and grid connection limits.

**Key-words:** Electrical railway system, Electric vehicle (EV), Hybrid energy storage system (HESS), Optimization sizing of the energy storage system, regenerative braking power, battery, supercapacitor, vehicle to grid (V2G)



## Abstract in lingua italiana

Negli ultimi anni, l'attenzione ai veicoli elettrici (EV) è aumentata dalle nazioni per ragioni ambientali e per la carenza di combustibili fossili. Nel frattempo, supportare la potenza richiesta delle diffuse infrastrutture di ricarica per veicoli elettrici (EVCI) sovraccaricherebbe la rete elettrica e causerebbe alcuni problemi. L'utilizzo del metodo di risparmio energetico intrinseco nei sistemi ferroviari elettrici (ERS) noto come energia di frenata rigenerativa (RBE) in punti strategici, come le aree di parcheggio vicino alle stazioni ferroviarie o le aree park-and-ride può aiutare la rete a evitare situazioni di sovraccarico e aumentare efficienza energetica. In questa ricerca, viene proposto un nuovo metodo di ricarica collaborativo per caricare le batterie dei veicoli elettrici tramite l'RBE dei treni e sfruttare l'energia delle batterie per alimentare i treni durante la modalità di accelerazione verso scopi di peak shaving. Inoltre, il sistema di accumulo di energia ibrido (HESS) è anche in grado di fornire energia alla rete attraverso la tecnologia da veicolo a rete (V2G) e mitigare la domanda di energia dalla rete e aumentare l'efficienza. L'ottimizzazione del dimensionamento HESS viene eseguita considerando diversi scenari di guida e richieste di potenza. I risultati mostrano che l'HESS può migliorare significativamente l'efficienza energetica del sistema ferroviario, riducendo al contempo il consumo energetico e i costi complessivi. I risultati della simulazione vengono forniti per convalidare l'efficacia del metodo proposto con il traffico ferroviario di 24 ore considerando il numero di veicoli elettrici con diverse velocità globali di carica/scarica e limiti di connessione alla rete.

**Parole chiave:** sistema ferroviario elettrico, veicolo elettrico, sistema di accumulo di energia ibrido, ottimizzazione del dimensionamento del sistema di accumulo dell'energia, potenza di frenata rigenerativa, batteria, supercondensatore, veicolo alla rete.



# Contents

<b>Abstract</b> .....	<b>i</b>
<b>Abstract in lingua italiana</b> .....	<b>iii</b>
<b>Contents</b> .....	<b>v</b>
<b>Introduction</b> .....	<b>1</b>
<b>1. Traditional method for recuperating regenerative braking energy</b> .....	<b>3</b>
1.1 Introduction.....	3
1.2 Timetable optimization.....	4
1.3 Energy storage systems.....	4
1.3.1 Flywheel.....	6
1.3.2 Electric double-layer capacitors (EDLCs) .....	7
1.3.3 Batteries.....	8
1.3.4 Supercapacitores.....	9
1.3.5 Hybrid energy-storage systems (HESS).....	9
1.3.6 Superconducting magnetic energy storage (SMES) .....	10
1.4 Reversible substation .....	10
1.5 Energy density and power density .....	11
1.6 Optimization technique .....	12
1.7 Discussion .....	22
<b>2. Utilizing EV batteries for recuperating regenerative braking energy</b> .....	<b>24</b>
2.1 Introduction.....	24
2.2 Electric vehicle charging infrastructure.....	24
2.2.1 Fast charging infrastructure (DC EVChs).....	25
2.2.2 Low-power AC EVChs.....	25
2.3 Integration of EV charging infrastructures.....	25
2.3.1 Employing regenerative braking energy.....	26

2.3.2 Meantime integration of ERSs and EVCIs.....	26
2.3.3 ESS-based integration of ERSs and EVCIs .....	27
2.4 Integration of EV charging infrastructures.....	28
2.4.1 Two-Stage DC Charging Infrastructures.....	28
2.4.2 Single-stage DC charging infrastructure .....	28
2.5 Different architectures of ERS and EVCI integration.....	29
2.5.1 Low-voltage DC hub-based integration .....	29
2.5.2 AC hub-based integration.....	31
2.5.3 Hybrid hub-based integration.....	32
2.6 Integration renewable energy source .....	33
2.7 Control management system .....	36
<b>3. Modeling and simulation of proposed system .....</b>	<b>40</b>
3.1 Introduction.....	40
3.2 Modeling of electrical railway .....	41
3.3 Energy management system.....	44
3.4 Modeling of hybrid energy store system (HESS).....	50
3.5 Simulation and result.....	52
3.5.1 Charging rate 20 kW .....	52
3.5.2 Charging rate 6 kW .....	59
3.5.3 Charging rate 6 kW + HESS.....	66
3.5.4 HESS (Battery and Supercapacitor).....	74
3.6 Discussion and Comparison .....	78
<b>4. Conclusion and future development .....</b>	<b>80</b>
<b>Bibliography.....</b>	<b>83</b>
<b>List of Figures.....</b>	<b>91</b>
<b>List of Tables.....</b>	<b>95</b>
<b>5. Acknowledge .....</b>	<b>96</b>





# Introduction

The transport industry is a major contributor to the world's energy usage, with member states of the International Energy Agency reporting a 36% consumption rate [1]. In light of global efforts to decrease reliance on fossil fuels and lower carbon emissions, the transportation sector is a prime target for change, particularly through the adoption of electric vehicles. This shift to electrification impacts both personal and public transportation, necessitating continuous improvements to infrastructure to accommodate the heightened demand for electricity on power grids.

Although electric vehicles (EVs) are impacting public transportation, such as through the use of electric buses, railway electrification is the primary mode of electrifying mass transportation.

The adoption of electric transportation presents difficulties for the broader electric power infrastructure. Moving away from the use of fossil fuels leads to an overall increase in electricity consumption, and unregulated charging of a growing number of electric vehicles creates surges in power demand that could potentially overload regional distribution networks. This problem becomes especially pronounced when EV charging coincides with the high-power demands of electric rail vehicles, leading to the risk of substation overloads. Furthermore, the rise in electricity usage due to electric transportation coincides with greater fluctuations in the electricity supply.

Efforts to address the challenges related to electricity supply intermittent usually involve utilizing energy storage technologies. For electric rail systems, which are significant consumers of power, energy storage can be employed as a form of demand-side management. In this context, energy storage can assist in alleviating peak power demand pressures on the electricity grid that are caused by the traction power needs of electric trains, particularly during acceleration, when traction power requirements can reach several megawatts depending on the rail system.

Energy storage can be advantageous in the recovery of brake energy in electric train systems. This energy can be stored in a storage device and utilized later to power the vehicle. The implementation of regenerative braking in electric rail networks and vehicles has resulted in notable advancements in energy efficiency and diminished operational expenses.

A different approach to energy storage is suggested: utilizing a V2G network near an electric rail system in conjunction with a hybrid energy storage system (HESS). V2G is an energy storage concept that aggregates the battery packs of stationary electric vehicles and utilizes them to provide various grid services by charging or discharging them. V2G differs from other energy storage technologies because it makes use of already-existing storage that would otherwise be unused (the batteries of parked EVs). However, due to a shortage of available EVs and their slow charging rate, a hybrid energy storage system is employed in conjunction with V2G.

In this work, the combination method is proposed to employ the advantages of both methods and remove the disadvantages of them. It is used for covering the traction power with the lowest power demand and also lowest pick power.

# 1. Traditional method for recuperating regenerative braking energy

## 1.1 Introduction

The electrification of both individual and mass transportation necessitates ongoing infrastructure upgrades in both areas to accommodate the increased demand for electricity on power grids [1-2]. Typically, electric trains are powered by overhead transmission lines or third and fourth rail systems. As a result, the process of electrifying pre-existing railways necessitates substantial investment in local power infrastructure. Moreover, the shift towards electrification in transportation poses a challenge to the broader electric power grid. As the move away from fossil fuels leads to a rise in overall electricity demand and may result in power demand peaks that could overwhelm local distribution networks. The electrification of transportation is not the only significant transformation occurring in our electricity systems. In fact, it is accompanied by significant shifts towards generating electricity from renewable sources. Consequently, the increased electricity consumption resulting from electric transportation coincides with greater variability in electricity supply. Efforts to address issues related to electricity supply variability typically involve the use of energy storage technologies. Large-scale consumers of electricity like electric rail systems may also use energy storage as a way to control demand. Energy storage can assist in reducing the stress on the power grid caused by peak power demands from electric trains during acceleration, when traction power demand can reach several megawatts depending on the rail system. Local energy storage could supply some or all of this traction power, thus decreasing the strain on the electric power grid. Energy storage can also be advantageous in the realm of train brake energy recovery. By storing and then reusing power generated through brake energy recovery, energy storage can facilitate efficient regenerative braking within the grid networks [2]. The literature offers various proposals to maximize the reuse of regenerative braking energy. One solution is train timetable optimization, which involves synchronizing the operation of multiple trains to enable one train to brake

and feed regenerative energy back to the third rail, while another train simultaneously accelerates and absorbs this energy from the third rail. Another solution is energy storage systems (ESS), where regenerative braking energy is stored in an electric storage medium such as supercapacitors, batteries, or flywheels, and released to the third rail when required. The storage medium can be placed onboard the vehicle or beside the third rail. Lastly, a reversible substation is suggested, which provides a path for regenerative energy to flow in the opposite direction and feed power back to the main AC grid [3].

## 1.2 Timetable optimization

The idea of train timetable optimization has been suggested to make the most out of regenerative braking energy. This involves coordinating the braking and acceleration of two nearby trains to happen at the same time, allowing an accelerating train to use some of the energy produced by a decelerating one. Several studies have found that optimizing the timetable in this way can result in energy savings of up to 14% [4]–[5]. Research on train timetable optimization can be divided into two primary categories based on their goals: reducing the peak power demand and maximizing the utilization of regenerative braking energy [6]. Recently, there has been research focused on using train timetable optimization to maximize the utilization of regenerative braking energy. The main objective of this research is to synchronize the acceleration and deceleration intervals of nearby trains. To achieve this, most of the studies have concentrated on optimizing the dwell time, which refers to the stop time at each station, in order to increase the likelihood of coordinating the acceleration and deceleration of trains. These studies can be found in references [3], [5], and [7]–[9]. Other studies have been centered on finding the best time overlap between multiple trains, as can be seen in references [10]–[12].

## 1.3 Energy storage systems

Another solution involves energy storage systems (ESS) where regenerative braking energy is stored in an electric storage medium such as a super capacitor, battery or flywheel and then released to the third rail when required. This storage medium can be placed onboard the vehicle or next to the third rail. If an energy storage system is appropriately created, it has the ability to collect the energy generated by a train during braking and release it when required. This, in turn, lowers the amount of energy consumed from the primary grid, as supported by references [7], [8], and [13]. Furthermore, incorporating an ESS can decrease the maximum level of power required, which has advantages for both the railway transport system and the power

supplier. The ESS can also function as a means to offer services to the primary grid, including peak shaving, as stated in reference [14].

The types of energy storage technologies utilized in the railway sector can be classified into two groups: on-board energy storage systems (OESS) and stationary energy storage systems (SESS). OESSs are incorporated into the train and designed to store energy recovered from a single train. Consequently, the power and energy capacity required for OESSs are lower than those needed for SESSs. Nevertheless, OESSs must have the ability to meet the peak power generated during braking as well as the energy demand of the train itself (a train's peak power consumption can reach up to 24MW [15]).

When choosing an on-board energy storage device, factors to consider include the power demands of the electric multiple unit (EMU), which can exceed 1 MW for a standard 4-wagon, 200-ton EMU. In addition, it is important to consider the size of the storage device, particularly for EMUs, and safety concerns, particularly for trains carrying passengers.

Storage devices can serve three primary functions when integrated into railway cars: lowering energy consumption, decreasing peak power requirements, and enabling catenary-free operation [16]. Catenary-free operation refers to a mode of operation where an electrically powered train runs on an electrified track using energy from an energy storage device. Trains operating in this mode require storage devices that can supply both high peak power and high energy capacity, which poses a significant challenge for current storage technologies. For example, a typical electric train hauled by a locomotive with a load factor of 40% consumes roughly 1 kWh per passenger.

In some instances, incorporating on-board energy storage devices may not be practical or cost-effective, particularly for heavy haul trains. In these cases, stationary energy storage systems (SESSs) may be a more viable solution [17]. Compared to on-board storage systems, SESSs require a higher energy capacity but offer greater flexibility in terms of system sizing. An effective stationary storage system should possess both high power and energy capacity, as well as a long charge/discharge cycle [18]. Today, various forms of ESSes—such as flywheels, electric double-layer capacitors (EDLCs), batteries, fuel cells and superconducting magnetic energy storage (SMES) devices—have been proposed and utilized in railway systems for different purposes: [19].

### 1.3.1 Flywheel

In most cases, a flywheel energy storage system (FESS) is made up of four main parts, namely, a rotor, a rotor bearing, an electrical machine, and a power electronics interface [20]. Fig. 1.1 illustrates the schematic diagram of a FESS.

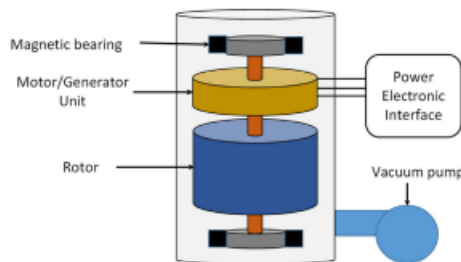


Figure 1.1: schematic diagram of an FESS [19]

The process involved in a flywheel energy storage system (FESS) is the conversion of electrical energy into kinetic energy, which is then stored in a high-speed rotor. The rotor is connected to an electrical machine through a bearing, and the kinetic energy is reconverted to electrical energy when required. [19]

To reduce or eliminate friction loss, the rotor in a flywheel energy storage system (FESS) is typically placed in a vacuum or low-pressure containment [21]. The influence of rotor geometry on FESS performance was analyzed in studies [22-24]. The maximum rotational speed of the rotor is determined by the material's tensile strength because the centrifugal force is related to the square of the rotational speed [25]. The use of high-strength composite materials improves FESS performance by allowing for higher rotational speeds [26].

Various methods have been proposed for selecting suitable materials for flywheels, as these materials play a significant role in determining flywheel performance [27, 28]. The use of traditional mechanical bearings in modern high-speed FESSes is not feasible due to high friction and consequent energy losses. Therefore, mechanical bearings necessitate lubrication to decrease friction and require regular maintenance [29]. Alternatively, magnetic bearings, which rely on magnetic levitation, have minimal friction and are a better option [19].

Magnetic bearings are typically categorized into two groups: active magnetic bearings (AMBs) and passive magnetic bearings (PMBs). AMBs provide excellent control, but the primary drawback is the power loss caused by biased current [30]. On the other hand, PMBs employ permanent magnets, eliminating the need for input power [31]. However, PMB design is typically challenging due to the limitations of

Earnshaw's theorem [32, 33]. When a FESS is charging, an electrical machine may act as a motor, whereas it may serve as a generator when discharging. There are several types of electrical machines employed in FESSs, with synchronous and asynchronous machines being the most common categories.

The permanent magnet synchronous machine (PMSM) is a widely used synchronous machine in FESSs due to its high overall efficiency [34]. Since the rotor flux is created by the permanent magnet in PMSMs, the rotor loss is relatively low [20]. The primary drawbacks of PMSMs are their high cost and low material tensile strength. Compared to induction machines (IMs), PMSMs are more vulnerable to temperature changes because intrinsic coactivity drops as temperature rises [21]. IMs are widely used in high-power applications due to their torque, robustness, construction, and cost benefits, as a typical asynchronous machine [29]. The rotor design of IMs, on the other hand, is more complicated because the rotor needs wires and electric brush connectors [21]. Moreover, for high-speed FESS applications, IMs have a speed limitation, which is another disadvantage. [35].

Flywheels have similar properties to EDLCs, but they have a slightly higher charge-discharge time. There are not many studies on the application of flywheels in electrified railways. Flywheels have to store energy by using kinetic energy, which means that they need more maintenance in comparison with EDLCs. Stationary flywheels have quite big dimensions and they are also heavy. Onboard flywheels need space in the bogie for being accommodated, which require a bigger space than EDLCs. After the diffusion of EDLCs, the applications of flywheels in electrified railways are reduced because of the superior properties of EDLCs in terms of maintenance, weight and size. [36]

### 1.3.2 Electric double-layer capacitors (EDLCs)

The EDLC is comprised of a pair of electrodes separated by a separator that permits ion movement [37]. Unlike standard capacitors, the electrodes of an EDLC are immersed in an electrolyte and the capacitance is established by the accumulation of electrostatic charge at the boundary between the electrode and electrolyte [38], the load circuit causes electrons to flow from the positive electrode to the negative electrode, which results in the accumulation of cations and anions in the negative and positive electrodes, correspondingly. When the EDLC is in the discharging phase, electrons move from the negative electrode to the positive electrode via the load circuit, and the anions and cations start to intermingle again [39].

Typically, carbon-based materials are utilized for the electrodes in an EDLC due to their widespread availability and relatively low cost. Activated carbon is the most

commonly used type of carbon-based material in EDLCs because of its low cost and high specific surface area, which can range from 1000 to 2000 square meters per gram [40]. The activation process for creating activated carbon can be accomplished through a physical or chemical approach at high temperature or by mixing chemicals, respectively [39]. However, optimizing the distribution of pore size in activated carbon materials is challenging due to the limited control over pore size during the activation process [40]. Carbide-derived carbon (CDC) is an alternative carbon-based material employed in EDLCs as its pore size can be suitably tailored [41]. Typically, EDLCs constructed with CDCs have a larger capacitance as the CDC structure determines capacitance [42]. Graphene, a single layer of carbon atoms arranged in a honeycomb crystal lattice, has received significant attention in recent years. EDLCs using graphene could potentially provide exceptional performance as they possess desirable features such as high cycle capability, flexibility, electrical conductivity, and excellent thermal stability [43].

### 1.3.3 Batteries

**Nickel Cadmium (Ni-Cd):** This developed battery technology possesses numerous advantages, such as extended lifespan, high dependability, low self-discharge, exceptional durability, and the ability to operate in a wide temperature range, which renders it a suitable choice for heavy-duty purposes. However, it has some drawbacks, including the memory-effect and the environmental risks associated with cadmium, a hazardous material, which makes the disposal of these batteries a significant challenge.

**Nickel-Metal Hydride (Ni-MH):** This type of battery technology shares similarities with Ni-Cd batteries in terms of positive electrode and electrolyte, but uses hydrogen instead of cadmium in the negative electrode. As a result, NiMH batteries do not have the same harmful impact on the environment as Ni-Cd batteries. Additionally, Ni-MH batteries have a greater energy density and specific energy, and importantly, do not suffer from the same extent of memory-effect as Ni-Cd batteries. However, Ni-MH batteries have some limitations. For example, overcharging can cause overheating and hydrogen release, leading to a severe fire hazard. This necessitates the use of complex charging circuitry. Furthermore, when used in high-current applications such as heavy transportation, their lifespan is reduced significantly, with only 200-300 cycles possible. [44].

**Lithium-Ion (Li-Ion):** Currently, this battery technology is the most commonly used in portable electronic devices, and due to a decrease in manufacturing costs and strong incentives towards cleaner transportation, it has gained significant popularity among electric vehicle manufacturers. It has replaced Ni-Cd and Ni-MH technologies

due to its high cell voltage, high energy density, long lifespan with no memory effect, and lack of environmental concerns associated with Ni-Cd and Ni-MH technologies. Despite still being expensive, improvements in the manufacturing process and economies of scale have significantly reduced costs [44].

### 1.3.4 Supercapacitores

These devices store energy in an electrochemical double layer. Compared to batteries, their specific power is much higher (500–10000W/kg) but their specific energy is considerably lower (0.2–5Wh/kg). In transportation applications they are principally used for power assist during acceleration and hill climbing and for regenerative braking. In hybrid systems, supercapacitors are used together with other electric storage devices (e.g. Li-Ion) to provide with high specific power and high specific energy.

### 1.3.5 Hybrid energy-storage systems (HESS)

The primary idea of a hybrid energy storage system (HESS) is that various energy storage systems (ESS) have complementary features, particularly when it comes to power density and energy density [19]. Through the combination of these diverse ESS, their benefits can be blended together to achieve better performance instead of relying solely on one type of ESS. In the context of railway applications, an HESS usually comprises a minimum of two ESS types, where one is intended for high energy demand while the other is meant for high power requirements [19]. The ESS that has a high capacity for energy can be used as a source of long-term energy, whereas the ESS with a high capacity for power can be utilized to meet short-term high power demands. Numerous HESS setups have been suggested to incorporate two ESS devices into one power source. These setups can be generally classified into three categories: passive parallel, cascade, and active. The passive parallel configuration connects the two ESS devices without utilizing any power electronic device. Although this design is easy to execute, the output voltage fluctuates during both the charging and discharging processes. The cascade configuration is more effective than the passive parallel design, but it also incurs higher costs and necessitates an additional converter between the ESS devices. This process separates the ESS devices and allows for active energy management, but it is restricted by scalability concerns and lacks the flexibility of a control strategy. Alternatively, the active parallel configuration is the most versatile, with each ESS device linked to a dedicated power converter. This permits each ESS device to operate under its optimal conditions and enables maximum power-point tracking [19].

### 1.3.6 Superconducting magnetic energy storage (SMES)

SMESs store energy in a magnetic field created by the flow of DC current in the superconducting coil. In order to maintain the superconducting state, the coil is immersed in liquid helium and cooled to a cryogenic temperature, which should be lower than its superconducting critical temperature. Therefore, a refrigerator is necessary to keep the superconducting coil operating under the cryogenic temperature. Since the resistance of the coil is almost zero in its superconducting state, the resistive loss is negligible. Therefore, when the SMES is charged, the electrical energy is converted to magnetic energy, which can be stored in the magnetic field indefinitely. The magnetic energy can be stored indefinitely because there is no degradation of the coil current. When the SMES is required to deliver energy to the external load, the stored magnetic energy is converted to electrical energy by discharging the superconducting coil. Recent progress in this area includes the utilization of high-temperature superconducting materials in order to offer higher performance and economic advantages. Compared with the other types of ESS, SMESes have high energy efficiency, high power density, excellent fast charging/discharging performance and extremely long cycle life (almost infinitely). The main drawbacks of SMESs are their high cost and the generation of enormous electromagnetic forces when they are utilized as a massive energy storage device.

## 1.4 Reversible substation

Finally, a reversible substation can also be used to enable regenerative energy to flow in the reverse direction and feed power back to the main AC grid.

Fig. 1.2 illustrates an alternative method for recycling regenerative braking energy which involves the use of reversible substations. These substations, also called bidirectional or inverting substations, utilize an inverter to establish a connection that allows regenerative braking energy to flow back to the upstream AC grid. This energy can then be consumed by other AC-based equipment present in the substation, such as escalators or lighting systems. [47].

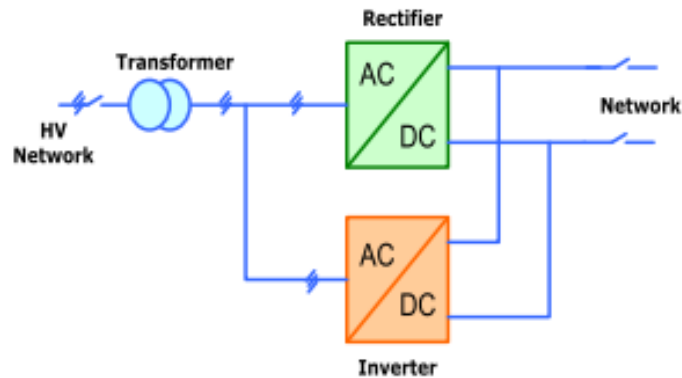


Figure 1.2: Block diagram of a reversible substation [2]

Depending on the regulations and guidelines established by the electricity distribution network, the energy obtained can also be redirected back to the main grid. However, in order to ensure the power fed back into the grid meets acceptable quality standards, reversible substations must take measures to minimize the level of harmonics present. [47]. While reversible substations are designed to enable the redirection of regenerative braking energy back to the upstream network, in order to achieve optimal energy recuperation, it is recommended to prioritize the exchange of energy between trains on the DC side of the power network.

There are two primary techniques for creating a reverse energy flow path. The first approach involves using a diode rectifier along with a DC/AC converter, which may be a pulse width modulation (PWM) converter or a thyristor line commutated inverter (TCI) [48]. This method has the advantage of being able to retain the existing diode rectifier and transformer, requiring only additional equipment to establish reversible energy conduction. On the other hand, the second method involves utilizing a reversible thyristor controlled rectifier (RTRC), which requires replacing the diode rectifiers with RTRCs and modifying the rectifier transformers, making it a more complex and expensive approach. Despite this, RTRCs provide certain benefits, such as voltage regulation and fault current limitation [49].

## 1.5 Energy density and power density

The terms gravimetric energy density and gravimetric power density refer to specific energy and specific power, respectively, and are used to describe the amount of energy and power that an energy storage system (ESS) can hold per unit of mass. When an ESS has a high specific energy or specific power, it can store a certain amount of energy or power with less weight. Conversely, volumetric energy density and volumetric power density are used to measure the total amount of energy and power that an ESS can hold per unit of volume. Energy storage devices that have

high energy density and power density are ideal for situations where weight and size are key factors. This attribute is particularly crucial for applications that are on-board rather than stationary. For example, when an ESS is installed on a railway vehicle, the weight of the vehicle increases, requiring more power to maintain its performance. If an ESS with low specific energy is selected, the energy efficiency is reduced. Additionally, on-board ESS size is limited due to safety regulations and financial constraints. Based on Table 1.1, EDLCs are identified as having exceptionally high gravimetric and volumetric power density, which makes them more appropriate for high-power applications. Flywheels, Ni-MH batteries, Li-ion batteries, and SMESs also have a relatively high power density and are commonly utilized in power-delivery applications. In general, battery-based ESSs and HFCs have higher energy densities than other ESSs, making them more suited for applications with high energy demands. Depending on the chemical components used, Li-ion batteries can be designed to have either high energy density or high power density, but not both, as indicated in references [50] and [51].

Table 1.1: Comparison of energy and power densities of ESS systems [19]

Technology	Gravimetric energy density (Wh/kg)	Gravimetric power density (W/kg)	Volumetric energy density (Wh/L)	Volumetric power density (W/L)
Flywheel	5–100	400–1500	20–80	1000–2000
EDLC	5–15	5000–10 000	10–30	>100 000
Lead-acid	30–50	75–300	50–90	10–400
Ni-Cd	50–75	150–300	60–150	75–700
Ni-MH	54–120	200–1200	190–490	500–3000
NaS	150–240	150–230	150–250	140–180
ZEBRA	100–120	150–200	150–180	220–300
Li-ion	150–250	500–2000	400–650	1500–10,000
VRFB	10–30	166	25–35	< 2
HFC	800–10 000	5–800	500–3000	>500
SMES	0.5–5	500–2000	0.2–2.5	1000–4000

## 1.6 Optimization technique

Modern transportation vehicles (TVs) use high energy density storage systems that have a long enough discharge time to improve the efficiency of the system and reduce costs, weight, and volume. However, using only battery systems in modern TVs can cause damage due to higher peak power, current, regenerative braking energy, and other factors that cause battery degradation, which reduces their lifespan. Therefore, using a high energy storage system (HESS) is essential to minimize these harmful effects on batteries. Assigning greater peak power needs to a resilient energy storage system (ESS), such as SC (superconducting magnetic energy storage), lithium-ion capacitor, and flywheel, can reduce the negative effects mentioned earlier. Even though these sturdy ESSs have a lower energy density compared to batteries, they possess a higher power density, which can lead to a longer lifespan. Additionally, they have the ability to absorb regenerative braking

energy and enhance acceleration power. On the other hand, batteries have a higher energy density and are appropriate for low-power vehicle applications. Nevertheless, due to space constraints in modern vehicles and weight limitations, it is crucial to carefully choose the size of the high energy storage system (HESS) used in these vehicles. This is necessary to ensure that the performance meets the requirements of the vehicle's customers or automotive manufacturers, as well as renewable energy power systems. Additionally, it is not enough to size the HESS alone, as neglecting energy management strategies can result in an unreliable system. As a result, numerous researchers have concentrated on integrating the sizing of HESS with an energy management strategy, which has led to the development of multi-objective optimization methods. This section examines various HESS sizing techniques that have been reported in the literature. Figure 1.3, located below, depicts additional methods that have been used to size HESS. Additionally, the optimization of ESS sizing involves selecting appropriate proportions for various hybrid energy storage system (HESS) devices. Different methods for optimizing ESS sizing in railway applications can be found in [52-54].

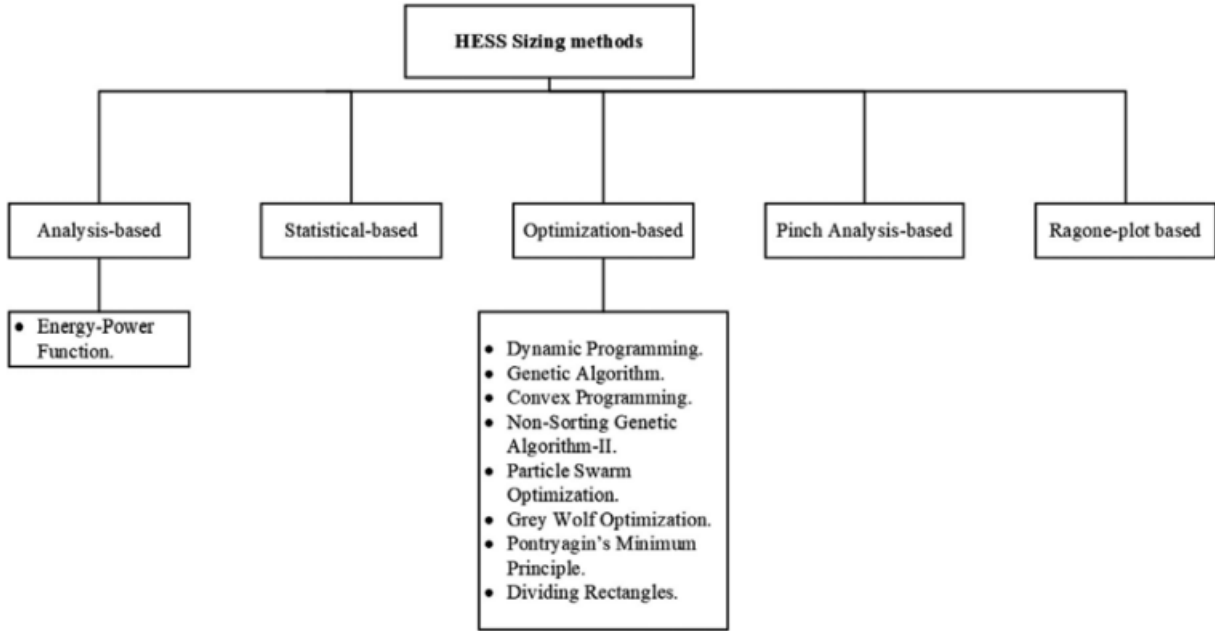


Figure 1.3: Hybrid energy storage system sizing methods [55]

Optimization techniques are crucial in determining the appropriate size of hybrid energy storage systems (HESS) as they enable the system to maintain its operational limits, such as SOC, voltages, and current. The sizing of HESS and its energy management are closely linked, and the driving pattern and road geometry are the most important factors in ensuring the system's effectiveness. By using optimization methods, it is possible to enhance energy/power distribution between ESSs, reduce

HESS energy loss, and improve vehicle daily operating costs, fuel economy, ESS lifespan, distance traveled, and HESS cycle life. An effective optimization model can help to achieve the aforementioned goals. [55]

The integration of battery and supercapacitor technology in a hybrid energy storage system (HESS) has gained significant interest for potential use in transportation vehicles (TVs). The popularity of this technology can be attributed to the decreasing cost of HESSs and the advancements in electrode materials for improved energy storage systems. The existing energy storage systems, such as batteries, face several scientific challenges, including a short lifespan, lower power density, and limited ability to improve vehicle performance, particularly in terms of acceleration and rapidly recovering regenerative braking energy, while also being susceptible to environmental conditions. Studies indicate that the energy and power density of HESSs rely significantly on the voltage matching of each individual energy storage system during development, especially when implementing a passive parallel topology to power a standard TV. While this topology is practical for use in TVs, it offers little improvement in battery lifespan due to the unregulated flow of energy and power between the ESSs. Therefore, this topology may be useful in supporting the starting, lighting, and ignition functions of internal combustion engine (ICE) vehicles in the future, thus reducing the need for high starting battery current and potentially enhancing battery lifespan with the help of a supercapacitor. [ 55]

The aim is to explore options for utilizing energy efficiently, including regenerative substations and energy storage systems, whether stationary or on board. However, this particular text is concentrating on stationary energy storage systems. The proposal involves a HESS which facilitates energy transfer between multiple storage units. The transfer occurs via an AC/DC converter and corresponding DC/DC converter, allowing for flow between the catenary and any storage systems. Additionally, if financially feasible, power can move between batteries and ultracapacitors, or even between different batteries. These options are illustrated in Fig. 1.4. It's important to note that the primary focus of this study is the proper sizing and operation of the hybrid system, rather than the design of its individual components.

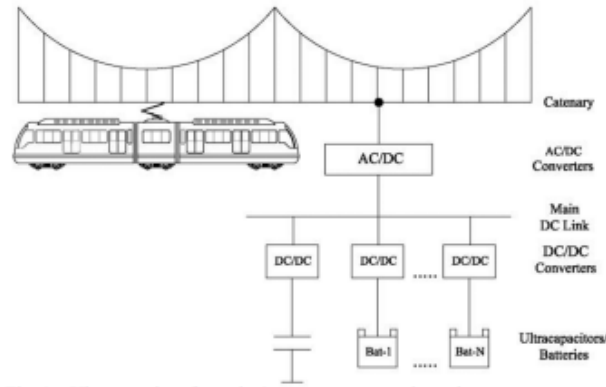


Figure 1.4: Ultracapacitors/batteries/converters connection scheme [56]

This paper presents a model that aims to determine the ideal quantity of minimum battery units (MBUs) and minimum ultracapacitor units (MUUs) that should be implemented in a specific section of an electric railway system for maximizing the associated profits. The model employs a mixed integer linear programming problem, which encompasses all the technical and economic constraints mentioned earlier, as well as some additional equations outlined below:

$$\begin{aligned}
 & \text{Minimize} \\
 & \sum_{h=1}^H (\varepsilon \cdot \Delta t \cdot P_{gen}^h) + \sum_{g=1}^G (C_B^g \cdot N_B^g) + C_U \cdot N_U \\
 & + \sum_{j=1}^J (N_{AD}^j \cdot C_{AD}^j) + \sum_{i=1}^I (N_{DD}^i \cdot C_{DD}^i) \\
 & \quad \forall g \in \Omega_g, \forall i \in \Omega_i.
 \end{aligned} \tag{1}$$

The optimization problem's objective function, expressed in (1), aims to minimize the total expenses associated with investing in and operating the system during the time horizon of interest. The function comprises several terms. The first one calculates the total energy cost, which is defined as the product of the energy purchased from the electric system and the corresponding energy price. The next term computes the investment made in batteries, which is equivalent to the number of MBUs installed multiplied by its daily cost. The cost of ultracapacitors is also calculated similarly. Lastly, the function incorporates the investment cost of all power electronics converters. In order to finalize the model, it is necessary to incorporate the total power balance condition, as presented in (2). This constraint stipulates that the total power exchanged via the DC link must be equivalent to the train's net demand. The balance equation takes into account several terms, including power purchased from the electric grid, power sourced from both batteries and ultracapacitors (adjusted for efficiency), power injected into batteries and ultracapacitors, and a term that accounts for the possibility of excess power generated through regenerative braking that cannot be stored, resulting in energy loss:

$$\begin{aligned}
& P_{gen}^h + \eta_{syst} \cdot (P_{B-}^h + P_{U-}^h) - P_{B+}^h - P_{U+}^h \\
& - P_{exc}^h = P_{dem,T}^h - P_{gen,T}^h \\
& \quad \forall h \in \Omega_h, \forall g \in \Omega_g.
\end{aligned} \tag{2}$$

The problem of optimally sizing hybrid energy storage systems (HESS) installed in electric railway systems, considering the effect of regenerative braking is studied in [56]. HESSs combine traditional batteries and newly developed ultracapacitors, taking advantage of the high energy capacity of batteries and of the flexibility and ability to capture high power density of ultracapacitors. A novel mixed integer linear programming formulation that includes the counting of battery cycles is presented. Some particularities of battery operation are included in the model, like the dependence of its performance on the number of cycles and the depth of discharge (DOD).

This method provides the optimal results in a fast and accurate manner. We have modeled in detail the operation of batteries, ultracapacitors and the necessary power electronic converters; more specifically, we have demonstrated a formulation that efficiently takes into account the cycling constraints of batteries; to the best of our knowledge this has not been done previously by any other researchers. Also included in the model is the capability to store regenerated energy from braking operations.

In [57] a probabilistic algorithm has been applied to calculate the on average lost energy by the trains during the braking phase. Subsequently, the size of the supercapacitors needful to save and reuse this energy, both in the normal conditions and in black out case, has been determined. During the recovery situations the energy coming from the trains is stored in the supercapacitors and given back to the trains in the starting phase as soon as it is possible: the supercapacitors are continuously charged and discharged. The following step is to quantify the number and the characteristics of the supercapacitors needed to create the storage system. Considering the standard solutions on the market and the conventional sizing, each module is constituted by 24 cells in series of 5000 F each one, that give a total capacity of the module equal to 210 F, a value 24 times less than the one of a single cell because the various cells in the module are connected in series.

The regenerative braking energy (RBE) generated during the braking of high-speed trains affects the power quality of the power grid. Recovery of RBE is problem that needs to be solved urgently. The RBE of high-speed railway features high power and high energy. It is difficult to recover it only by using high power density supercapacitors or high energy density batteries. In [59], a hybrid energy storage system (HESS) composed of supercapacitors and lithium-ion batteries and its optimal configuration method are proposed for the purpose of obtaining maximum

economic benefits for railroad systems. Then the economic benefits when using the HESS and the single energy storage system are compared from the perspective of whether the regenerative braking energy is fully recycled or not. [58]

The primary purpose of the HESS is to lower the expenses associated with the power supply system for high-speed railways by repurposing regenerative braking energy and lowering electricity purchase costs. This is accomplished by minimizing the overall daily operating costs of the power supply system. However, it is essential to maintain power balance restrictions. As a result, the energy management strategy flowchart for the HESS is presented in Figure 1.5.

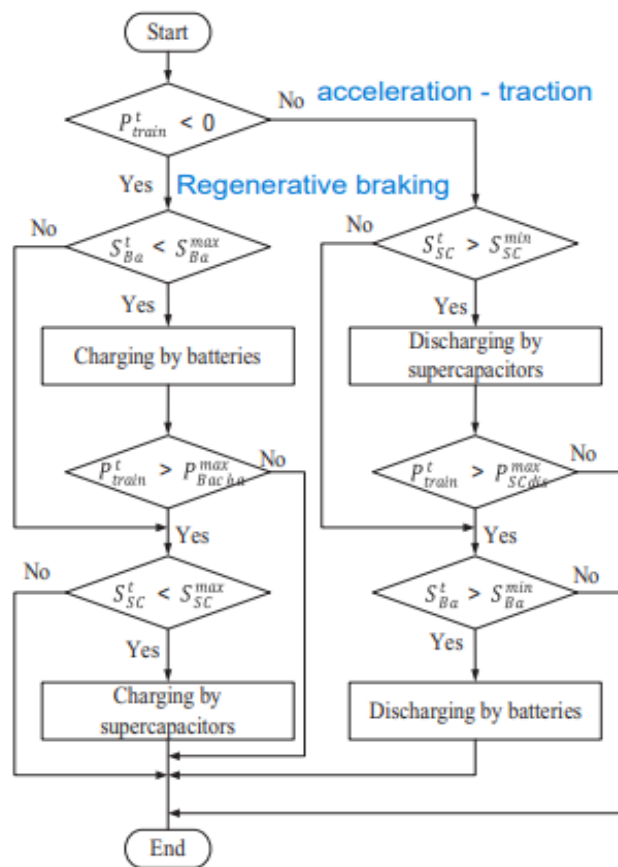


Figure 1.5: Energy management flow chart of HESS [58]

The HESS operates in a charging state when the power consumed by the high-speed railway is less than 0, and the batteries are activated simultaneously. On the other hand, when the power consumed by the high-speed railway is greater than 0, the HESS enters the discharging state. Initially, the supercapacitors are discharged quickly, ensuring that they have enough capacity to store the next regenerative braking energy. However, when the discharging power of the supercapacitors cannot match the power required by the system, the battery is used to discharge energy.

The process of optimizing the capacity configuration of HESS is illustrated in Figure 1.6. Initially, the life cycle investment cost of the energy storage system and converters is modeled, and parameters such as high-speed rail load, electricity price, and SOC range are input. This is followed by constrained optimization with the aim of minimizing the overall daily cost of the high-speed railway power supply system. Finally, the optimal cost and the quantity of supercapacitors and batteries required are output.

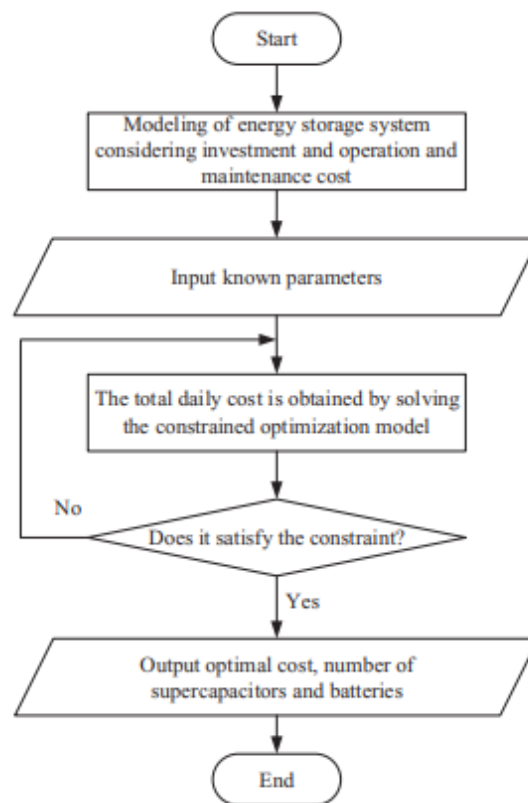


Figure 1.6: Optimization flow chart [58]

In [58], a method is proposed for optimal allocation of HESS capacity for regenerative braking energy recovery and utilization in high-speed railway.

The conclusions are as follows:

- The maximum regenerative braking power of the high-speed railway in the example reaches 11 MW, and the total regenerative braking energy in one day reaches 9.58 MWh, whose power and energy are large, and it is necessary for the railway system to recycle it. Regenerative braking energy requires energy storage systems with both high power density and high energy density to recycle it. This paper uses HESS combined with supercapacitors and batteries to recycle.

- The HESS configured to fully recycle regenerative braking energy has a large capacity. But as the regenerative braking peak power duration is short, the capacity utilization of the batteries in the HESS is very low, and the savings in electricity costs are difficult to meet the investment costs of the HESS, it cannot save the total cost of the system.
- When partially recovering regenerative braking energy, the capacity utilization rate of the HESS is high, and the electricity cost saving is higher than the investment cost of the HESS. The total daily cost saving is 3%, and the solution can recover the cost in the 8th year.

The co-phase power supply system shown in Fig. 1.7 transports electricity from a traction transformer system (TSS) to an active power conditioner (APC). from traction network (P<sub>Load</sub>) to grid (P<sub>Grid</sub>) [60], where VRB and SC are connected to the APC via DC/DC converters, respectively.

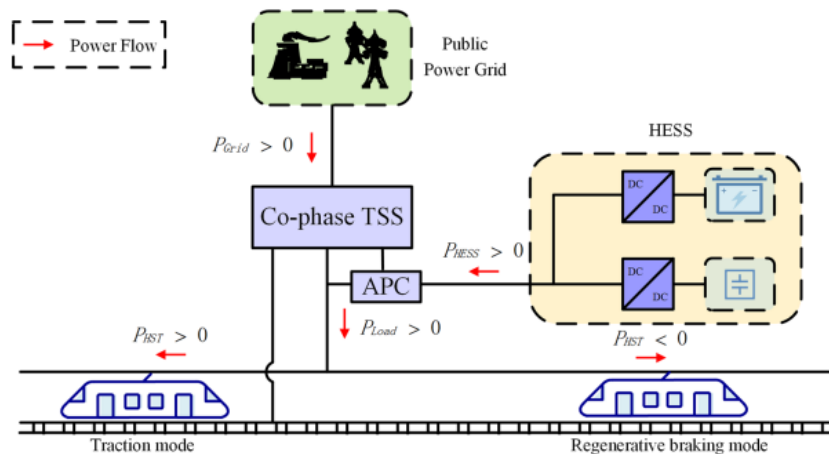


Figure 1.7: Traction power supply system with HESS structure [59]

While the HST is in traction mode, the HST power for P<sub>HST</sub> is greater than zero, and when the HST is in regenerative braking mode, P<sub>HST</sub> is fed back to the catenary from the HST. The power flow of HESS (i.e., P<sub>HESS</sub>) is responsible for peak shaving or valley filling as the load power surpasses the threshold region.

Taking into account the payment method, HESS is used to lower the demand for peak power and reserves energy during times of low load. In order to do this, the power allocation criterion is developed using the charging threshold line PL1 and the discharging threshold line PL2. Fig. 1.8 depicts a portion of the load power and demand curve of a TS.

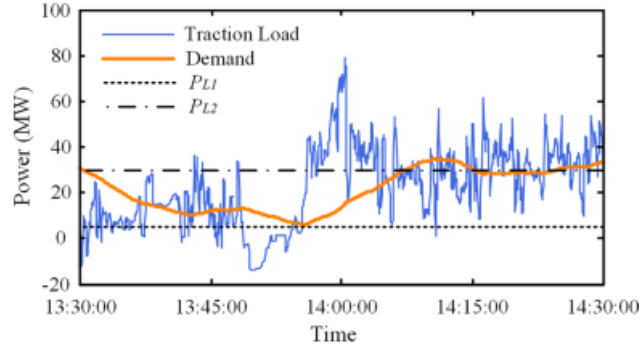


Figure 1.8: Feeder traction load power curve [59]

On the basis of this, a demand reduction strategy is developed for energy management. If the traction power exceeds  $PL_2$ , HESS is configured to discharge. HESS is charging if the traction power is less than  $PL_1$ . The HESS is sometimes in standby mode. Formulas below can be used to express it specifically:

$$P_{HESS}(t) = \begin{cases} P_{H,r}, P_{Load} > P_{L2} \\ 0, P_{L1} < P_{Load} \leq P_{L2} \\ P_{Load} - P_{L1}, P_{L1} - P_{H,r} < P_{Load} \leq P_{L1} \\ -P_{H,r}, P_{Load} \leq P_{L1} - P_{H,r} \end{cases} \quad (3)$$

where  $P_{H,r}$  is the rated power of HESS, and  $P_{HESS} > 0$  indicates HESS is discharging state. Two popular HSRS schemes are ESS for traction substation and ESS for onboard. For onboard ESS, the effects of the ESS volume and weight change on the vehicle operation performance are significant [61]. Traction substations, on the other hand, are situated in suburban areas with sufficient usable space, thus ESS volume and weight are not a significant restriction [62].

In the optimal problem of HESS capacity, when the HESS capital cost and maintenance cost are taken into account, cost restrictions are typically applied. Yet, the HESS size also significantly affects maximum demand and RBE utilization, suggesting that cost constraints are insufficiently used to examine the case's economic effectiveness.

For the purpose of evaluating HESS's economic effectiveness, the Net Present Value (NPV) is included. The HESS sizing problem's objective function, or NPV, is denoted by equation (4)

$$\begin{aligned} \min f = -NPV = & - \sum_{i=1}^{N_p} (-C_{CC}[i] - C_{MC}[i] - C_{RC}[i] \\ & + \Delta C_{EC}[i] + S_V[i]) \times (1 + F)^{-i} \end{aligned} \quad (4)$$

When the train is in traction mode, the train power is greater than zero, and conversely, train power is fed back to the catenary from the train in regenerative braking mode. As the load power exceeds the threshold region, the power flow of EVs in the park & ride is responsible for peak shaving or valley filling. However, whole during the day it cannot supply the total train power, so in the proposed method if the load power exceeds the second threshold, the HESS is in charge of supplying the remain load power and vice versa.

A hybrid energy-storage system (HESS) is a concept that involves combining different types of energy-storage systems (ESSs) that have different characteristics, such as power density and energy density [45]. This integration allows the strengths of each ESS to work together, resulting in improved performance compared to using a single ESS. In railway applications, an HESS typically combines at least two types of ESS devices, one with high energy demand and another with high power requirements. The high-energy device is used to meet long-term energy needs, while the high-power device is used to fulfill short-term high power demands. In railway systems, batteries and fuel cells are commonly integrated into an HESS to meet the energy requirements.

If properly designed, an energy storage system can collect the energy produced by a braking train and discharge it when necessary. This reduces the amount of energy drawn from the primary power grid [63 - 65], and also reduces peak power demand. This is beneficial not just for the rail transit system, but also for the power utility, as the ESS can offer services such as peak shaving. By capturing the energy produced by a braking train, an ESS can minimize the need for onboard or wayside dumping resistors. This results in a reduction in the costs associated with heat waste and ventilation systems [66].

The regenerative braking energy of high-speed railway features high power and high energy. It is difficult to recover it only by using high power density supercapacitors or high energy density batteries. Therefore, a hybrid energy storage system (HESS) composed of supercapacitors and lithium-ion batteries and its optimal configuration method are proposed for the purpose of obtaining maximum economic benefits for railroad system [67].

Then the economic benefits when using the HESS and the single energy storage system are compared from the perspective of whether the regenerative braking energy is fully recycled or not.

The batteries are composed of battery cells in series and in parallel. The number of batteries mainly depends on the power and capacity required. Lead acid battery and lithium-ion battery have become more mature in the market. As the characteristics of

lithium-ion battery better than lead-acid battery in cycle life and energy density, lithium-ion battery is used in HES.

Batteries require more time to recharge energy in each cycle due to the electrochemical reaction that occurs inside them, which distinguishes them from flywheels and EDLCs. As a result of this property, batteries are suitable for installation trackside, as they can provide ample energy to electrified systems and have fewer life cycles than some other energy storage devices, which can make them difficult to maintain. Trackside installation allows for easier maintenance and replacement of batteries. In Japan, batteries are installed both stationary and aboard in electrified railway systems for various applications, such as energy saving, voltage regulation, and power compensation. While academic articles by Japanese researchers report large battery capacities, they do not provide sufficient details about the connected circuits, battery specifications, protection circuits, or control strategies for charging and discharging the batteries [68].

## 1.7 Discussion

Although energy storage systems can reduce the peak demand and carry out peak shaving and also store regenerative braking, it needs to invest huge budget to implement, manufacture and maintain and impose prominent cost on the railway system. Thus, in the next section novel methods are introduced and evaluated which employs battery of electric vehicle (EV) as energy storage system. This kind of method, unlike other energy storage technologies, utilizes already existing storage that would otherwise lay dormant (batteries of parked EVs). When combined with smart charging technologies, EVs could be turned from a burdensome load on the power grid, into a valuable tool for maintaining grid stability.



## 2. Utilizing EV batteries for recuperating regenerative braking energy

### 2.1 Introduction

Over the past few years, countries have invested heavily in the development of electric vehicles (EVs) and charging infrastructures for EVs and E-buses, in an effort to reduce carbon emissions and the use of fossil fuels. However, the widespread use of power supply EV charging stations (EVCs) can put a strain on the main power grid and lead to indirect emissions. Electric railway systems (ERSs) have the potential to generate a significant amount of energy through regenerative braking, which can be utilized as a supplementary power source. Since EVs are often parked for long periods of time, their batteries can be used as energy storage systems (ESSs) to store regenerative braking energy (RBE) from trains or even as a secondary power source for ERSs. Integrating ERSs and EV/E-bus charging stations at strategic locations, such as parking areas near ERS stations or rail freight intermodal terminals, can improve the efficiency of the system and reduce costs. Different integration architectures can be used depending on the type of electrical railway system (ERS), utilizing either the DC or AC energy hub concept. The concept of train-to-vehicle (T2V) and vehicle-to-train (V2T) technologies will also be explored, along with the challenges of designing future sustainable transportation systems. The existing electric railway system (ERSs) can be classified into two main categories, based on the primary power supply system they use - DC and AC systems [69].

### 2.2 Electric vehicle charging infrastructure

Electric vehicle charging infrastructures (EVCIs) consist of different levels that can be categorized into two groups: low-power AC EVCIs and high-power DC EVCIs.

### 2.2.1 Fast charging infrastructure (DC EVChs)

This category refers to the charging infrastructure used nowadays for mid (up to 25 kW) and fast (up to 150 kW) charging, equipped with Combo 2 and/or ChAdeMO plug. These chargers can charge most of the current and future EVs, with the preference for the Combo 2 connection chosen by the European Union as the charging standard. To accommodate the low power value, it is preferable to connect them to the low-voltage DC section. These charging systems need to support vehicles with batteries up to 1000 V. Mid charging infrastructure is suitable for a charging time of 1-2 hours, while fast charging is mainly used to reduce the charging time to half an hour [69].

### 2.2.2 Low-power AC EVChs

This group of EVChs allows EVs to be connected directly to a single-phase/three-phase AC grid through an internal battery charger, making them suitable for large-scale installation of charging stations that can accommodate a wide range of EVs. They are widely used today and come with a household socket (NEMA 5-15) with 120/240 V and around 32A as standard. However, these chargers have low charging power, typically up to 22 kW, making them a slow charging method that takes 2-8 hours. They are suitable for home use or when the vehicle can remain parked for an extended period of time, typically a few hours. This basic level of EVCS is considered the slowest charging method. [69]

## 2.3 Integration of EV charging infrastructures

Combining ERSs and EVChs is a crucial step towards achieving sustainable transportation systems. There are two perspectives to consider when integrating these systems. The first is intermodal transportation, which involves flexible connections between roads and railways at strategic points. This perspective is mainly concerned with geographical and geopolitical factors and is beyond the scope of this chapter. The second perspective, which will be discussed in the following sections, is the integration of power supply systems and charging infrastructure for both ERSs and EVs. To achieve T2V/V2T integration, different frameworks can be evaluated based on the intrinsic characteristics of ERSs:

- Employing regenerative braking energy (RBE)
- Assuming EVs as stationary ESSs and distributed energy resources
- Utilizing ERS lines as energy hubs preparing suitable connection areas for renewable energy sources (RESs)

### 2.3.1 Employing regenerative braking energy

The concept of regenerative braking energy (RBE) in ERSs is an important subject that has gained a lot of attention due to its potential to improve energy efficiency and sustainability. Modern trains are typically fitted with an electrical braking system to prevent the waste of energy through the use of rheostats. This section will explore the potential of using RBE to power EVCIs and enable train-to-vehicle (T2V) technology. The rate at which RBE is produced is dependent on several factors such as train speed, train mass, total inertia, and braking duration. Additionally, AC ERSs generally have a wider range of total energy than DC ERSs, making the production of RBE in AC and high-speed ERSs particularly important. Based on actual measurements, the percentage of RBE produced can range from 4% to 13% [69].

### 2.3.2 Meantime integration of ERSs and EVCIs

The first integration mode involves transferring RBE from ERSs to EVCs without any interruption. Figure 2.1 illustrates the proposed plan for this scenario. However, the main challenge of this mode is the difference between the produced and consumed powers. The power generated by trains during braking is in the megawatt range, while the power required by EVs is only a few kilowatts. Therefore, numerous EVs should be parked in the area, or multiple EVCs connected along the ERS line, to absorb and consume RBE on a large scale. This method is feasible in areas where there are large EVCs, such as commercial centers and business buildings with numerous parking spaces. According to reports, vehicles typically stay parked for about 8 hours in such areas. Similarly, TPSSs located near metropolitan areas and highways with high parking volumes are ideal for this integration. However, the main challenge of this scenario is the intermittent production of RBE. As a result, an additional connection between the grid and EVCS is required to charge EVs directly through G2V technology during periods of no RBE production. An accurate aggregator must be employed to assess the status of EVs and determine the maximum charging rate available to prioritize integration based on calculations. [69]

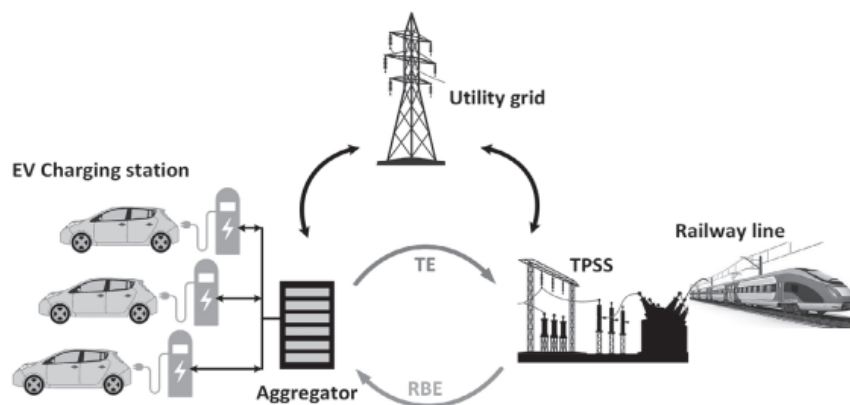


Figure 2.1: Scheme of meantime integration between ERSs and EVCIs [69]

### 2.3.3 ESS-based integration of ERSs and EVCI

The meantime integration scenario may not be feasible for implementation as most of the current EVCSs are small to medium-sized. Therefore, an alternative indirect approach involves using ESSs as an intermediary between ERSs and EVs. The additional energy generated during braking can be stored in ESSs, and when there is no RBE available, EVCSs can be powered from the grid. This approach allows for the continuous transfer of power and the absorption of RBE with a small number of EVs. Unlike the meantime approach, there is no requirement for an additional connection to the grid. The scheme for ESS-based integration is depicted in Figure 2.2.

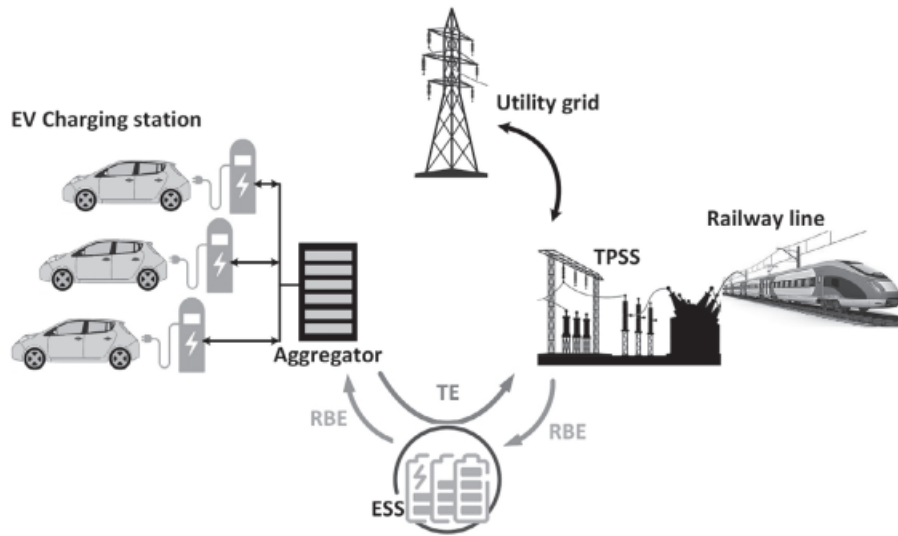


Figure 2.2: Scheme of ESS-based integration between ERSs and EVCI [69]

One way to supply traction energy (TE) to trains is by using the power flow from EVCI to ERS, which can be achieved by utilizing the dedicated batteries in EVs. This mode of power flow can be implemented during peak hours or when the trains are accelerating. The aggregator can manage the fully charged EV batteries as distributed energy resources to supply energy to the ERS as an auxiliary source. By involving a large number of EVs, a general power threshold ( $P_g$ ) for EVCSs can be established, which matches the accelerating traction power ( $P_{at}$ ) of the trains. In this method, the following equation must be satisfied to completely provide the accelerating train with power.

$$\begin{cases} \sum_{m=1}^N P_{d,m} \geq P_g \\ P_g \geq P_{at} \end{cases} \quad (5)$$

where  $P_{d,m}$  is discharging power rate and N is the total number of participated EVs. The amounts of  $P_{at}$  for each TPSS should be evaluated based on the average threshold powers of departure trains. From an EVCI point of view, the implementation of such integration depends on the number of EVs, the charging/discharging power rate of EVs, and their SOC. In case of insufficient EV number, ESS-based connection can be proposed, taking advantage of hybrid ESSs as

an auxiliary device. Thus, during acceleration of trains or peak shaving intervals, ESSs collaborating with EV batteries can supply trains. Literally, ERSs can be supplied by cheaper energy through this integration since EVs are often charged by lower tariffs or RESs [69].

## 2.4 Integration of EV charging infrastructures

Two architectures can be proposed to integrate the charging infrastructure into the DC catenary system of the ERPS, and they are applicable for both low- and high-power charging stations.

### 2.4.1 Two-Stage DC Charging Infrastructures

As it is shown in Figure 2.3, the two-stage chargers are applicable for low-power purposes, where the first-stage solid-state transformer (SST) as a DC-DC converter is isolated and interlinks the DC catenary.

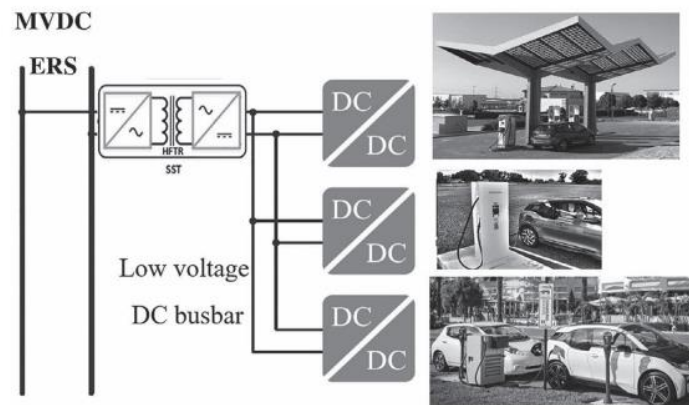


Figure 2.3: Integration configurations two-stage charging station [69]

system with the charging station. The second-stage DC-DC converter can be chosen to be isolated or non-isolated, and it is mainly installed to be able to charge various types of EVs with different voltage requirements.

### 2.4.2 Single-stage DC charging infrastructure

The architecture of a single-stage charging station can be seen in Figure 2.4 in which one power electronic converter is directly interlinking the DC catenary system with various types of chargers, including mega chargers for E-buses and E-trucks. In this type of charger, the single power electronics converters are isolated in order to provide the system with galvanic isolation for meeting the safety factor [69].

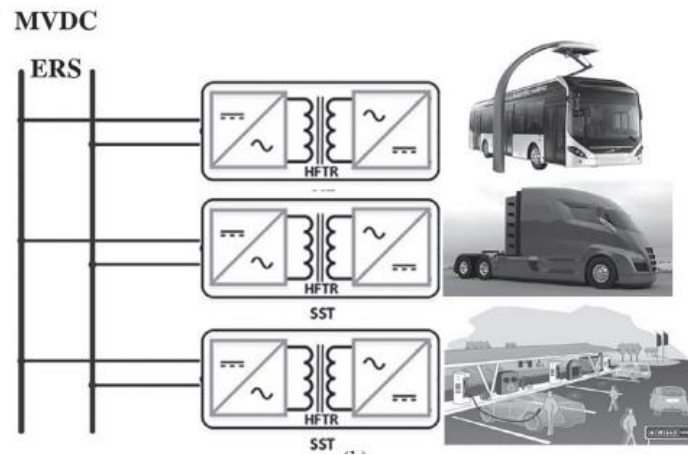


Figure 2.4: Integration configurations single-stage charging station [69]

## 2.5 Different architectures of ERS and EVCI integration

The previous sections have discussed several frameworks for integrating Electric Road Systems (ERSs) and Electric Vehicle Charging Infrastructures (EVCI). The remarkable advantages of this integration have inspired the authors to explore and evaluate the integration of Renewable Energy Sources (RESs) into the system. This section aims to present different integration configurations, including both DC and AC systems, and the concept of an energy hub [69].

### 2.5.1 Low-voltage DC hub-based integration

Low-power DC ERSs are commonly found in heavily populated metropolitan and urban areas, with dedicated DC lines distributed throughout the city to supply them. Meanwhile, most DERs, such as PV and ESSs, are based on DC networks or include a DC component, as are wind generators [70]. In the same vein, DC-based mid and fast charging EVCI are situated in close proximity to railway lines or stations, which increases the potential for interconnection. Figure 2.5 illustrates the general concept of T2V/V2T integration in low-voltage ERSs. Typically, low-power transportation systems such as urban rails, trams, light rails, and subways make use of LVDC ERSs (0.6-1.5 kV) for short and medium distances. As a result, low-power components can be integrated into such a system. The proposed architecture involves a shared DC busbar that serves as the integration point and energy hub. This can be implemented in two locations: at the substation or along the railway line. Substations are a favorable location because they have pre-existing switching and protection devices, as well as buildings that can be used for new connections. Additionally, the close proximity to the AC mains enables higher power transfer. On the other hand, integration along the line may be more complicated but provides an opportunity to supply EVCI at strategic points, such as parking lots near railway stations.

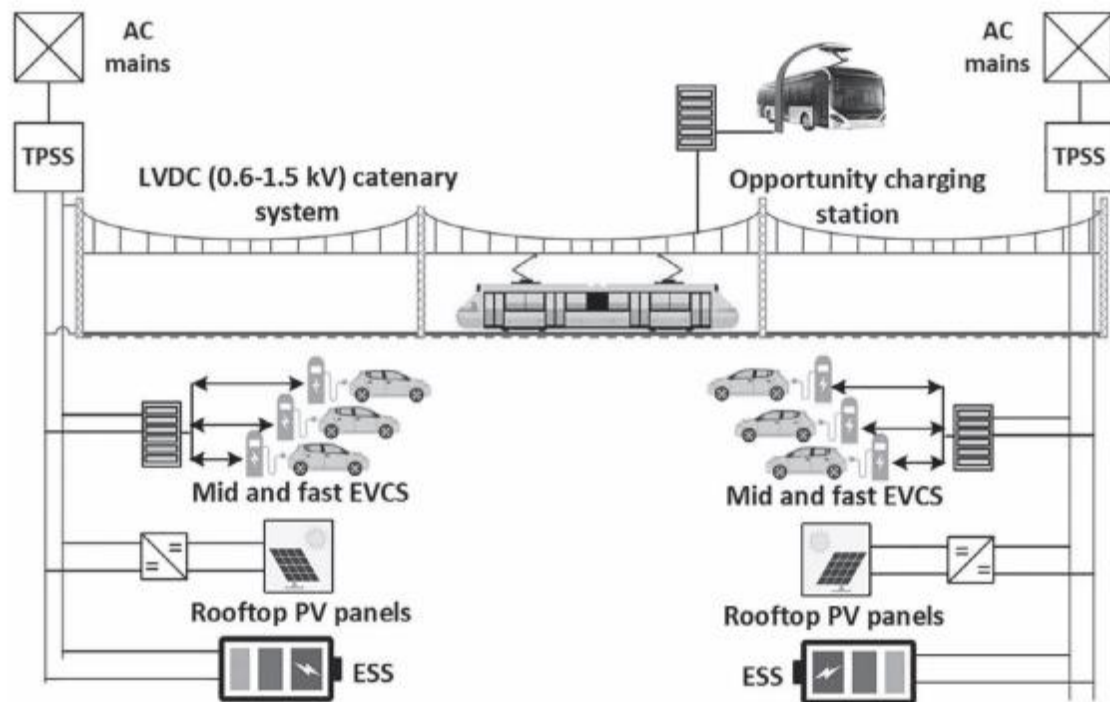


Figure 2.5: T2V/V2T integration architecture in LVDC ERSs [69]

Also, a balancing block is used in this system to handle voltage changes caused by the trams' varying power consumption. To manage the energy flow between the DC microgrid, the balancing system's BESS, and RBE for optimal use and power quality control, an SPS control system is implemented. The tramway's RBE is utilized to power charging stations instead of being wasted, even if there is no balancing system present and only E-bus opportunity charging systems are connected to the traction DC microgrid. By implementing a balancing mechanism, the possibility of integrating EV or E-bus charging stations to the tramway DC microgrid can be increased, resulting in substantial cost reductions and improved energy efficiency. [71].

Worth mentioning that controlling the charging system in the integration system is a vital role. The objective of the presented electric transportation power supply system is to enhance energy efficiency and lower costs in charging stations for railway networks and electric vehicles. To accomplish this, maintaining a stable voltage range in the tramway DC microgrid near the E-bus opportunity chargers, a stabilizing module has been installed. This balancing system improves the voltage profile of the grid, directly impacting the efficiency and quality of the fast opportunity chargers. Rather than constructing additional grid wiring, the current DC grid can be utilized. The stationary battery energy storage system (BESS) can store the RBE of trams and send it back to the DC grid when required using a reversible DC/DC converter in the balancing module. The authors of this article have previously worked on this issue and presented their findings in [72] using a more straightforward conversion scheme in the balancing system. The dual active bridge

(DAB) converter model studied in this paper isolates the DC grid from the battery using its high-frequency transformer. Additionally, changes have been made to the system's overall structure to improve its performance. a railway power flow controller combined with a DC/DC buck converter has been developed to recover energy from the shared DC hub and transfer it to the EV charging stations. A hierarchical control system has been adjusted to manage all tasks related to power transfer, optimal energy utilization, and power quality control.

### 2.5.2 AC hub-based integration

While MVDC ERSs offer several benefits, they require a significant amount of time for development and expansion. Therefore, an alternative to high-power railway lines is to use AC ERSs, which are now a mature technology. However, these systems face significant power quality (PQ) issues that necessitate additional compensators. Additionally, unlike LVDC ERSs, RBE transfer between trains is less likely due to neutral sections, and it is possible to return RBE to the utility grid. Such a system is known as AC ERSs. As a result, T2V/V2T technologies in this type of system require some limitations. The concept of integrating AC ERSs with EVCI. Figure 2.6 shows the general idea of this integration, which involves traction transformer-based substations with 25 kV OCS in an insulated area. The AC bus serves as an energy hub that can be implemented in two formats, either concentrated in the substation or distributed along the line. To integrate the elements into the AC hub, DC/AC converters are mainly used, but their switching frequencies may cause PQ issues. Therefore, the power flow capacity must be limited to avoid such problems. As a result, RESs connected to AC ERSs are usually low-power systems. Although this structure may not be suitable for mega chargers or ultrafast charging systems, it can integrate mid and fast EVCIs through special rectifiers and low EVCIs through step-down transformers. However, integrating the elements through the rectification process can exacerbate PQ issues in AC ERSs. [69]

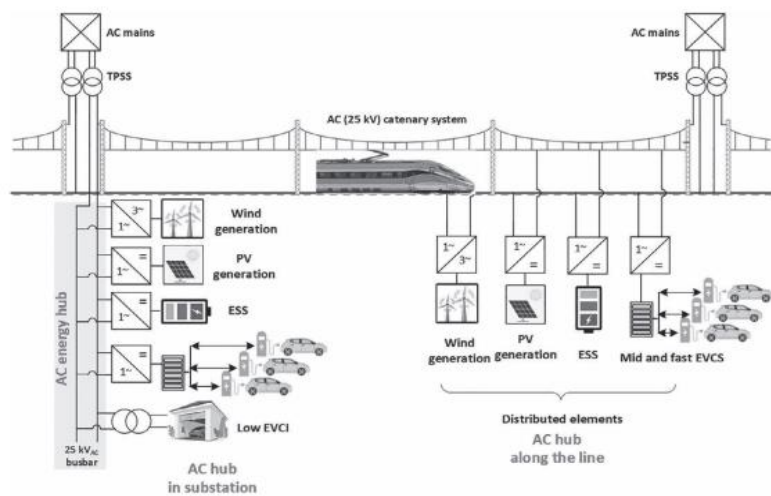


Figure 2.6: T2V/V2T integration architecture in MVDC ERSs [69]

### 2.5.3 Hybrid hub-based integration

To overcome the problems of AC-based architecture and increase the power-flow capacity, a hybrid configuration can be proposed. In hybrid architecture, taking advantage of a high-power interfacing device (different kinds of interface converters or compensators [73]), a joint DC bus can be established to facilitate the connections of elements. Depending on the interface device, various configurations can be proposed for hybrid architecture, which is explained in detail in [70]. The scheme of hybrid architecture for T2V/V2T integration is shown in Figure 2.7. Interface converter can create an increased bidirectional power flow between AC and DC buses. The high-power capability of hybrid architecture allows the direct connection of high power RESs. Meanwhile, from an EVCI point of the view, this system can provide the realization of mega EVCI, which could be problematic in the AC architecture. It must be noted that during busy times with high consumed loads if all the elements work at their full rates, the suitable control interface device, and consequently PQ controlling, will be very complicated. Due to the high cost of implementing DC bus along the line, this architecture it is better to be realized in the substation position. [69]

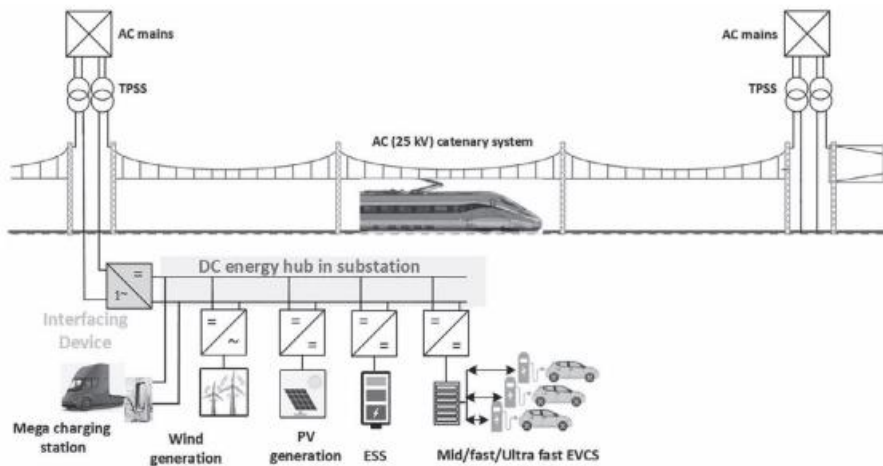


Figure 2.7: T2V/V2T integration architecture in hybrid ERSs [69]

This [74] proposes a new system that integrates a large-scale hybrid renewable energy source (RESs) and an electric vehicle (EV) fast-charging station into a medium voltage (MV) DC electric railway power system (ERPS). Figure 2.8 displays a proposed micro grid for a DC railway that incorporates a hybrid system consisting of PV panels, wind turbines, and storage. The main objective is to provide power to the train and EV fast-charging station through a large-scale hybrid system that operates in two modes: standalone (grid-OFF) and grid-connected (grid-ON). The PV and storage systems are linked together through a unidirectional DC/DC boost converter and a bidirectional DC/DC buck-boost converter. The boost converter is used for maximum power point tracking (MPPT) to obtain the maximum power from the PV panels, while the buck-boost converter is utilized to charge and discharge the storage

system based on the system's operating conditions. The wind turbine is connected to the overhead catenary system through a diode bridge rectifier and DC/DC boost converter for MPPT to obtain the highest power output. To connect the common point of the PV and storage system to the DC bus, a unidirectional PSFB DC/DC converter is employed. In this study, the PSFB converter boosts the voltage from 1 kV to 1.5 kV, and the DC catenary system is energized in either standalone or grid-connected mode based on the availability and operational conditions of the grid, PV, wind, storage system, and loads.

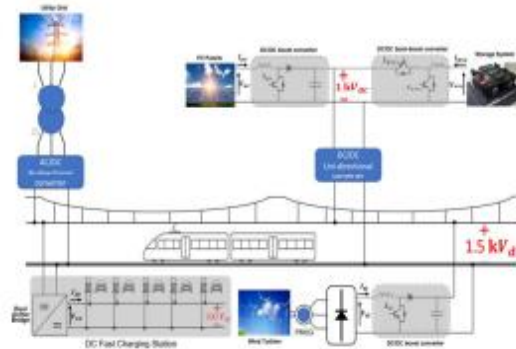


Figure 2.8: PV/wind/storage hybrid system general architecture[74]

To connect the fast-charging infrastructure to the DC catenary system, a bidirectional DC/DC dual active bridge (DAB) converter is used, which enables power to flow in both directions, from the grid to the vehicle (G2V) and vice versa (V2G), although the latter is not part of this study and is reserved for future development. The DAB converter lowers the voltage of the DC bus from 1.5 kV to 500 V, which is used to power five parking slots. Moreover, a two-level bidirectional AC/DC converter is employed to connect the utility grid to the DC catenary system. a storage system is also connected to the system to avoid blackouts and reduce the burden on the utility grid during peak hours due to the intermittent nature of wind and solar irradiance. To increase the voltage to 1.5 kV DC and connect the photovoltaic (PV) arrays and storage system to the railway catenary system, a unidirectional DC/DC power converter is used. Additionally, the DC/DC converter provides galvanic isolation between the storage and utility grids for safety reasons. [74].

## 2.6 Integration renewable energy source

On other side, the [75] describes a DC power grid consisting of PV/storage and DC/DC power converters, which is designed to provide the fast charging station with renewable energy and reduce greenhouse gas emissions caused by EVs. The proposed microgrid system is shown in Fig. 2.9. the PV and storage systems are linked together through a one-way dc/dc boost converter and a two-way DC/DC buck-boost converter. The DC/DC boost converter is used for Maximum Power Point Tracking (MPPT) to obtain the highest power from the PV panels. The bidirectional

buck-boost converter charges and discharges the storage system as needed. A unidirectional PSFB DC/DC converter is used to connect the common point of the PV and storage system to the DC bus. The PSFB converter increases the voltage from 500 V to 1000 V. The DC bus can be powered by either the PV-storage system or the main grid, depending on the availability and operational conditions of the grid, PV, and storage system. This study focuses on how the PSFB converter boosts the voltage and how the DC bus is energized. To connect the fast-charging infrastructure with the DC bus, a two-way bidirectional DC/DC Dual Active Bridge (DAB) converter is used. This converter enables power flow in both directions for Grid to vehicle (G2V) and Vehicle to Grid (V2G), but V2G is not included in this study since it is reserved for future development. The DAB converter lowers the DC bus voltage from 1000 V to 500 V, which is then distributed to five parking stations. Additionally, the main grid is linked to the DC bus using a two-level bidirectional AC/DC converter.

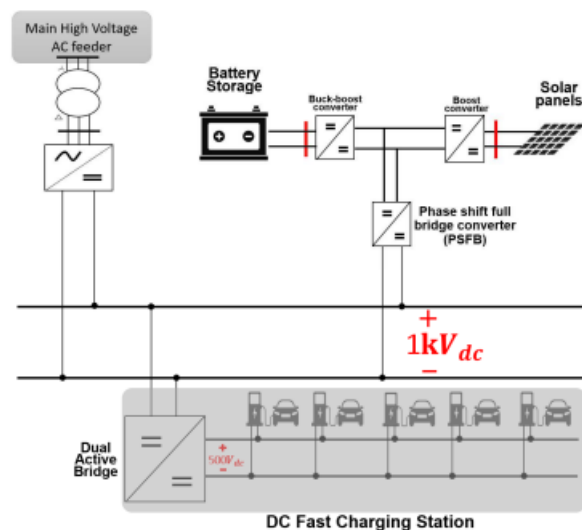


Figure 2.9: Microgrid general architecture [75]

[75] is suitable for installation alongside motorways where AC utility grids are unavailable, and energy can be transmitted via DC connections like the DC catenary system of the ERPS. The study assumes that the charging station's energy demand is primarily met by a PV/storage system, with the main utility grid supplying power to the DC bus as needed. Additionally, a storage system is used to compensate for fluctuations in PV output power. The phase shifts full bridge (PSFB) converter is implemented to increase the voltage to higher values, and it increases the reliability and redundancy of the PV-storage system because a lower number of PV and storage components will be connected in series; additionally, the galvanic isolation will be provided for safety reasons [75].

This paper proposes a smart DC railway architecture that integrates two types of renewable energy sources (wind and PV) into the DC catenary system. A storage unit is also used to address the intermittent nature of the renewable sources and work as a backup. Additionally, a DC fast-charging station is integrated into the smart DC

catenary system through a bi-directional DC-DC power converter dual active bridge (DAB), which provides galvanic isolation and two-way power flow. The smart DC catenary system is utilized as a DC hub in which the power flow is controlled between power generators and loads. The results of the study confirm that this smart architecture can lead to partial or even temporary full independence from the main utility grid suppliers. The interlink between two different transportation systems and the capability of power transferring revive the concept of sustainable transportation as the architecture of future power supply systems. Another study on integrating the DC catenary system of 3 kVdc electric railway power systems (ERPS) into a DC hub is also presented in fig. 2.10, which accommodates RESs, charging infrastructures, and storage units to increase the system's capacity and mitigate the voltage drop due to high penetration of loads. Furthermore, a power management system (PMS) is proposed to ensure the correct operation of the system under various working modes, while future research may consider evaluating the energy management system (EMS) and vehicle-to-grid (V2G) possibilities. [76]

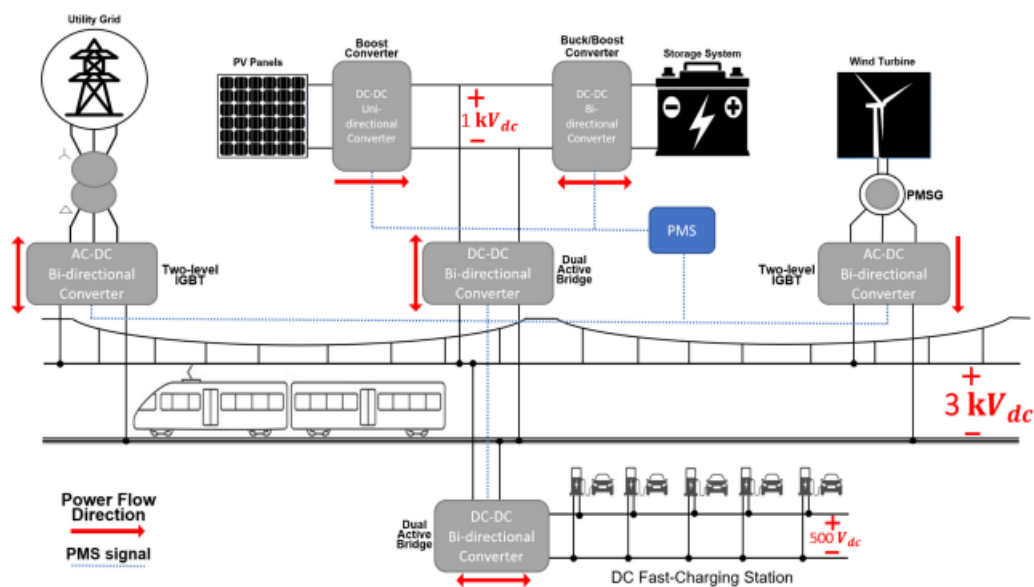


Figure 2.10: Smart DC catenary system architecture [76]

Using electric railway system (ERS) dedicated lines and infrastructure as an energy hub to connect with renewable energy sources (RESs) and improve the capacity of the railway grid is a step towards realizing the smart grid concept in the railway sector. The different integration architectures for DC and AC ERSs show that MVDC-based architecture can offer the advantages of both AC and LVDC types. In the study "sustainable MVDC," a 9 kV MVDC railway system is modeled and simulated based on an existing high-speed line as a real case study, with the integration of RESs and EV/E-bus charging infrastructures as auxiliary power supply to the proposed MVDC railway microgrid. A modified power management system considering the regenerative braking energy of trains is also presented. It is shown that integrating RESs into the railway system can increase its capacity and efficiency. Smart

integration control can also make voltage fluctuations of the catenary system smoother around the nominal value. In conclusion, MVDC ERSs are promising architectures to take advantage of RESs and achieve sustainable transportation systems due to the possibility of direct connections and lower converters. [77]

This piece of writing introduces a new scheduling approach for V2G systems, which takes advantage of repetitive power demand patterns and the decreased uncertainty that comes with recurring events. Specifically, an "event" is defined as a predictable pattern of power demand that occurs over a specific period, with a known start and end time. This scheduling technique is designed for use in large-scale, centrally controlled V2G networks and is comprised of three different scheduling layers. The predictive scheduling layer operates just before each event begins, scheduling each event separately. This layer assumes perfect knowledge of the event's duration and executes accordingly. A second reactive scheduling layer is used in real-time to adjust the schedule as needed. A third layer employs a distinct set of scheduling rules for periods without any events occurring. The strategy was demonstrated using an example scenario in which a V2G network is utilized to meet the power requirements of electric trains in the vicinity. In this particular context, an event was described as the arrival or departure of an electric train at a station, resulting in a sudden increase in power demand during train acceleration or a surplus of power during train deceleration facilitated by regenerative braking. The algorithms introduced were created based on a modular aggregator control approach that utilizes indirect communication through a shared SQL database across the entire network. To minimize the computational expense of scheduling, the EVs' ability to serve different types of events (CW and DCW) was predetermined within the database. The standards used to assess EV suitability are highly dependent on the specific V2G application and limitations on the EV population. During events (first layer), scheduling was carried out in one-second intervals, although a more precise resolution could be used at a higher computational expense. Reactive scheduling (second layer) and smart charging (third layer) were not restricted by fixed time intervals. The study demonstrated that a multi-layer scheduling strategy can result in a nearly immediate system response if power demands can be accurately forecasted. If there is a disparity between the predicted and actual power demands due to uncertainty, there will still be delays in the system response. However, the duration of these delays is influenced by the severity of the mismatch, which determines the number of schedule adjustments that must be performed by the reactive scheduling layer [2].

## 2.7 Control management system

In the proposed EV parking lot, the connected EV population would discharge into the rail system as electric trains speed up, generating a rise in the power demand for

traction, reducing the load on the nearby substation. As arriving trains decelerate using regenerative braking, the resulting spike in power from the rail system would be fed into the EV parking lot. But as EV parking lot is not able to supply whole power demand from train especially in the early morning and evening, Hybrid energy storage system (HESS) is employ to mitigate power demand from the grid. In order to manage the energy exchange, the power demand profile has been separated into three distinct 'events' 1) train departure event (acceleration from standstill, slow speed movement close to the station, then to travelling speed, traction power required), 2) train arrival event (deceleration from travelling speed to standstill, energy from regenerative braking needs to be dissipated) and 3) no traffic when there is no departure event or arrival event. The EV parking lot is assumed to utilize the same substation and share its power grid connection as the train system (see Fig. 19). It makes an effort to maintain the grid connection limit, or the power flow from this substation, at a steady level (a soft constraint rather than a true limit, defined by the proportion of the available power to be managed by the EV parking lot).[2]

The aggregator continuously analyzes EVs and uses a dual scoring system to rate them according to their suitability for consuming or supplying power. DCW and CW are the dual scores.

Charge Weighting (CW)\*: An unsigned float value measuring how well the electric vehicle (EV) is suited to receive power (the greater the value, the more likely it will be used for charging). When SOC reaches 100%, value is zero and an EV can no longer be charged. created using database calculations and other inputs.

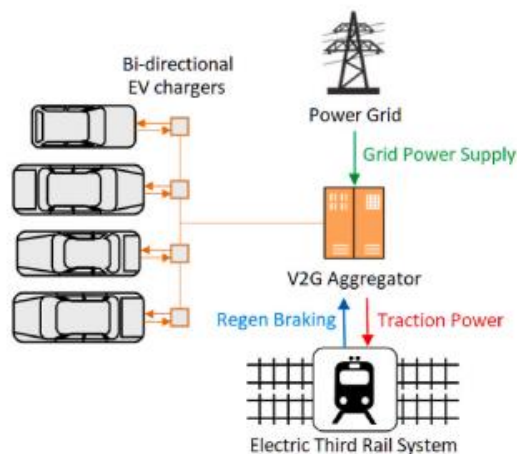


Figure 2.11: System overview and power flows [2]

Discharge Weighting (DCW)\*: An unsigned float value indicating how well-suited the EV is to provide power (the higher the value, the higher the chance of this EV to be allocated to discharging). Value is 0 when SOC is zero, making it unable to discharge an EV any further. created using database calculations and other inputs. In

order to calculate the DCW and CW index it is necessary to calculate state of charge (SOC) of every battery of EV parking lot and HESS.

The battery pack SOC at the time determines the maximum charging rate for each EV. So, regardless of the battery pack SOC, it is reasonable to assume that the battery pack can be depleted at least at this pace. Any of the bi-directional EV chargers' estimated charging/discharging limits are exceeded by this discharging rate.

For train departure events the aggregator switches grid connection power from EVs to train. Then aggregator for supplying the traction power, priorities EVs with high battery capacity, high maximum discharging rate and high SOC (each parameter is weighted equally in the scoring system). Such EVs are useful for train departures as they can provide a relatively large quantity of energy relatively quickly (compared to the EV population as a whole). Finally, if the power store in the EV parking lot cannot supply the traction power HESS which is consist of supercapacitor and battery is in charge of covering the remain traction power. When the discharging power of the supercapacitors cannot match the system load power, the battery is started to discharge energy. If the equation (6) during whole acceleration event would be true, the aggregator does not demand power from the grid. The main objective is to minimize the power demand from the grid network. Therefore, if aggregate meet the equation (6), we achieve our aim. However, if during part of the acceleration event equation (6) would not be true, the remain power must be demand from the grid and this situation is not satisfactory.

$$P_{Grid\ connection}^t + P_{EVs}^t + P_{Badis}^t + P_{SCdis}^t \geq P_{train}^t \quad (6)$$

On the other hand, during the braking event aggregator confront with two energy source, first grid connection power and regenerative braking power. In order to manage these two energy source, firstly aggregator share grid connection power between EVs. Based on the proposed algorithm EVs with high capacity, high maximum charging rate (at the time) and low SOC are prioritized. These EVs can quickly absorb a lot of electric energy (relative to the EV population). Then, if whole grid connection power is shared between EVs and still there is vacant space in the battery of EVs, regenerative braking energy fill the vacant space of the EVs battery to charge the EVs with maximum rate. After that, HESS is in the charging state, and the batteries starts to work first. When the maximum charging power cannot meet the regenerative braking power, the supercapacitors start charging at the same time to absorb the regenerative braking power. when the EV population is not able to supply sufficient traction power to the rail system, the power flow from the substation may exceed the grid connection limit to compensate for the deficit. In case of insufficient power absorption from regenerative braking of trains, excess power is assumed to be 'wasted' via heat dissipation (either through resistor banks or mechanical brakes) and not fed into the grid. In either case, the rail service is not compromised.

During events, the aggregator assigns EVs sequentially to charge/discharge at the maximum possible rate until the power drawn from the substation matches the pre-determined grid connection limit. The degree to which the V2G network can decouple the power demands of the rail system from the grid connection mainly depends on the following three parameters: the EV population size, the global charging rate limit (the maximum charging/discharging rates per EV as supported by the aggregator) and the anticipated grid connection limit [78].

The scheme outlined utilized Electric Vehicles (EVs) as a means of storing the braking energy of the railway electrical infrastructure. This involved implementing regenerative braking and utilizing the EV charging stations located near the train station. Additionally, the idle capacity of internal service and traction transformers was also taken into account as another source for charging EVs during normal operations. A novel optimization-based strategy has been developed, taking into account the benefits of the railway system and renewable energy sources. The findings indicate that utilizing the idle power capacity of service and traction transformers can help to minimize installation costs for charging station infrastructure. This is the first time such an approach has been proposed in the literature. In addition, combining a parking lot equipped with photovoltaic (PV) technology with regenerative braking energy (RBE) from the trains can greatly reduce the operational costs of the parking lot. It is also suggested that operational costs could be further reduced by implementing a 150% power capacity for two hours. It can be concluded that integrating regenerative braking energy (RBE) and Energy Storage Systems (ESS) is more cost-effective than using PV systems. Operating the traction transformer at its rated power level contributes to a reliable power system. In future studies, the cost of RBE power and purchasing power from the day-ahead electricity market can be included in the cost function. Additionally, including the Vehicle-to-Grid (V2G) option in the decision-making algorithm could also be considered.

# 3. Modeling and simulation of proposed system

## 3.1 Introduction

In the majority of the presence method hybrid energy storage system (HESS) is utilized to guarantee stability of the power network with storing energy in the braking mode and providing in acceleration mode. But it need to invest huge budget for manufacturing and maintenance dedicated energy storage systems for electric rails systems. The other method for storage the energy is a vehicle to grid (V2G) network in proximity to an electric rail system. With the idea of "V2G," parked road EV battery packs are combined and charged or discharged to provide a range of grid services. Frequency regulation (keeping the grid frequency at 50 or 60 Hz, depending on region), serving as a pseudo-spinning reserve, or load balancing are examples of common grid functions for V2G. (discharging EVs at periods of peak stresses on the grid and charging at low demand periods). In the system presented here, the V2G network works as a buffer between the power grid and the electric train system, as shown in Fig. 3.1.

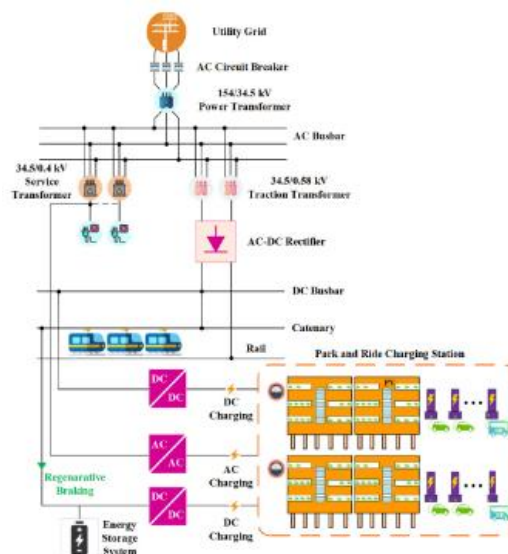


Figure 3.1: System overview and power flows [78]

Unlike other energy storage solutions, V2G makes use of storage that is already in place but would otherwise be idle (EV batteries that are parked). Existing EV batteries are given a secondary use rather than producing and maintaining specialized energy storage systems for electric trains systems. EVs could be transformed from a troublesome load on the electrical grid into a useful tool for preserving grid stability when combined with smart charging systems. The dependence on the availability of EVs in sufficient quantities is the primary drawback of V2G in comparison to alternative energy storage technologies. This research offers a preliminary analysis of the size of the necessary EV population.

### 3.2 Modeling of electrical railway

In this research, we proposed a new method to avoid drawback of the pervious method. based on suggestion method the hybrid energy storage system and battery of electrical vehicle (EV) are use both of them simultaneously. In [2] the DC fast charging (20kW) is utilized to manage power absorption and power demand completely only with more than 100EVs. But implementation of these instrument for at least 100EVs is not logical and practical. Therefore, in the proposed method we turned to the AC charging to be more practical.

on the other side, AC charging rate is not enough to cover the total power for acceleration and regenerative. Therefore, it is necessary to employ the HESS to compensate the remain capacity for storing energy and also, acceleration power. In order to meet both advantage of the pervious methods, a proposed method use the EVs battery and HESS simultaneously.

At first, this method tries to be close to the reality. So, it uses the AC charging (6kW) but the rate of the charging is so lower than DC fast charging (20kW). The only solution to compensate this difference is to increase the number of the EV. This solution is not logical and may be impossible. So this method employs the HESS to this. But the positive point in comparison to the method which is used only HESS, decrease the size of the battery and supercapacitor. Utilizing the HESS with lower size has important effect on the decreasing investing cost. Therefore, in this section we introduce the proposed method based on the EVs battery and HESS and after that evaluate this structure with the other pervious method.

The combined population of electric vehicles (EVs) can be used to supply power to nearby trains that are accelerating, thus decreasing the pressure on the grid during peak demand. Alternatively, the EVs can be charged with power generated by regenerative braking of the trains. When there are no trains nearby, the EVs can use the common connection to the power grid to charge. However, if the EVs participate in vehicle-to-grid (V2G) charging cycles, it may cause the batteries to degrade faster.

A model has been created to estimate the power consumption of trains along the entire railway line. This model takes into account not only the energy needed to propel the trains but also the potential energy generated by regenerative braking. The power demand profile of a single train starting from a stationary position and coming to a stop at a train station is used as the basis for this research. The track section is powered solely by the substation since it is single-ended. The speed and power demand of the train, with negative demand indicating power from regenerative braking, are illustrated in Figure 3.2 (a) and (b), respectively. This model is built upon previous work.

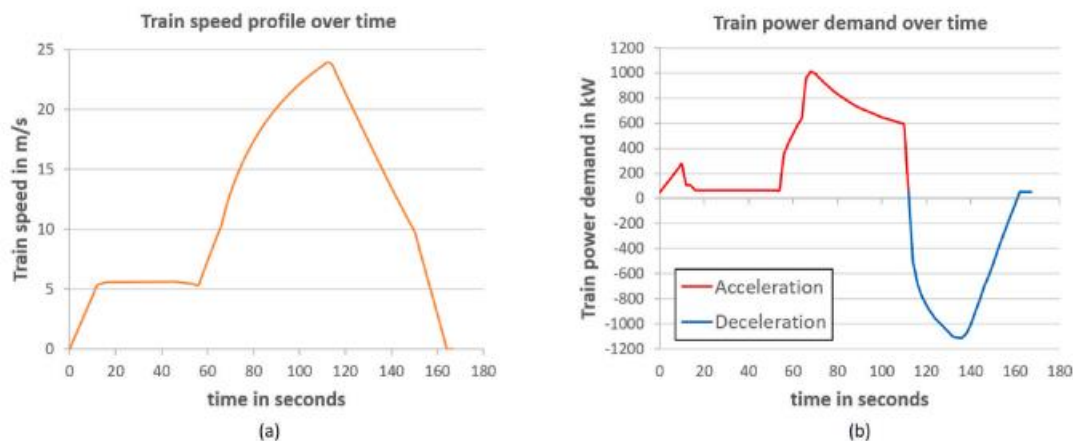


Figure 3.2: a) Assumed speed profile of simulated train (based on GPS data captured during real-life train journey); (b) Resulting train traction power demand (as experienced by the substation) during acceleration and regen power output during deceleration [2]

The power demand profile has been categorized into three separate "events" as mandated by the V2G aggregator control. These events include a train departure event which involves accelerating from a stationary position, gradually increasing speed close to the station, and then achieving traveling speed while requiring traction power. The second event is a train arrival event, which includes decelerating from traveling speed to a stationary position and dissipating the energy generated by regenerative braking. The third event pertains to a lack of traffic, meaning there are no trains present. This creates a highly idealized power demand profile. It does not capture any potential deviations that would be expected between train journeys in normal rail operation (e.g. differences in vehicle weight due to passenger numbers or driver behavior may alter power demands). Neither is any potential overlap of train arrival and train departure events considered (which should not occur if the public train schedule is strictly adhered to).

To support variable power demands, a V2G network must be able to adjust dynamically and be resilient. The 24-hour power demand model used in this discussion involves 117 train departures (Fig. 3.3), with 15% of the day requiring traction power for acceleration, and 6% of the day where regenerative braking could generate power. During the remaining 18.9 hours, there is no rail traffic, allowing

EVs on the V2G network to charge freely. Each train departure uses about 46 MJ or 12.7 kWh of energy, resulting in a total of 5382 MJ or 1486 kWh of energy consumed over 24 hours. Similarly, each arrival generates about 35 MJ or 9.7 kWh of energy, adding up to 4095 MJ or 1135 kWh per day.

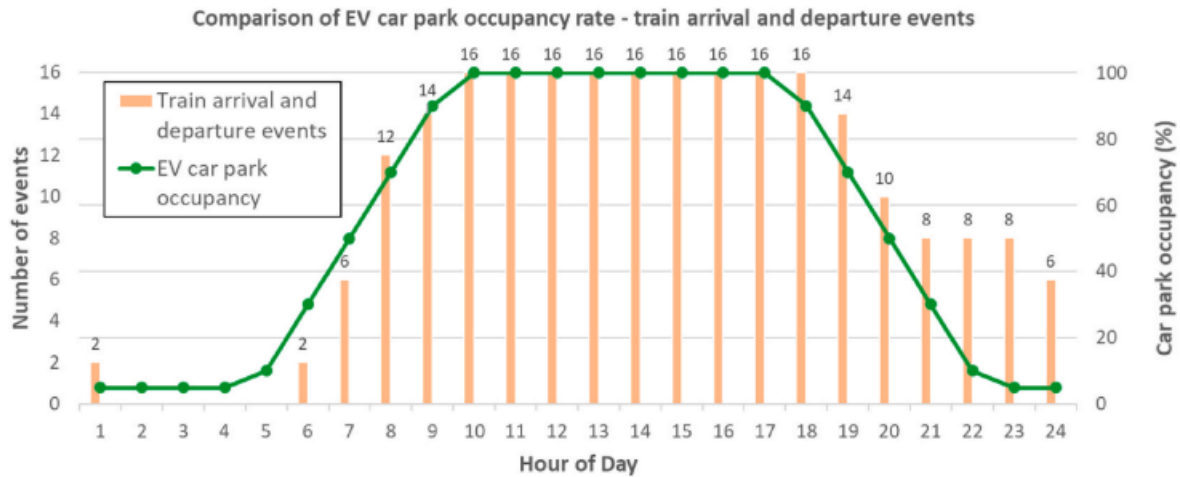


Figure 3.3: Assumed car park occupancy rate and number of train arrival/departure events over 24 simulation period [2]

The proposed system represents the EV population as a group of stationary electric vehicles located in the same parking lot. Each EV in this group is assumed to be connected to a bi-directional charger, and it is assumed that all connected EVs are participating in V2G operation. The analysis only considers the parking spaces equipped with chargers in the car park, with the train station assuming that 75, 100, or 150 of these spaces have EV chargers, respectively. The occupancy rate of the car park varies over the simulation period, with 0% occupancy representing no connected EVs and 100% occupancy indicating that all available EV chargers are being used by V2G enabled EVs. The occupancy rate during the 24-hour simulation period is presented in Figure 3.3. The assumption is made that the car park at a train station will be utilized in a similar manner. To obtain a complete 24-hour occupancy rate for the car park, additional assumptions were necessary. It was assumed that the occupancy rate during nighttime would be low at 5%, while during daytime, from the morning ramp up to the evening decline, it would be very high at 100%. The graph in Figure 3.3 indicates that times of heavy car park usage typically overlap with frequent rail traffic. The EV population follows the assumed car park occupancy rate in Fig. 3.3 by adding EVs to the network (i.e. initiating new instances of the EV simulator) until the assumed occupancy rate is reached or by removing EVs from the network whenever the occupancy rate is exceeded.

In this study, V2G aggregation assumes that all electric vehicles are connected to the same type of bi-directional EV chargers. The V2G network is assumed to share the same substation as the rail system and use its power grid connection (as depicted in Figure 3.1). The network aims to maintain a constant power flow from this

substation, which is restricted by the grid connection limit. If the EV population cannot provide enough traction power to the rail system, the power flow from the substation may surpass the grid connection limit to compensate for the shortage. If there is insufficient power absorption from the regenerative braking of trains, any excess power is assumed to be lost through heat dissipation instead of being supplied to the grid. In both cases, the railway service remains unaffected. As previously mentioned, the significant difference between the power requirements of trains (measured in megawatts) and electric vehicles (in kilowatts) means that high-power AC EV chargers or large AC EV charging infrastructures with multiple low-power chargers are the most suitable options for integration. In this regard, a parking lot with over 500 parking spaces is considered for integration, with 150 of those spaces equipped with AC EV chargers. The management of converters depends on various factors, including the aggregator management system, the number of available electric vehicles, the maximum charging/discharging power, and the state of charge of the EVs.

### 3.3 Energy management system

The proposed electric vehicle (EV) parking lot is designed to allow the connected EVs to discharge into the rail system as electric trains speed up, resulting in a rise in power demand for traction and a reduction in the load on the nearby substation. Conversely, when arriving trains decelerate using regenerative braking, there is a spike in power from the rail system that can be fed into the EV parking lot. However, the EV parking lot cannot fully supply the power demand from the trains, particularly during the early morning and evening periods. Therefore, a Hybrid Energy Storage System (HESS) is used to manage the power demand from the grid. To effectively manage the energy exchange, the power demand profile is separated into three distinct events: 1) train departure event, which requires traction power for acceleration from standstill, slow speed movement close to the station, and then to travelling speed, 2) train arrival event, which involves the dissipation of energy from regenerative braking during deceleration from travelling speed to standstill, and 3) no traffic, where there is no departure or arrival event occurring.

The EV parking lot is assumed to utilize the same substation and share its power grid connection as the train system (see Fig. 3.4). It makes an effort to maintain the grid connection limit, or the power flow from this substation, at a steady level (a soft constraint rather than a true limit, defined by the proportion of the available power to be managed by the EV parking lot).

**Charge Weighting (CW):** An unsigned float value measuring how well the electric vehicle (EV) is suited to receive power (the greater the value, the more likely it will be used for charging). When SOC reaches 100%, value is zero and an EV can no longer be charged. created using database calculations and other inputs.

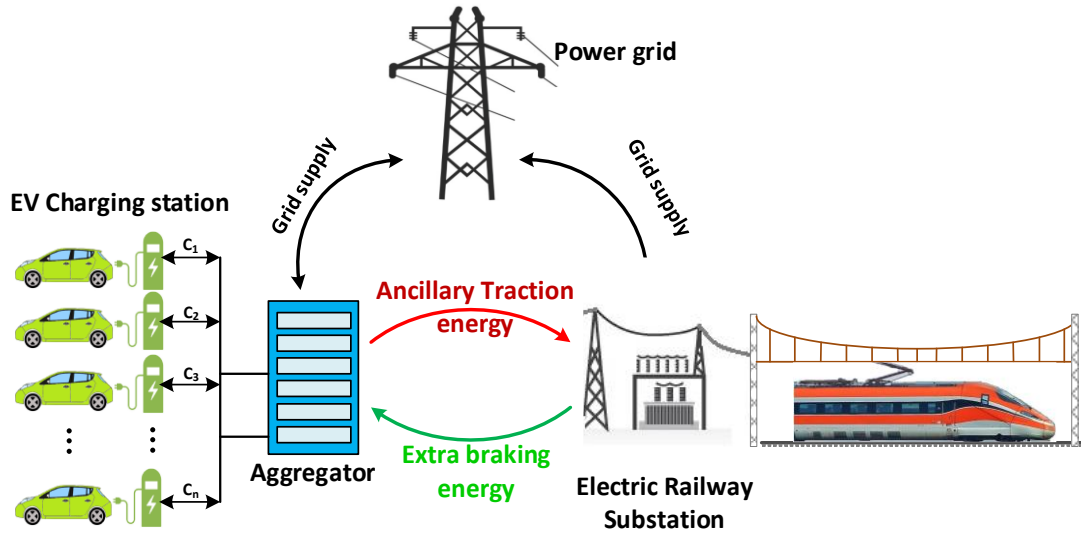


Figure 3.4: Proposed integration system in park & ride area.

Discharge Weighting (DCW): An unsigned float value indicating how well-suited the EV is to provide power (the higher the value, the higher the chance of this EV to be allocated to discharging). Value is 0 when SOC is zero, making it unable to discharge an EV any further. created using database calculations and other inputs.

In order to calculate the DCW and CW index it is necessary to calculate state of charge (SOC) of every battery of EV parking lot and HESS.

The mathematical model of state of charge for every EV, battery and supercapacitor are as follows: The state of charge (SOC) of them are shown in Equations (7-9). SOC represents the ratio of energy store to capacity of EV, Battery and supercapacitor.

$$S_{EV}^t = S_{EV}^1 + \frac{\sum_{t=1}^T P_{EVcha}^t \cdot \eta_{EV} \cdot C_{EV}^t \cdot t - \sum_{t=1}^T \frac{P_{EVdis}^t}{\eta_{EV}} \cdot D_{EV}^t \cdot t}{E_{EV}} \quad (7)$$

$$S_{Bat}^t = S_{Bat}^1 + \frac{\sum_{t=1}^T P_{Batcha}^t \cdot \eta_{Bat} \cdot C_{Bat}^t \cdot t - \sum_{t=1}^T \frac{P_{Batdis}^t}{\eta_{Bat}} \cdot D_{Bat}^t \cdot t}{E_{EV}} \quad (8)$$

$$S_{SC}^t = S_{SC}^1 + \frac{\sum_{t=1}^T P_{SCcha}^t \cdot \eta_{SC} \cdot C_{SC}^t \cdot t - \sum_{t=1}^T \frac{P_{SCdis}^t}{\eta_{SC}} \cdot D_{SC}^t \cdot t}{E_{SC}} \quad (9)$$

In Equations (7)-(9),  $t$  is the duration of charging or discharging,  $S_{EV}^t$ ,  $S_{Bat}^t$ ,  $S_{SC}^t$  are the SOC of EV, Battery and supercapacitor, respectively.  $S_{EV}^1$ ,  $S_{Bat}^1$ ,  $S_{SC}^1$  are the initial values of the state of the charge SOC of EV, Battery and supercapacitor, respectively. The  $C_{EV}^t$  and  $D_{EV}^t$  are the charging and discharging state of EV, respectively. Similarity,  $C_{Bat}^t$ ,  $D_{Bat}^t$  and  $C_{SC}^t$ ,  $D_{SC}^t$  are charging and discharging state of Battery and supercapacitor.  $P_{EVcha}^t$  and  $P_{EVdis}^t$  are the charging and discharging power of EV and  $P_{Batcha}^t$ ,  $P_{Batdis}^t$  and  $P_{SCcha}^t$ ,  $P_{SCdis}^t$  are the charging and discharging power of battery and supercapacitor, respectively. When they start to work, charging will increase their stored power, and discharging will reduce their stored power. However, there

is only one charging and discharging state at the same time, so  $C_{EV}^t$ ,  $C_{Bat}^t$ ,  $C_{SC}^t$  and  $D_{EV}^t$ ,  $D_{Bat}^t$ ,  $D_{SC}^t$  are introduced to represent the charging and discharging state of the EV, battery and supercapacitors, respectively, and their values can be 0 or 1, and they cannot be 1 at the same time. When  $C_{EV}^t$ ,  $C_{Bat}^t$ ,  $C_{SC}^t$  is 1, the first part of the equation represents the increment of electricity at time t. When  $D_{Bat}^t$ ,  $D_{Bat}^t$ ,  $D_{SC}^t$  is 1, the second part of the equation represents the decrease of electricity at time t. Therefore, by adding all the charging and discharging electricity before time t, we can get the variation value of the electricity stored in the EV or battery or supercapacitor from the initial time.

Equations (10) - (15) demonstrate the EV, battery and supercapacitors' charging and discharging efficiencies, respectively.

$$\eta_{EVchar} = \eta_{EVchar}^{ess} \cdot \eta_{DC/DC} \cdot \eta_{DC/AC} \quad (10)$$

$$\eta_{EVdis} = \eta_{EVdis}^{ess} \cdot \eta_{DC/DC} \cdot \eta_{DC/AC} \quad (11)$$

$$\eta_{Batchar} = \eta_{Batchar}^{ess} \cdot \eta_{DC/DC} \cdot \eta_{DC/AC} \quad (12)$$

$$\eta_{Batdis} = \eta_{Batdis}^{ess} \cdot \eta_{DC/DC} \cdot \eta_{DC/AC} \quad (13)$$

$$\eta_{SCchar} = \eta_{SCchar}^{ess} \cdot \eta_{DC/DC} \cdot \eta_{DC/AC} \quad (14)$$

$$\eta_{SCdis} = \eta_{SCdis}^{ess} \cdot \eta_{DC/DC} \cdot \eta_{DC/AC} \quad (15)$$

The charging and discharging efficiencies of EV, battery and supercapacitors themselves are represented in Equations (10)-(15) by  $\eta_{EVchar}$ ,  $\eta_{Batchar}$ ,  $\eta_{SCchar}$  and  $\eta_{EVdis}$ ,  $\eta_{Batdis}$ ,  $\eta_{SCdis}$  respectively. Efficiency of a DC/DC converter is expressed as  $\eta_{DC/DC}$  and that of a DC/AC converter as  $\eta_{DC/AC}$ .

The aggregator gives EVs with a large battery capacity, a high maximum discharging rate, and a high SOC priority during train departure events (when EVs are discharged to generate traction power) (each parameter is weighted equally in the scoring system). Such EVs are advantageous for train departures since they can supply a sizable amount of energy quickly (compared to the EV population as a whole). Similar to this, EVs with high capacity, high maximum charging rate (at the moment), and low SOC are prioritized when it comes to train arrivals (where EVs are charged to absorb power from regenerative braking on the rail system). These EVs have a high rate of electric energy absorption (relative to the EV population). Every EV is taken for granted to be capable of charging or discharging without any hardware or software limitations.

When the SOC of every EV, battery and supercapacitor are calculated, the underlying functions used to evaluate the dimensionless CW and DCW scores are highly dependent on the specific application. Generally, in situations when power

has to be fed into the car park, EVs are particularly useful to the aggregator if their battery pack SOC is low, their battery pack capacity is high and their current maximum charging rate is high. Similarly, when power has to be supplied by the car park, EVs are particularly useful if their battery pack SOC is high, their battery pack capacity is high and their current maximum discharging rate is high. Hence, for the scope of this paper we can define:

$$CW=(1-SOC)*\frac{Capacity}{Base\ Capacity}*\frac{Max\ Charging\ Rate}{Base\ Power\ Rating} \quad (16)$$

$$DCW=SOC*\frac{Capacity}{Base\ Capacity}*\frac{Max\ Discharging\ Rate}{Base\ Power\ Rating} \quad (17)$$

Base Capacity and Base Power Rating are chosen to be 1 kWh and 1 kW respectively.

The EV population can use the shared grid link to draw electricity during times when there is no rail traffic, maintaining a constant power flow from the system. The EV population uses the shared grid connection for smart charging when there is no train activity. Each EV receives a minimum power ( $P_{min}$ ) plus a share of the remaining power ( $P_{Rm}$ ) according to its ranking.

$$P_{Rm}=P_{Gr} - \sum_{i=1}^n P_{min} \quad (18)$$

$$P_{Sh}=\frac{P_{Rm}}{\sum_{i=1}^n CW_i} \quad (19)$$

$P_{Sh}$  is the share power which is allocated to every EV based on its rank. The rank of every EV is evaluated with equation 10. Power demand ( $P_{Dem}$ ) of every EV is calculated based on the equation (14). If the Power demand would be greater than max charging rate of EV, the Power demand is equal to maximum charging rate otherwise, EV absorb power corresponding to the its Power demand and the extra power is stored in battery and supercapacitor.

$$P_{Dem}=CW_i*P_{Sh} \quad (20)$$

The battery pack SOC at the time determines the maximum charging rate for each EV. The expected link between the maximum charging rate and SOC is depicted in Fig. 3.5 So, regardless of the battery pack SOC, it is reasonable to assume that the battery pack can be depleted at least at this pace. Any of the bi-directional EV chargers' estimated charging/discharging limits are exceeded by this discharging rate.

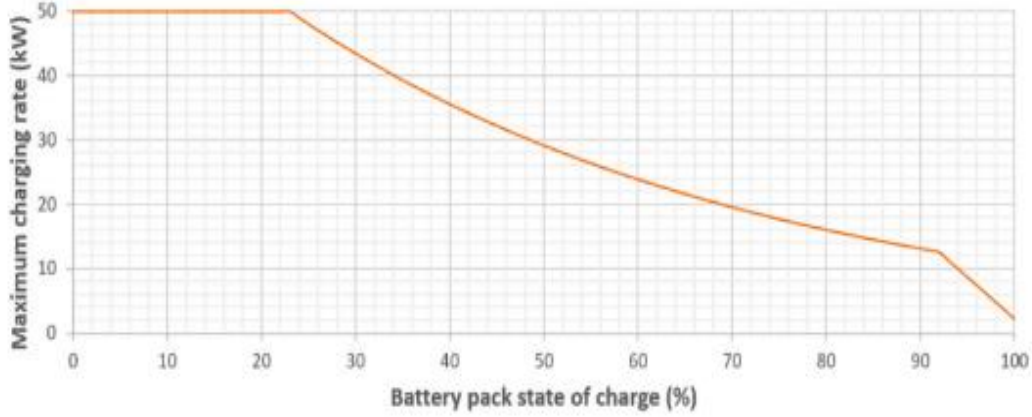


Figure 3.5 Assumed maximum charging rate against SOC for simulated EV population.

For train departure events the aggregator switches grid connection power from EVs to train. Then aggregator for supplying the traction power, priorities EVs with high battery capacity, high maximum discharging rate and high SOC (each parameter is weighted equally in the scoring system). Such EVs are useful for train departures as they can provide a relatively large quantity of energy relatively quickly (compared to the EV population as a whole). Finally, if the power store in the EV parking lot cannot supply the traction power HESS which is consist of supercapacitor and battery is in charge of covering the remain traction power. When the discharging power of the supercapacitors cannot match the system load power, the battery is started to discharge energy. If the equation (21) during whole acceleration event would be true, the aggregator does not demand power from the grid. The main objective is to minimize the power demand from the grid network. Therefore, if aggregate meet the equation (21), we achieve our aim. However, if during part of the acceleration event equation (21) would not be true, the remain power must be demand from the grid and this situation is not satisfactory.

$$P_{Grid\ connection}^t + P_{EVs}^t + P_{Badis}^t + P_{SCdis}^t \geq P_{train}^t \quad (21)$$

In equations of (22) - (24) constraints conditions for EV, battery and supercapacitore are explained to avoid occurrence of overcharging or over discharging. Also, they charging or discharging power range and the restrictions that they can only be charged or discharged at time t are also included in the calculations.

$$\left\{ \begin{array}{l} S_{EV}^{min} \leq S_{EV}^t \leq S_{EV}^{max} \\ S_{EV}^1 = S_{EV}^T \\ 0 \leq C_{EV}^t + D_{EV}^t \leq 1 \\ C_{EV}^t \in \{0,1\} \\ D_{EV}^t \in \{0,1\} \\ 0 \leq P_{EVcha}^t \leq P_{EVcha}^{max} \\ 0 \leq P_{EVdis}^t \leq P_{EVdis}^{max} \end{array} \right. \quad (22)$$

$$\left\{ \begin{array}{l} S_{Bat}^{min} \leq S_{Bat}^t \leq S_{Bat}^{max} \\ S_{Bat}^1 = S_{Bat}^T \\ 0 \leq C_{Bat}^t + D_{Bat}^t \leq 1 \\ C_{Bat}^t \in \{0,1\} \\ D_{Bat}^t \in \{0,1\} \\ 0 \leq P_{Batcha}^t \leq P_{Batcha}^{max} \\ 0 \leq P_{Batdis}^t \leq P_{Batdis}^{max} \end{array} \right. \quad (23)$$

$$\left\{ \begin{array}{l} S_{SC}^{min} \leq S_{SC}^t \leq S_{SC}^{max} \\ S_{SC}^1 = S_{SC}^T \\ 0 \leq C_{SC}^t + D_{SC}^t \leq 1 \\ C_{SC}^t \in \{0,1\} \\ D_{SC}^t \in \{0,1\} \\ 0 \leq P_{SCcha}^t \leq P_{SCcha}^{max} \\ 0 \leq P_{SCdis}^t \leq P_{SCdis}^{max} \end{array} \right. \quad (24)$$

On the other hand, during the braking event aggregator confront with two energy source, first grid connection power and regenerative braking power. In order to manage these two energy source, firstly aggregator share grid connection power between EVs. Based on the proposed algorithm EVs with high capacity, high maximum charging rate (at the time) and low SOC are prioritized. These EVs can quickly absorb a lot of electric energy (relative to the EV population). Then, if whole grid connection power is shared between EVs and still there is vacant space in the battery of EVs (based on the charging capacity figure 3.5), regenerative braking energy fill the vacant space of the EVs battery to charge the EVs with maximum rate. After that, HESS is in the charging state, and the batteries starts to work first. When the maximum charging power cannot meet the regenerative braking power, the supercapacitors start charging at the same time to absorb the regenerative braking power. The V2G scheduling – the process by which charging/discharging decisions for individual EVs are made – uses the event-based scheduling strategy outlined in figure 3.6.

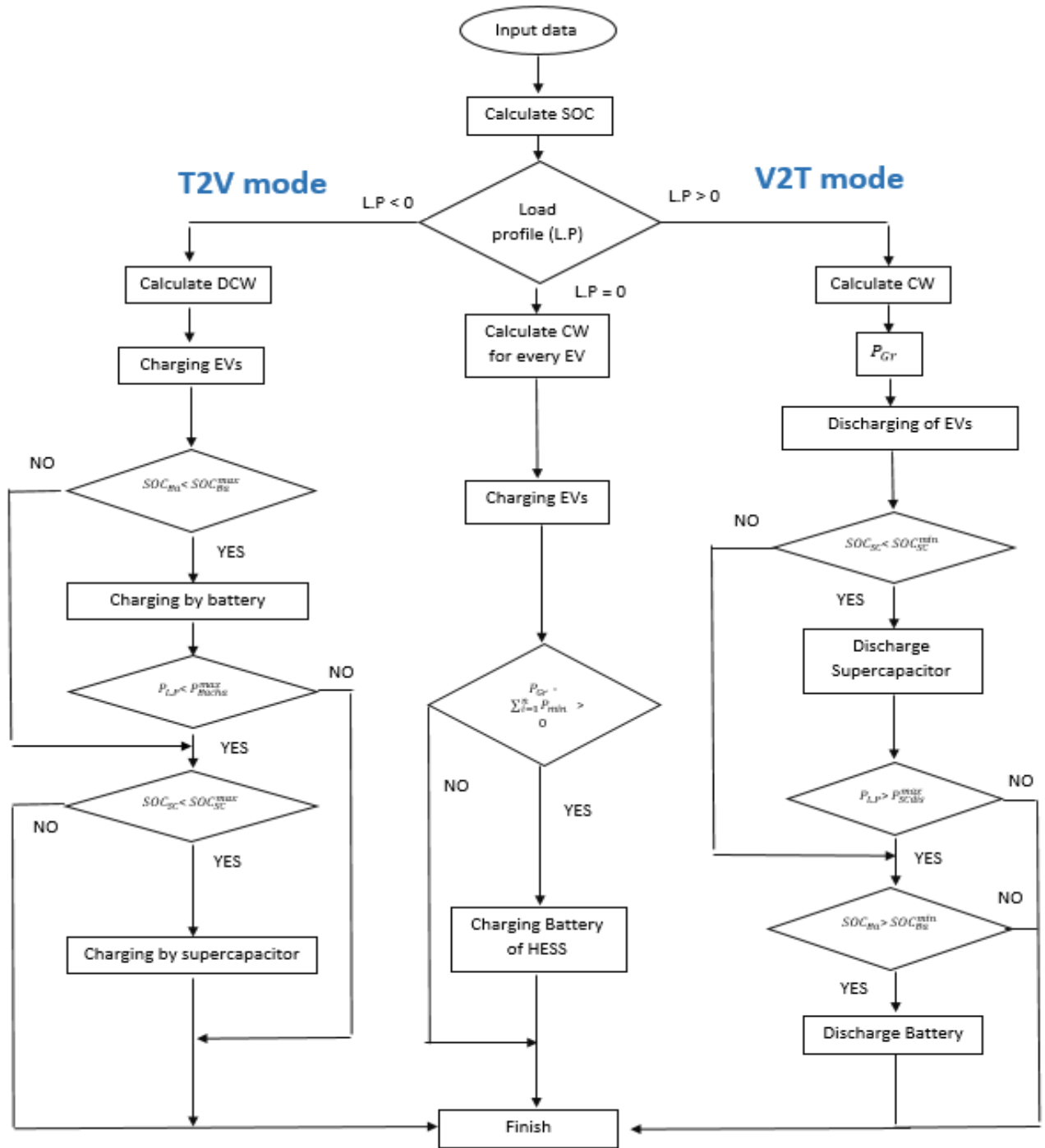


Figure 3.6: Flowchart of the proposed algorithm

### 3.4 Modeling of hybrid energy store system (HESS)

As previously mentioned, the main reason for choosing the charging rate with the rate of 6kW is that EV charging infrastructures (EVCIs) for AC 6 kW for 100 or 150 EVs is more practical in terms of technical issue in comparison with the 20kW charging rate. However, on the other side, this charging rate is not able to support and cover power demand from the grid completely and confine the grid connection

power which absorb by the system from grid. In addition, this system has not capacity to absorb regenerative braking energy completely and The power grid's power quality is impacted by the regenerative braking energy produced by high-speed trains when they brake. The regenerative braking energy possessed by high-speed railways is characterized by its high power and energy levels. Therefore, it is necessary to modify the system (V2G) to acquire the advantages of both systems. Hence, the system with 6 kW charging rate is embedded with hybrid energy storage system (HESS). Using just high power density supercapacitors or high energy density batteries alone is not enough to effectively recover the energy. To address this issue, the study introduces a hybrid energy storage system (HESS) that combines both supercapacitors and lithium-ion batteries, along with an optimized configuration approach to achieve maximum energy recovery.

It is important to note that it is preferable to clarify the simulation's parameters before assessing the report's findings. The parameters are all given based on Table 3.1. The first row relates to the HESS's specifications. There is an ESS that works with traction power and can hold RBE. Table 3.1 lists the technological requirements. Additionally, 0.95 is assumed for the efficiency of the DC-DC and AC-AC converters at the EV parking area. Besides, it is considered that there are 3 different scenarios for charging the EV (20 kW, 6 kW and 6 kW + HESS) and one type of electric vehicle in the EV parking lot (Nissan Leaf). The technical specifications for EVs are given in Table 3.1. In addition, the parameters of the load profile and the corresponding power demand curve is shown in the Table 3.1.

Table 3.1: Parameters of the proposed system

	Parameters	Value
HESS	Battery charging rate	55*6 kW - (330 kW)
	Battery Capacity	12*55 kWh - (2376000 kJ)
	Supercapacitor charging rate	100 kW
	Supercapacitor capacity	4000 kJ
Load profile	Nominal traction power of train	1009 kW
	Nominal Braking Power of Train	1109 kW
EV Station	DC fast Charging rate	20 kW
	EV battery capacity	40 kWh
	AC charging rate	6 kW

### 3.5 Simulation and result

The scheduling method distinguishes between "in-event" periods and non-event periods, or times when electricity is transferred between the EV population and the train system. The aggregator distributes EVs sequentially to charge/discharge at the highest pace possible throughout events, doing so until the power drawn from the substation reaches the predetermined grid connection limit. The size of the EV population, the global charging rate limit (the maximum charging/discharging rates per EV as supported by the aggregator), and the anticipated grid connection limit all have a significant impact on how much the V2G network can decouple the power requirements of the rail system from the grid connection.

Before evaluating these parameters, considering the condition of the network such as DC or AC charging and rate of the charging is necessary. Therefore, this research considers three network with different condition which is consist of a) DC 20 kW, b) AC 6 kW and c) AC 6 kW embedded with HESS.

#### 3.5.1 Charging rate 20 kW

DC 20 kW:

V2G application was proposed in which aggregated parked EVs are charged and discharged to support nearby DC-powered rail systems. Three main factors determining the performance of such a V2G system were identified and examined: the EV population size, the EV charging rates and the power made available to the whole system through the shared power grid connection. Size of EV population: The size of the linked EV population is the primary element affecting the performance of the planned V2G system (i.e. the number of EVs connected). In order to look into this, the 24-hour system functioning was simulated with EV populations of up to 150, 100, and 75 EVs, respectively, with the grid connection limit and the maximum global charging rate per EV remaining constant at 20 kW and 200 kW, respectively.

It should be noted that the time axis is equal 24hour (86400 second). In each of the three scenarios, the potential aggregated power output from the V2G network is depicted in Fig. 3.7. The aggregate potential power output of the system is 20 kW times the number of EVs connected at any given moment because the global discharging limit of 20 kW is much lower than the maximum power output that individual simulated EVs may provide (at no point are any of the EVs entirely discharged). The V2G network is considered capable of fully powering a train departure event (i.e. maximum peak power demand reduction as experienced by the power grid) whenever the power provision potential exceeds the threshold of ~1009 kW (i.e. the peak power demand of the train departure event). As seen in Fig. 3.7, all three scenarios exceed this threshold from ~06:00 to ~19:00 and ~07:00 to ~18:00.

The diagram in Fig. 3.8 demonstrates how the power supply potential of electric vehicles (EVs) can decrease peak power demands experienced by a substation. In Fig. 3.8 (a), the substation's original power demands for train traction power are displayed before taking V2G integration into consideration. As per the rail system model, there are 117 instances of short power demand peaks of approximately 1009 kW due to train departures between periods of no power demand. Fig. 3.8 (b), on the other hand, shows reduced power demand peaks when utilizing a connected V2G network under scenario 2's conditions (selected as the 'middle ground' scenario). It is evident that, except for a minor peak of around 400 kW in the morning (where insufficient EVs were connected to fully support the first train departure), peaks throughout most of the day (before approximately 19:00) were almost entirely eliminated (as a constant 200 kW were utilized for both EV charging and train traction power).

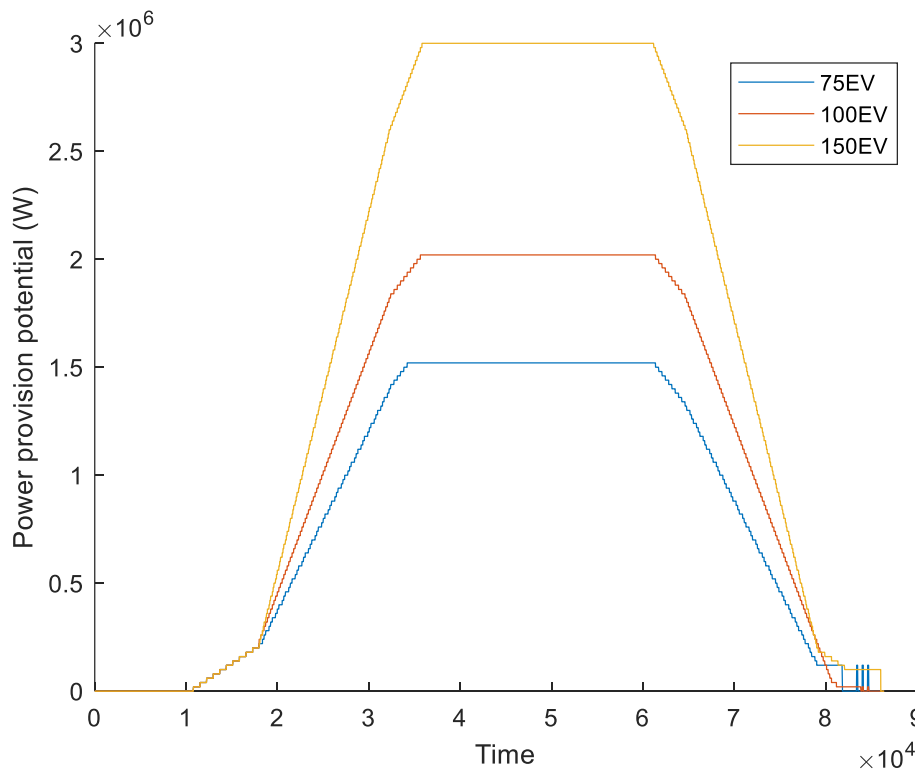


Figure 3.7: Total power provision potential of EV populations of varying size over 24 h (20 kW)

However, in the later hours of the day, the V2G network can no longer entirely support traction power, and peaks increase over time, almost reaching a megawatt (849 kW in the final power peak). This indicates that the proposed system is reliant on a sufficient EV population for peak power reduction. Although a V2G network with an EV population like the one modeled in this research is insufficient to eliminate all power demand peaks, temporary peak reduction is still highly beneficial to the local power grid, reducing the need for other grid balancing measures. In scenario 2 and 3 we evaluate the power draw with 100 and 150 EVs in

parking and is shown in fig. 3.9 and 3.10. based on these figures whatever the number of the EVs increase, the peak demand power would reduce and This is a positive point.

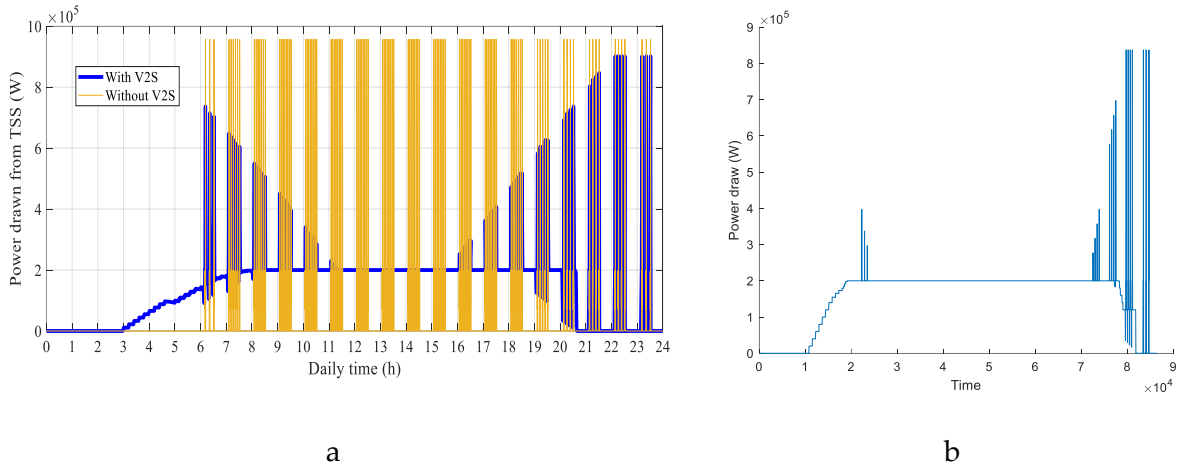


Figure 3.8: (a) Power draw from substation for rail system traction power without connected V2G network over 24 h; (b) Power draw from substation for the rail system and EV population power demands with connected V2G network over 24 h – 75EVs

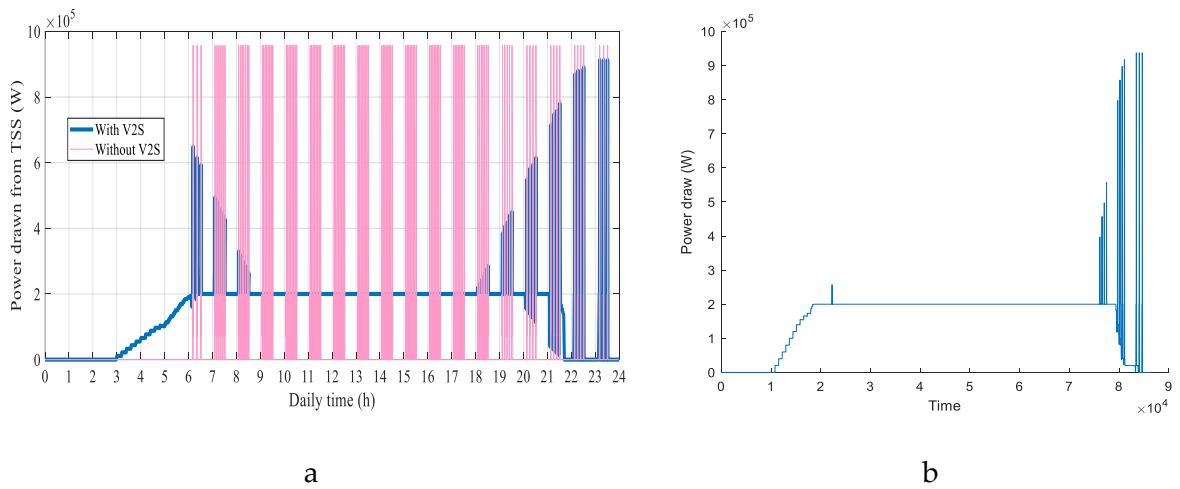


Figure 3.9: (a) Power draw from substation for rail system traction power without connected V2G network over 24 h; (b) Power draw from substation for the rail system and EV population power demands with connected V2G network over 24 h – 100EVs

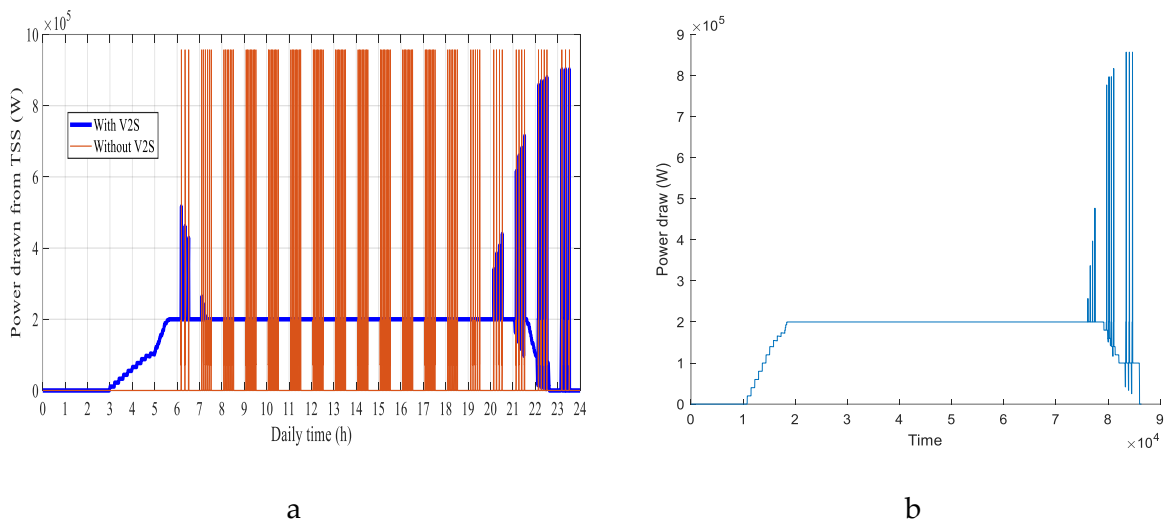


Figure 3.10: (a) Power draw from substation for rail system traction power without connected V2G network over 24 h; (b) Power draw from substation for the rail system and EV population power demands with connected V2G network over 24 h – 150EVs

Fig. 3.11 displays the V2G network's capacity for receiving power over time, which is the sum of all EVs' maximum charging rate at any given moment, limited to the global charging limit of 20 kW. However, the maximum charging power that each EV can receive is determined by its current SOC, as depicted in Fig. 3.5, and may not reach 20 kW, making this different from Fig. 3.7. For the V2G network to be able to fully absorb power from regenerative braking on the rail system, the aggregated power absorption capacity must exceed the threshold of around 1109 kW, which is the peak output of the rail system during a train arrival event. As shown in Fig. 3.11, this threshold is never surpassed in scenario 3 (EV population up to 75 EVs). Only in scenarios 1 and 2 (up to 150 EVs) is the V2G network capable of fully absorbing regenerative braking power for an extended period (from approximately 7:00 to 18:00, encompassing 85 of the 117 train arrivals, around 73%). The other scenarios demonstrate that even when the car park is less fully occupied, a significant contribution can be made to storing regenerated energy.

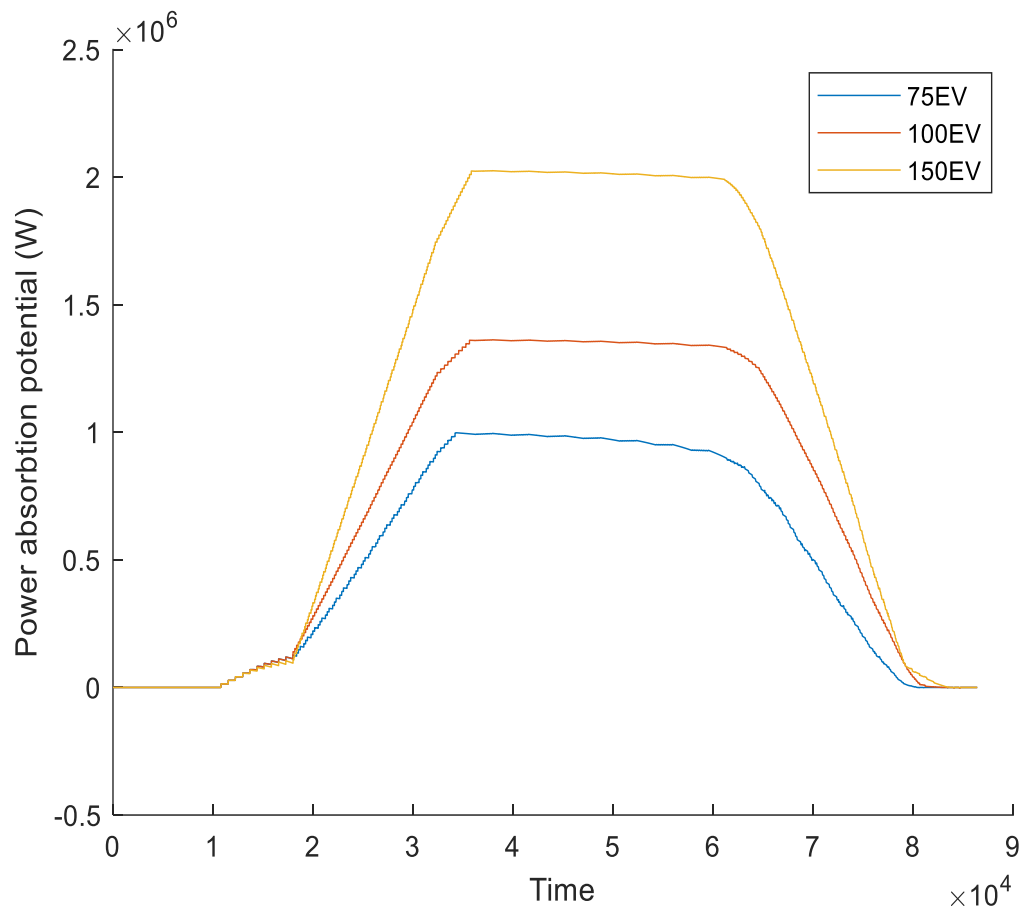


Figure 3.11: Total power absorption potential of EV populations of varying size over 24 h (20kW)

When comparing Figs. 3.7 and 3.11, it's worth noting that if an EV population's power absorption capacity surpasses the threshold needed to fully absorb power from a train's regenerative braking, the power provision potential also surpasses the threshold necessary to fully supply traction power. Additionally, since the regenerative braking threshold is of a greater magnitude than the traction power threshold, and each EV's maximum discharge rate is equal to or greater than its maximum charging rate, any EV population capable of fully absorbing regenerative braking energy from an arrival event is also capable of fully providing traction power for a departure event of the same train in this study. As this study doesn't consider complex scenarios with multiple train arrivals and departures simultaneously, the analysis below will not include the power provision potential of EV populations.

After examining the V2G network's effectiveness in separating the electric rail system from the power grid, it's important to assess its ability to charge individual EVs over time. Fig. 3.12 illustrates how the SOC of the three control EVs evolves in each of the three scenarios (75, 100, and 150 EVs), while Table 3.2 displays the final SOC values for each control EV. In all three scenarios, each control EV significantly increased its SOC. As expected, the SOC gains per EV are higher with lower EV population sizes

because the grid connection limit was fixed at 200 kW for all three scenarios, which limits the amount of power that can be shared between EVs during smart charging periods. Although only the control EVs are depicted, the observed SOC gains are indicative of the behavior of the entire EV population.

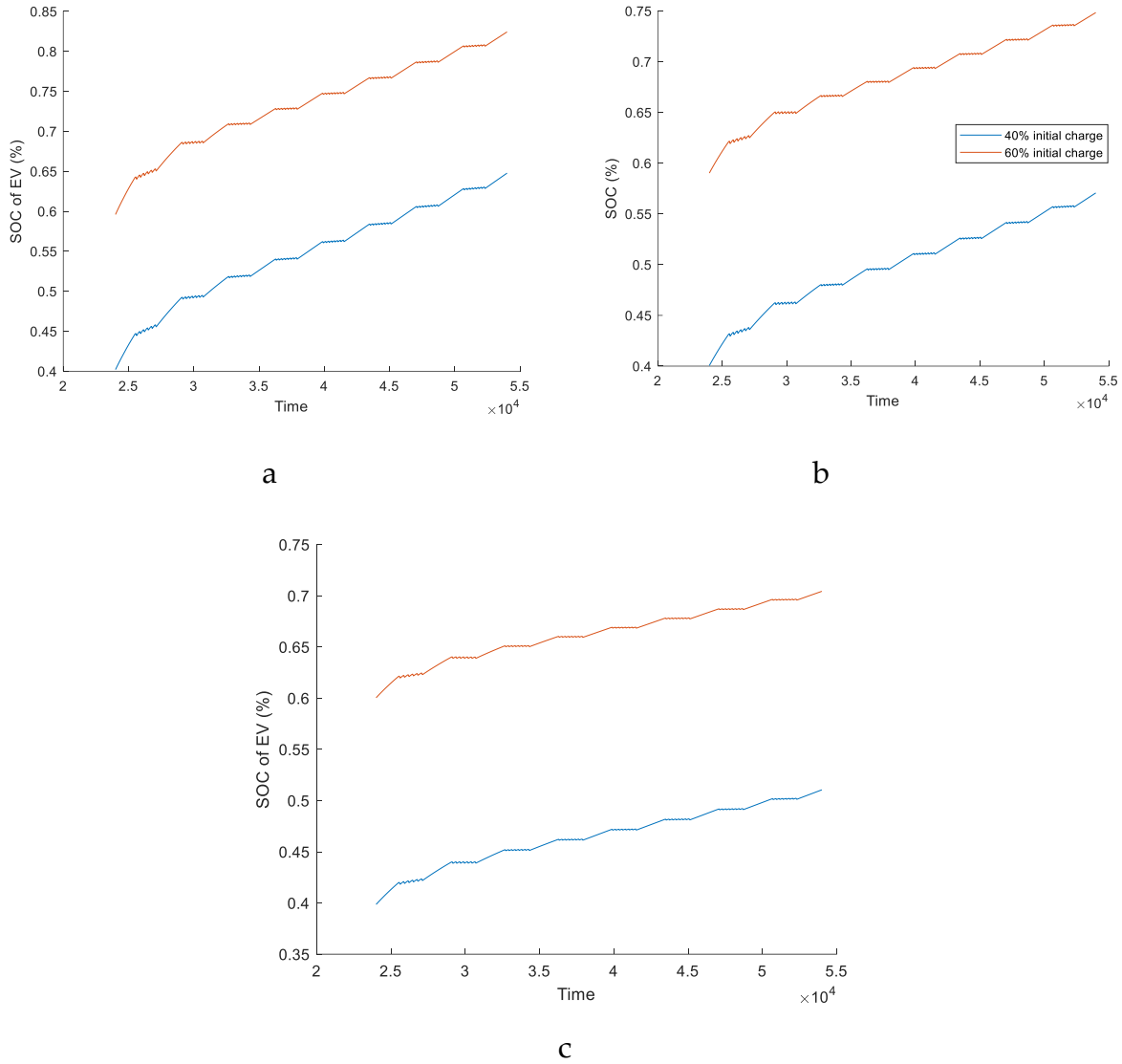


Figure 3.12: changes in SOC over time of three control EVs (20kW)

In this study, the final factor that affects the system's performance is the power that is shared between the electric rail system and EVs via a grid connection. To analyze this, the researchers conducted multiple simulations of 24-hour system operation with different grid connection limits, ranging from 100 to 400. The EV population size remained constant at 75, 100, and 150 EVs for all simulations.

Scenario 1: 100 kW grid connection limit

Scenario 2: 200 kW grid connection limit

Scenario 3: 300 kW grid connection limit

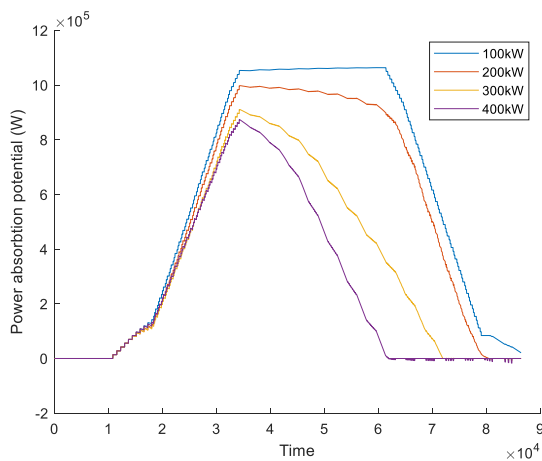
Table 3.2: Comparison of Control EV battery pack SOC at departure time for EV populations of varying sizes (20kW)

Initial charge	75EV	100EV	150EV
40%	64	57	51
60%	82	74	70

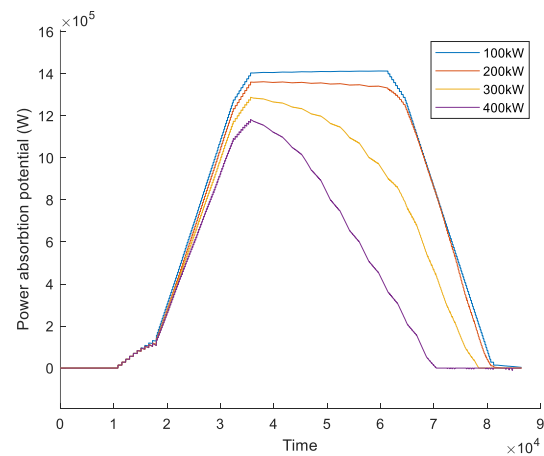
#### Scenario 4: 400 kW grid connection limit

The effect of increasing the grid connection limit on the ability of the EV population to absorb power from the rail system is illustrated in Fig. 3.13. The impact on power absorption potential is more noticeable in the afternoon and evening compared to the early hours of the day. While the power demand of the rail system remains unchanged across scenarios, an increase in the power made available to the system leads to faster gains in SOC for connected EVs due to increased charging rates. However, as shown in Fig. 3.5, the maximum charging rate for individual EVs decreases with SOC. Therefore, the power absorption potential of the EV population decreases not only when some EV batteries are fully charged, but also as they approach higher SOC levels.

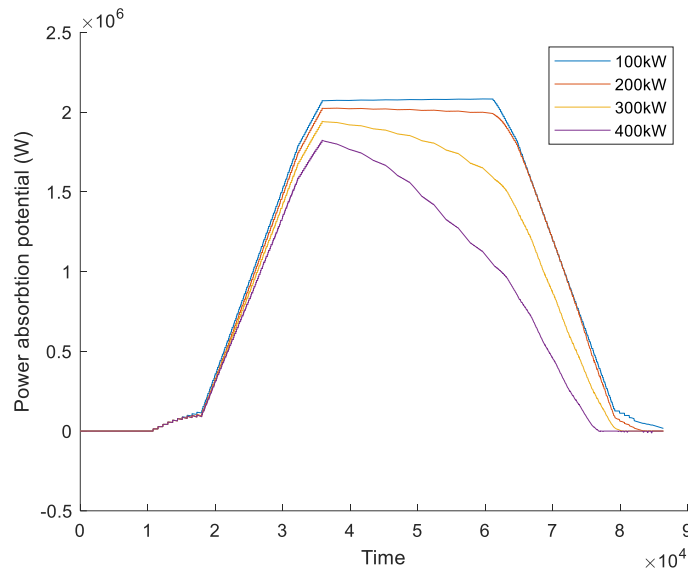
The problems mentioned above are partly due to the simplification of keeping the grid connection limit constant throughout the day. More complex scheduling rules that adjust this parameter to the number of connected EVs may help prevent a decrease in power absorption potential. However, any measures that limit EV charging rates need to be carefully considered, as the V2G network relies heavily on the participation of EV owners and users. Defining acceptable charging rate limitations for EV owners requires consideration of social and behavioral sciences, which is outside the scope of this study.



a



b



C

Figure 3.13: Total power absorption potential at varying grid connection limits over 24 h (20 kW). a)75 b)100 c)150

### 3.5.2 Charging rate 6 kW

As previously mentioned, the implementation of the EV charging infrastructures (EVCIs) for DC 20kW for 100 EV is not easy and not logical. Therefore, we consider the AC 6kW charging because this EVCIs is conventional and in terms of implementation is more practical. In this part the results of the AC 6kW charging EV is evaluated and compare with EVCIs for DC 20kW.

AC 6kW:

The previous section identified that the number of EVs connected is a significant factor affecting the effectiveness of the V2G system. To explore this further, simulations were conducted to observe the system's 24-hour operation with different EV populations of 150, 100, and 75 EVs. The charging rate limit per EV and the grid connection limit remained constant at 6 kW and 200 kW, respectively.

Scenario 1: 75 EVs

Scenario 2: 100 EVs

Scenario 3: 150 EVs

The Fig. 3.14 displays the possible combined power output of the V2G network over time for each of the three situations. Since the maximum power output of any simulated EVs never reaches the global discharging limit of 6 kW, the total potential power output of the system is 6 kW multiplied by the number of connected EVs at any given time. If the system can generate more than ~1009 kW of power, which is the peak power demand of a train departure event, it is deemed capable of

completely powering such an event. However, as shown in Fig. 3.14, the system cannot provide enough power for acceleration in all scenarios, and the grid connection must make up for this power deficit. But if the grid connection power is sum up with power provision potential, the summation of two these source of energy can cover the attraction power. This may lessen the need for investment in sub-station feeds from the grid.

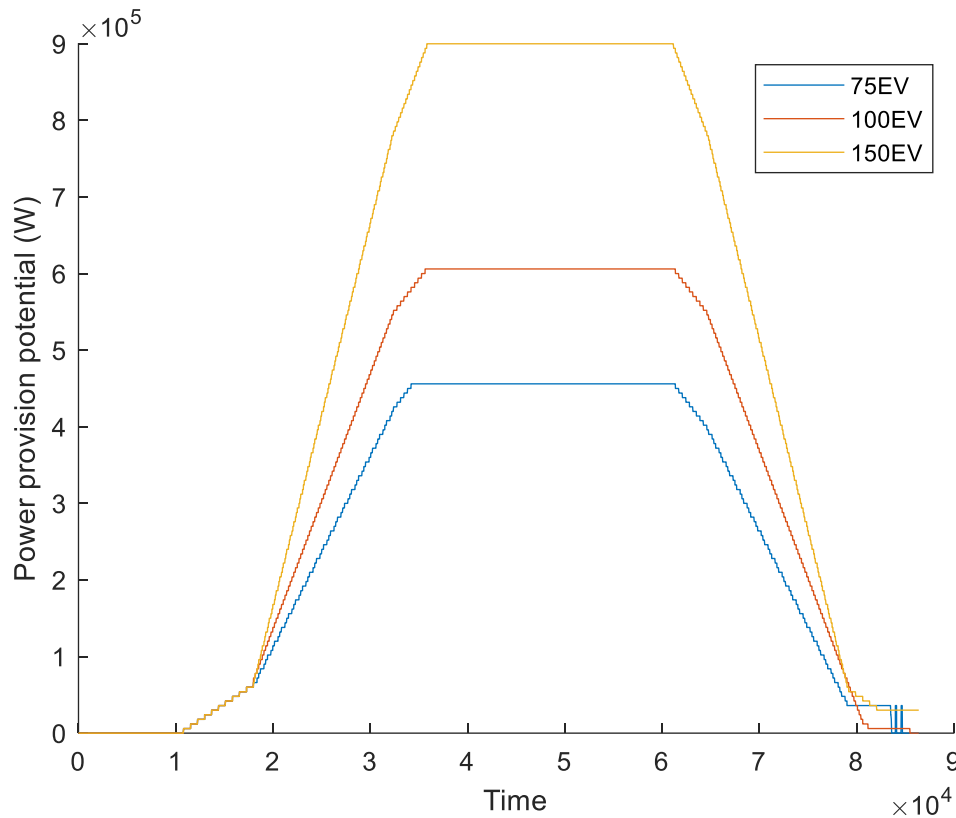


Figure 3.14: Total power provision potential of EV populations of varying size over 24 h (6kW)

Figure 3.15 demonstrates how the power provision potential of the EV population helps to decrease peak power demands experienced by the substation. In Figure 3.15(a), the original power demands required by train traction power are shown, which the substation must provide before considering V2G integration by 75 EVs. According to the rail system model, the substation experiences around 117 short power demand peaks of approximately 1009 kW from train departures, which are interspersed with periods of no power demand. In contrast, Figure 3.15(b) depicts power draw from the grid for 100 EVs. based on the fig 3.15, Scenarios 1 and 2 cannot contain power demand at the grid connection, while in scenario 3, the system can only meet the power demand from 9 mornings up to 18 when not enough EVs were yet connected to fully support the first train departure. This means that with charging rate 6kW the system needs to the at least 150 EVs to cover all power demand from the train without need to make a peak demand on the power grid. Throughout most of the day (before ~19:00), peaks are nearly eliminated and instead,

a constant 200 kW is drawn for both EV charging and train traction power. However, in the later hours of the day, the V2G network cannot fully support traction power, and peaks increase over time until they almost reach a megawatt (~849 kW in the final power peak). This highlights the proposed system's dependence on a sufficient EV population for peak power reduction. Although a V2G network with the modeled EV population cannot eliminate all power demand peaks, temporary peak reduction still greatly benefits the local power grid and reduces the need for other grid balancing measures.

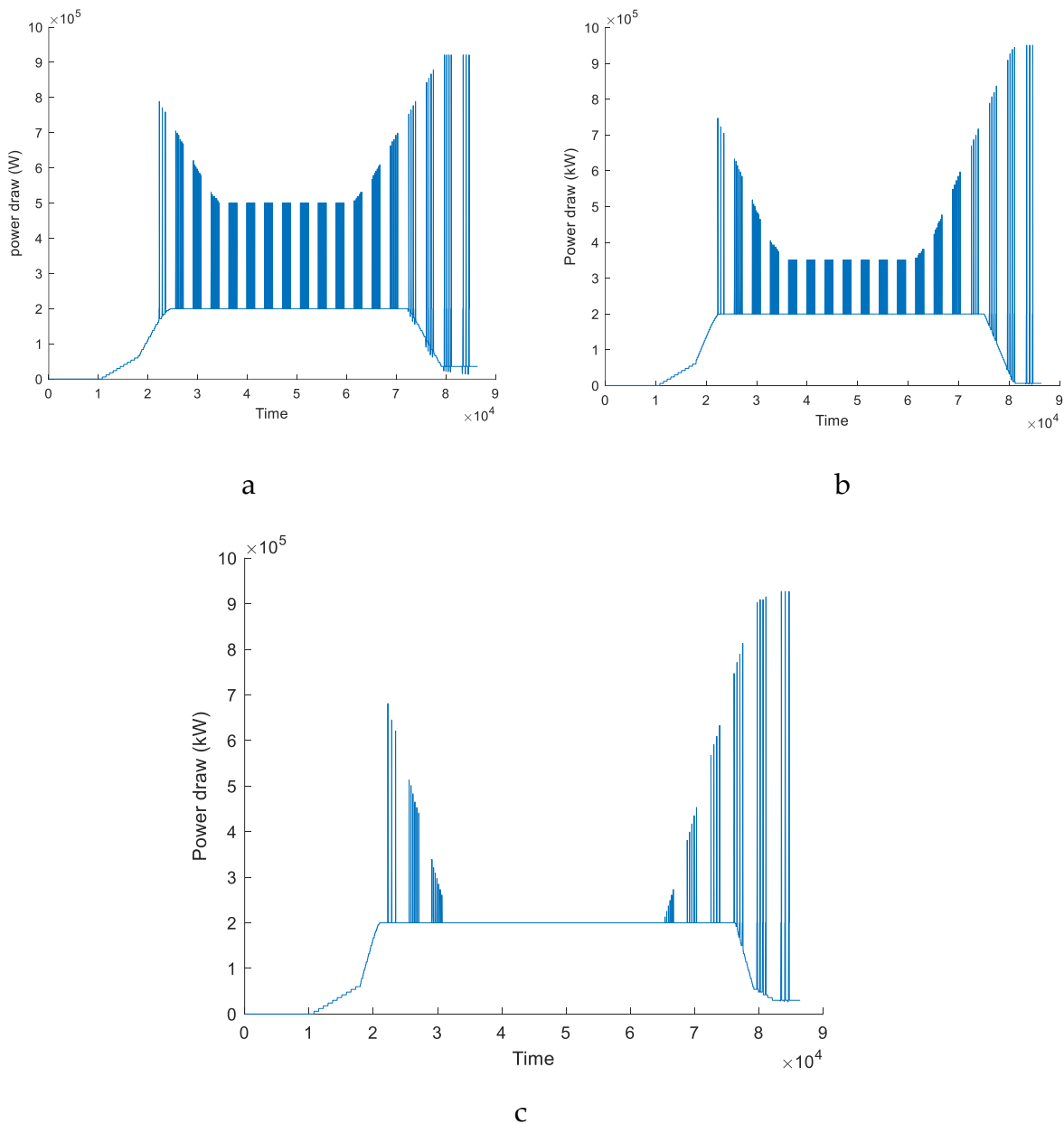


Figure 3.15: Power draw from substation for the rail system and EV population power demands with connected V2G network over 24 h (6kW). a)75 b)100 c)150

The information presented in Figure 3.16 pertains to the potential for the V2G network to receive power over time, which is the sum of the maximum charging rate of all connected EVs at any given time, up to the global charging limit of 6 kW. It should be noted that the maximum charging power for each EV is dependent on its current state of charge (SOC), and may not reach the maximum limit of 6 kW. In order for the V2G network to fully absorb power from the regenerative braking of the rail system, the total power absorption potential must exceed the threshold of approximately 1109 kW, which is the peak output of the rail system during a train arrival event. Figure 3.16 illustrates that this threshold is not reached at any point for three scenarios (75, 100, 150 EVs), and only store major part of the energy. In fig. 3.16 it is not possible to absorb total regenerative power so some contribution of total power is wasted and it is not efficient. Only in scenario 1 (up to 150 EVs) the system can absorb the maximum regenerative power and this rate of the power is around 60% of total regenerative power. In the other scenario the power potential absorption is around 410kW and 300kw for 100 and 75 EVs respectively.

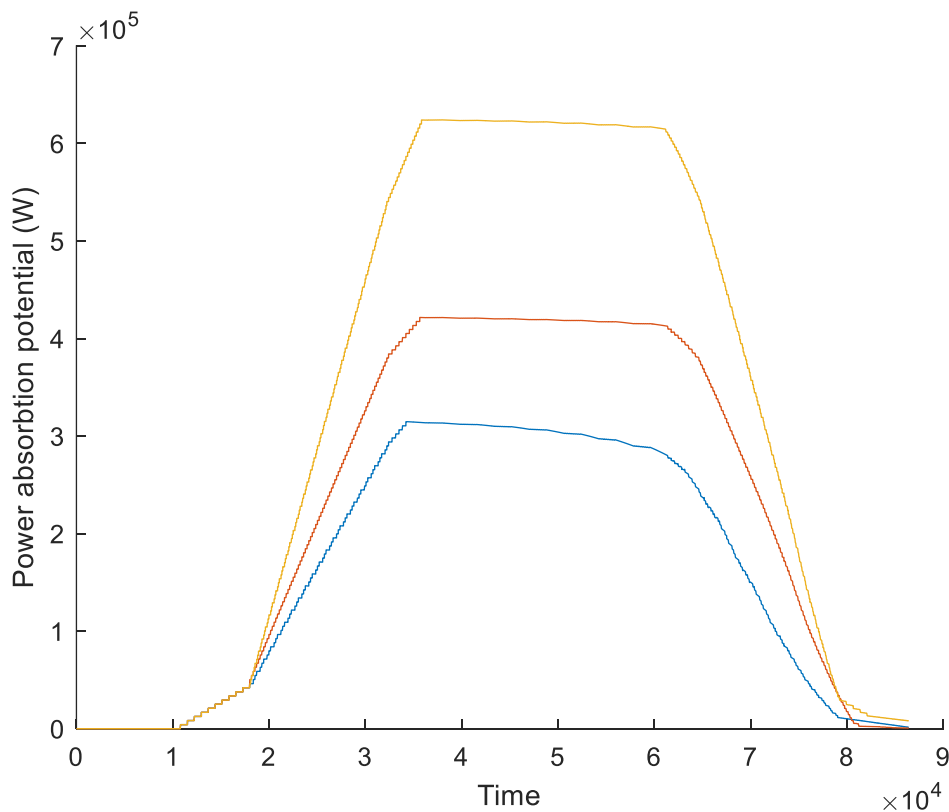


Figure 3.16: Total power absorption potential of EV populations of varying size over 24 h (6kW).

After considering the V2G network's effectiveness in decoupling the electric rail system and the power grid, its ability to charge individual EVs over time needs to be analyzed. Fig. 3.17 shows how the SOC of the three control EVs develops in each of the three scenarios. Table 3.3 shows the final SOC values for each control EV. In any

of the three scenarios, each control EV significantly gained in SOC. As expected, given that the grid connection limit was fixed at 200 kW for all three scenarios (limiting how much power can be shared between EVs during smart charging periods), the SOC gains per EV are higher at lower EV population sizes. While only the control EVs are shown, the observed gain in SOC is indicative of the behavior in the whole EV population.

Table 3.3: Comparison of Control EV battery pack SOC at departure time for EV populations (6kW)

Initial charge	75EV	100EV	150EV
40%	52	51	50
60%	72	70	69

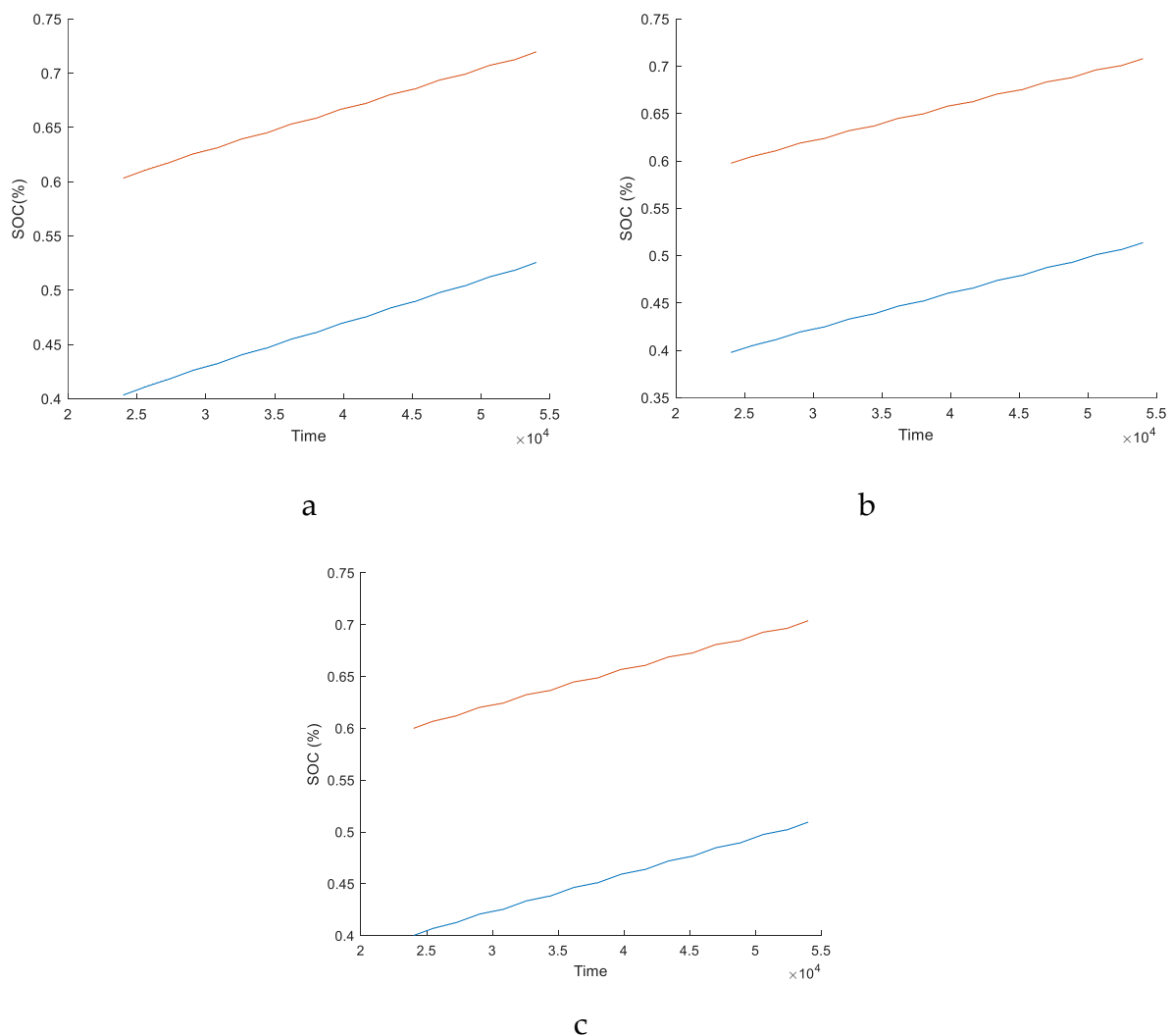


Figure 3.17: Changes in SOC over time of the three control EVs within EV populations of varying size (6kW)

This result is related to the 6kW charging rate. Comparing between charging rate 20kW and 6kW shows that rate of the SOC during the evaluation time is depend on the number of EV and charging rate. Whatever the charging rate decrease, the final SOC would be lower in comparison to the higher charging rate. The other factor that has influence of the SOC is number of the EVs. When the number of the EVs increase, the share power for every EV would decrease and the final situation of the SOC is lower and it take more time for charging.

Another aspect that this study aims to investigate in relation to system performance is the amount of power that can be shared between the entire system (comprising the rail and EVs) via a common grid connection. To achieve this, the system was simulated for 24 hours, with the grid connection limit (which determines the maximum proportion of power that can be supplied from the substation controlled by the V2G network) being varied between 100, 200, 300, and 400 kW in different runs. The number of EVs used in the simulations remained constant at 75, 100 and 150 EVs and the maximum charging limit per EV was set at 6 kW.

Scenario 1: 100 kW grid connection limit

Scenario 2: 200 kW grid connection limit

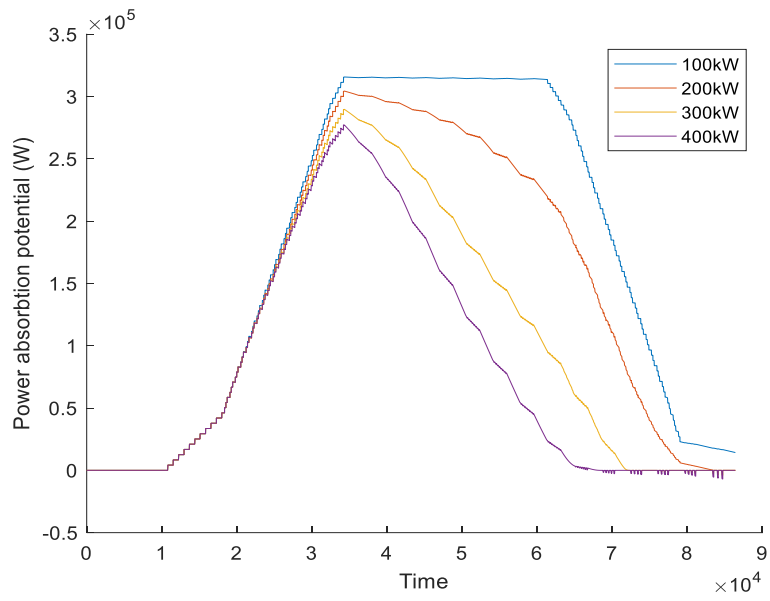
Scenario 3: 300 kW grid connection limit

Scenario 4: 400 kW grid connection limit

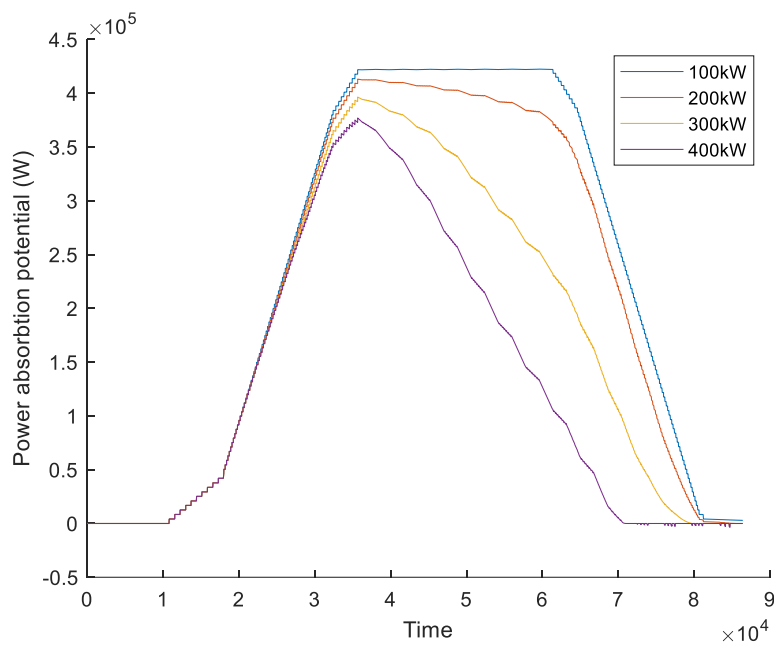
As depicted in Fig. 3.18, raising the grid connection limit significantly reduces the ability of the combined population of EVs to consume power from the rail system.

It is worth mentioning that this effect is more evident in the afternoon and evening hours than in the early hours of the day because the number of the active EV in the park and rid is decreasing. So, the share power would rise and the vacant capacity of any EVs battery decrease dramatically. Therefore, in the evening both the number of the active EVs and vacant capacity would decrease, so the capacity of the absorption regenerative power dramatically decreases and the trend of fig. 3.18 fall down in the evening and night. The other factor which consider is grid connection power has influenced on the capacity of the power absorption. As seen in fig 3.18, whatever the grid connection power increase, the share power increase and the rate of the charging would increase. So batteries of EVs charge more quickly. Therefore, in the evening the vacant of the batteries dramatically decrease and the fig 3.18 had the reducing trend.

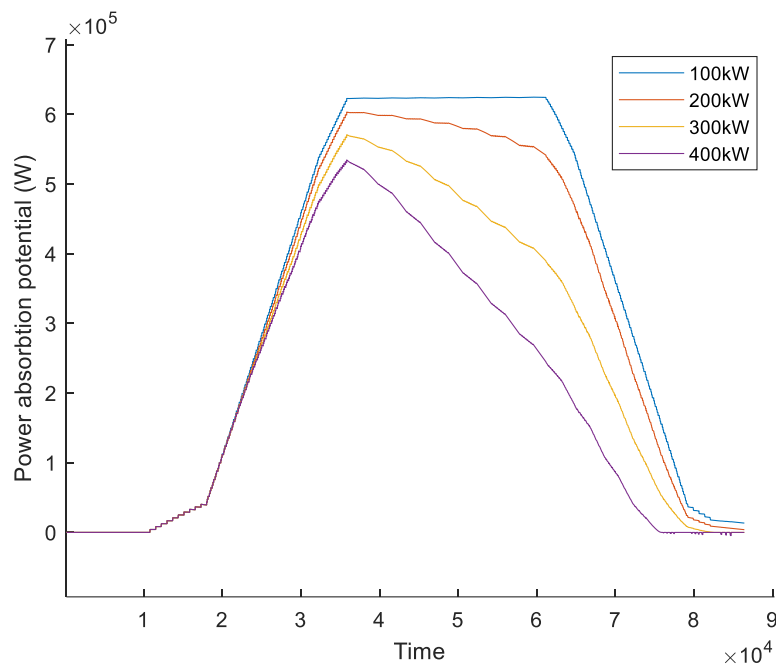
Since the power demand of the rail system remains unchanged across all scenarios, any increase in the power made available to the system results in an increase in the rate at which EVs charge, leading to quicker gains in the SOC of connected EVs. Hence, the ability of the combined population of EVs to absorb power decreases not only when some EV batteries are fully charged, but also as they approach higher SOC levels.



a) 75EVs



b) 100EVs



c) 150EVs

Figure 3.18: Total power absorption potential at varying grid connection limits over 24 h (6kW)

### 3.5.3 Charging rate 6 kW + HESS

AC 6kW embedded with HESS:

Similar to the previous section, the primary factor that affects the performance of the proposed vehicle-to-grid (V2G) system is the size of the connected electric vehicle (EV) population, or the total number of EVs connected to the system. To investigate this, a simulation was conducted using EV populations ranging from 75 up to 150 EVs, while maintaining a constant global charging rate limit per EV and grid connection limit of 6 kW and 200 kW, respectively. Additionally, the system is equipped with a hybrid energy storage system (HESS) to further optimize energy efficiency and absorb more regenerative braking energy.

Scenario 1: 75 EVs

Scenario 2: 100 EVs

Scenario 3: 150 EVs

As the same of the pervious section, fig. 3.19 illustrates the potential power output of the vehicle-to-grid (V2G) network over time in each of the three scenarios. As the global discharging limit is set at 6 kW, which is lower than the maximum possible power output of the simulated EVs (none of the EVs are ever fully discharged), it is necessary to compensate the remain power for the traction power. Therefore, the potential power output of the system is summation of the output of the hybrid energy storage system (HESS) and the output power of the EVs which is equal to the

charging rate of any EV (6 kW) multiplied by the number of connected EVs at any given time. So, these two sources of the power can cover the total traction power for acceleration and in this construction although we employ the lower charging power to implement the EVCI but thanks to the HESS, the traction power is supported and the problem of second structure is solved.

The V2G network is deemed capable of providing enough power to fully power a train departure event (i.e., peak power demand reduction) when the power provision potential exceeds approximately 1009 kW, which is the peak power demand of the train departure event. As shown in Figure 38, in scenarios 1 and 2, the system surpasses this threshold from around 06:00 to 19:00, covering 95 out of 117 daily train departures (approximately 81%), and from around 07:00 to 18:00, covering 85 departures (approximately 73%). Despite using the HESS in scenario 3 to provide more power, the system is unable to supply the total acceleration power required, although it could potentially reduce the investment required in sub-station feeds from the grid.

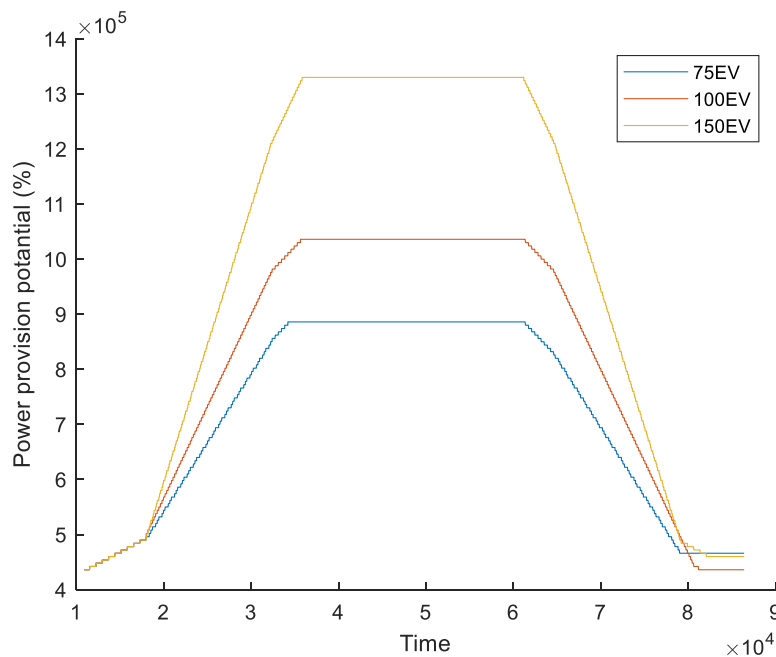
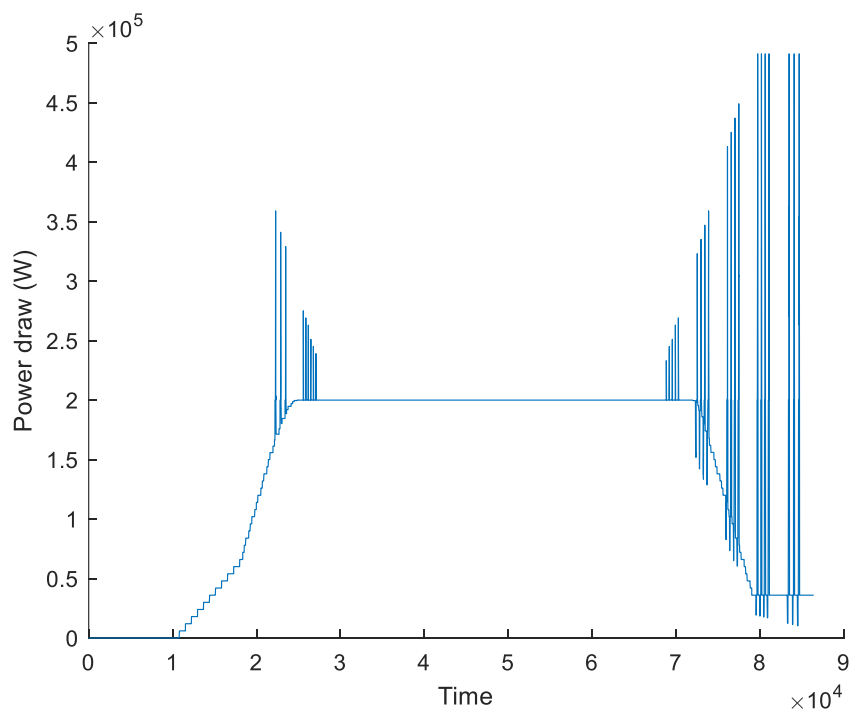


Figure 3.19: Total power provision potential of EV populations of varying size over 24 h with (6kW+HESS)

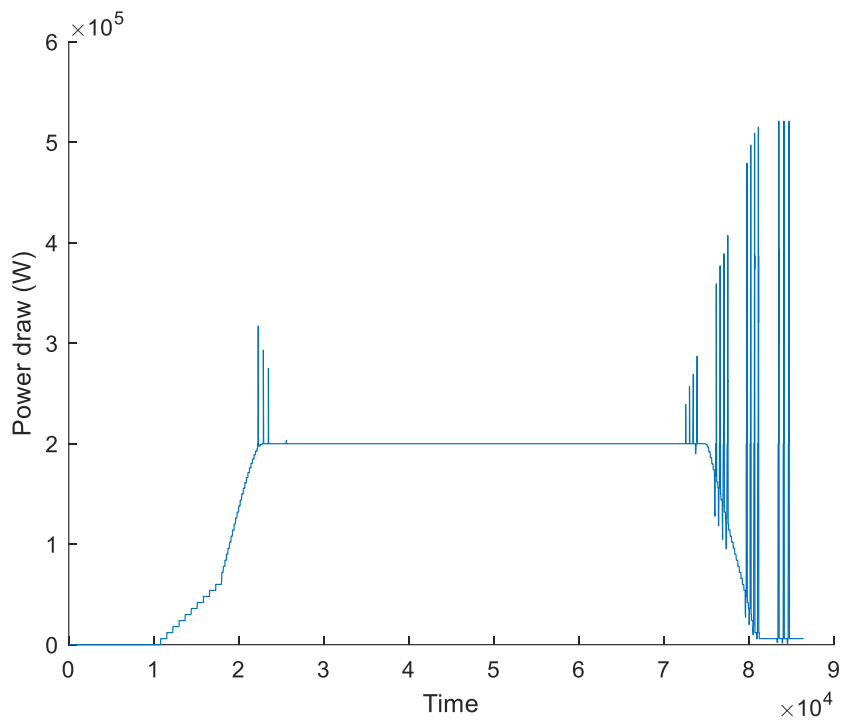
The diagram in Figure 3.20 depicts how the ability of electric vehicles (EVs) to provide power can reduce peak power demands at a substation by the system which compose of EVs battery and the HESS. In comparison with the V2G which 6kW charging rate and is not embedded with HESS, the performance of the EVs + HESS is better.

Unlike the pervious method, the system EVs + HESS in all scenario has the acceptable performance and the power demand from the grid specially in the middle of the day is confined to the grid connection (200kW). Also, thanks to the HESS the

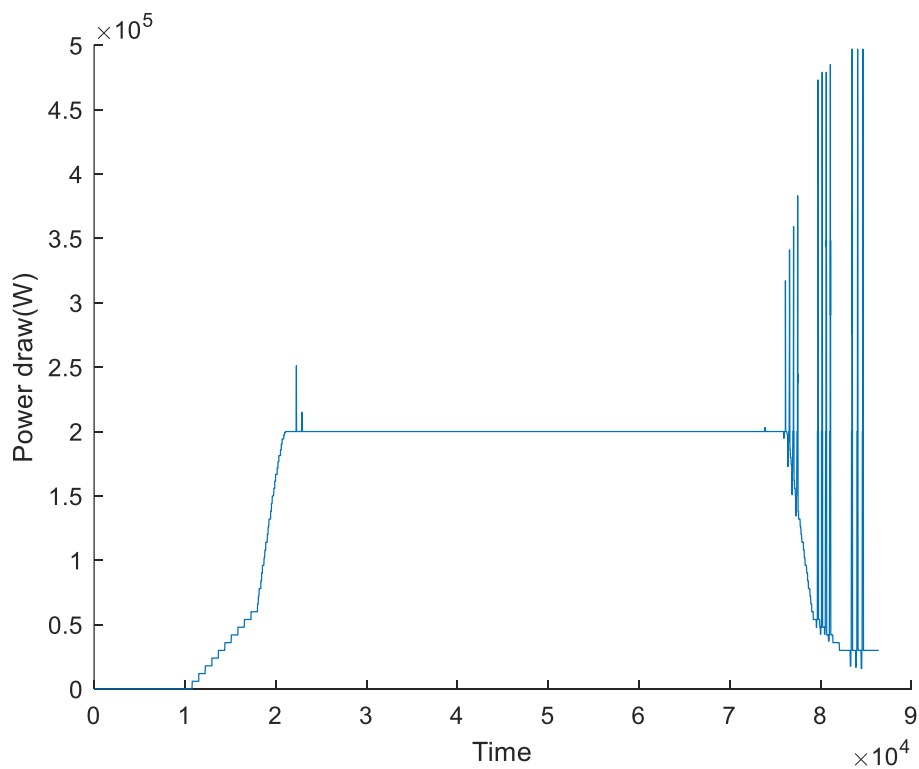
power demand from the grid at night has been confined to the 480 kW. This amount of power demand in comparison with previous method (890 kW) has fallen down and it is one of the prominent advantages of the EV+HESS system. In Scenario 1, 2, and 3, the use of a connected vehicle-to-grid (V2G) network is shown to reduce power demand peaks throughout most of the day, except for a minor peak in the morning. During these times, a constant 200 kW is drawn for both EV charging and train traction power, greatly benefiting the local power grid and reducing the need for other grid balancing measures. However, in the later hours of the day, the V2G network is unable to fully support traction power, and peak demands gradually increase until almost reaching a megawatt. This highlights the importance of having a sufficient population of EVs to achieve peak power reduction. While the V2G network modelled in this study is not enough to eliminate all power demand peaks, the temporary reduction still provides significant benefits. In comparison to previous methods, Scenario 3, which employs a hybrid energy storage system (HESS) that is independent of park and ride capacity, results in a peak demand of around 480 kW at the end of the day, demonstrating the effect of the HESS on power demand from the grid.



a) 75 EVs



b) 100 EVs



c) 150EVs

Figure 3.20: Total power provision potential of EV populations of varying size over 24 h with 6kW+HESS

The diagram in Figure 3.21 displays the V2G network's ability to receive power over time, which is determined by the maximum charging rate of all EVs at any given point (limited to a global charging limit of 6 kW plus HESS). Each EV's maximum charging power depends on its current state of charge (SOC) and may be much less than 6 kW. Similar to the previous method, number of the active EVs has profound effect on the power absorption. Therefore, whatever the number of the EVs decrease, the capability to absorbed regenerative power decrease because the vacant capacity has the direct relation to the number of the EVs. But the slop of the fall down is so slight because in this system (EVs +HESS) the other factor in absorption is HESS and it independent to the variation of the number of the EVs.

In order for the V2G network to absorb power from the regenerative braking of the rail system, the aggregated power absorption potential must exceed approximately 1109 kW, which is the peak output of the rail system during a train arrival event. However, as shown in Figure 3.21, this threshold is not reached in three scenarios. Only in Scenario 1 (with up to 150 EVs) is the V2G network capable of absorbing the majority of regenerative braking power for an extended period. The other scenarios demonstrate that even when the car park is less fully occupied, a significant contribution can still be made to storing regenerated energy.

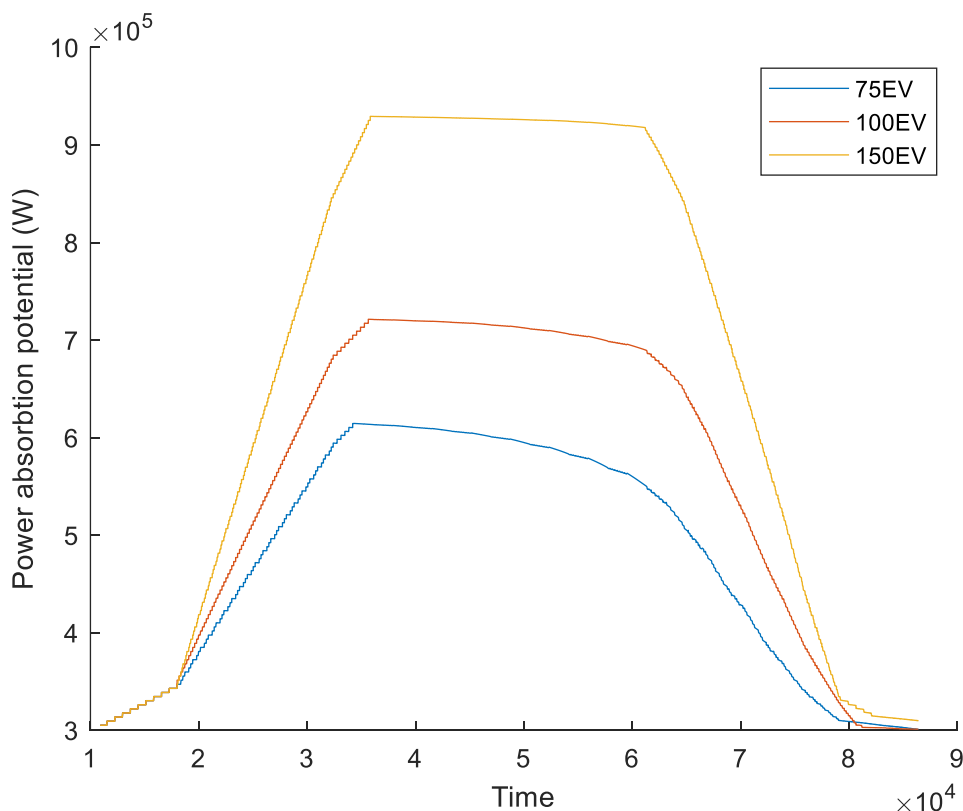


Figure 3.21: Total power absorption potential of EV populations of varying size over 24 (6kW+HESS)

After considering the V2G network's effectiveness in decoupling the electric rail system and the power grid, its ability to charge individual EVs over time needs to be

analyzed. Fig. 3.22 shows how the SOC of the three control EVs develops in each of the three scenarios. Based on this fig, the maximum charging rate is considered 6kW and the charging rate is done based on the SOC of the battery which means the rate of absorption power has the relation to the SOC. This relation is illustrated in fig. 3.5. Although the charging rate is low (6kW) in comparison with 20kW, the final position of the battery (SOC) is acceptable. In the proposed method, our first priority is to charge the EVs during the EV is connected to the system and try to rise the SOC of the every EV. So, in the first step regenerative power is injected to EVs. Then if there exist remain power of the regenerative power, it is injected to the HESS.

In any of the three scenarios, each control EV significantly gained in SOC. As expected, given that the grid connection limit was fixed at 200 kW for all three scenarios (limiting how much power can be shared between EVs during smart charging periods), the SOC gains per EV are higher at lower EV population sizes. While only the control EVs are shown, the observed gain in SOC is indicative of the behavior in the whole EV population.

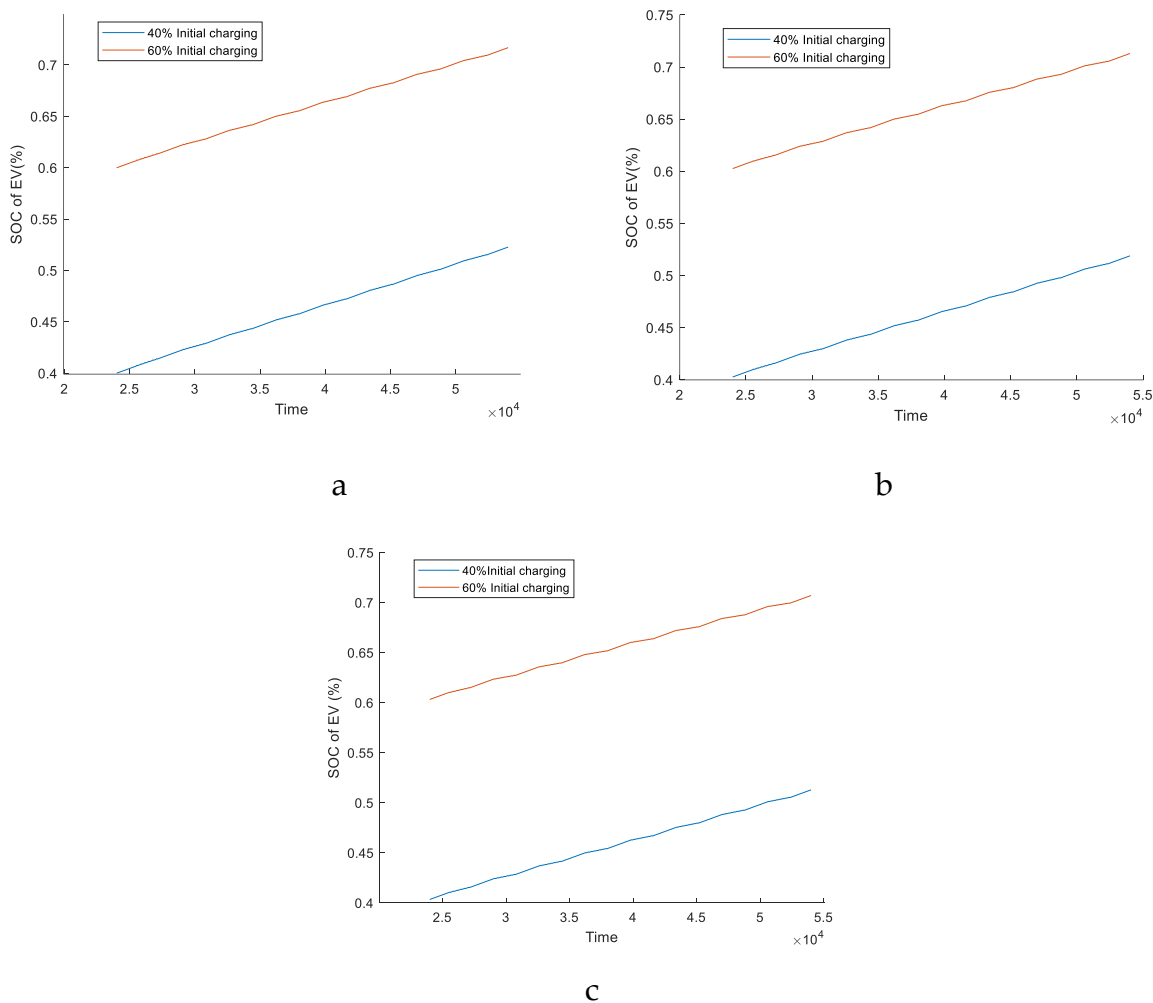


Figure 3.22: Changes in SOC over time of the three control EVs within EV populations of varying size (6 kW + HESS)

The final factor that this study considers, which affects system performance, is the amount of power available to the entire system (comprising the rail and EVs) through a shared grid connection or constant power demand from the grid. To investigate this, the 24-hour operation of the system was simulated multiple times while adjusting the grid connection limit (which is a flexible constraint on the proportion of power accessible from the substation managed by the V2G network) to 100, 200, 300, and 400, respectively. The simulation maintained a consistent EV population size of 75, 100, and 150 EVs, and the maximum charging limit per EV was set at 6 kW, plus the HESS.

Scenario 1: 100 kW grid connection limit

Scenario 2: 200 kW grid connection limit

Scenario 2: 300 kW grid connection limit

Scenario 4: 400 kW grid connection limit

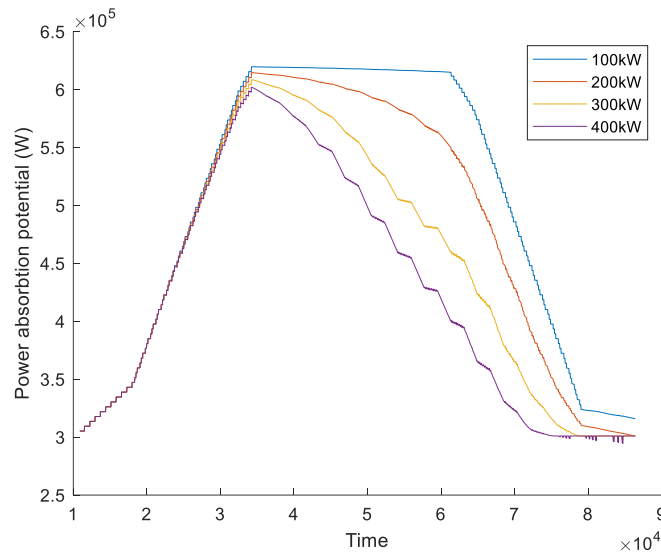
As depicted in Fig. 3.23, a higher grid connection limit has a notable negative impact on the ability of the combined EV population to take in power from the rail system. Similarity, two important factor have effect on the power absorption potential. The first factor is the grid connection power which system absorb power from the power network consciously. In this simulation this power should be acquired constant during the day and this power depend the mode of the algorithm inject to the EVs (no traffic and regenerative braking) or to the train (acceleration mode). Based on the proposed algorithm, the grid connection power is shared between the EVs and every EVs absorb its contribution correspond to its SOC (fig. 3.5). Therefore, whatever, the grid connection power rise, the contribution of the every EV from the grid connection would increase and capacity for absorption of regenerative power would decrease. So, during the evening and night the capacity of the potential absorption dramatically decrease.

The second factor is the number of the EV. Similarity, the number of the active EVs has the same effect on the power absorption potential.

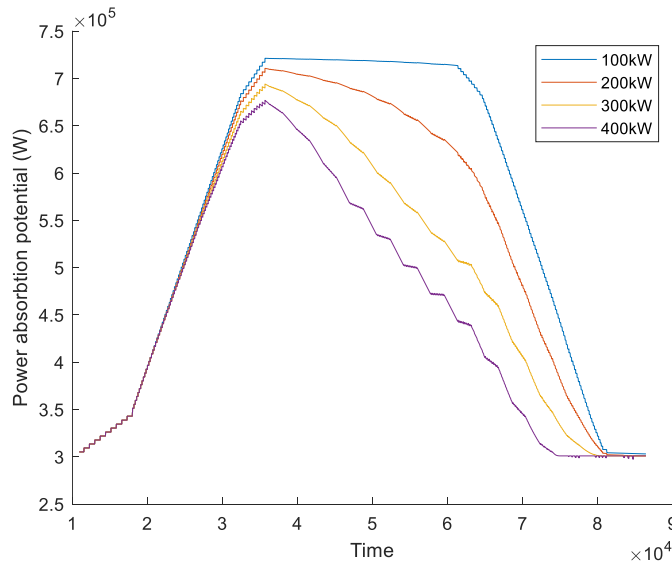
It's worth noting that this effect on the power absorption potential is more noticeable in the afternoon and evening than in the earlier hours of the day. Although the power demand of the rail system stays constant across scenarios, any rise in the power available to the system leads to an increase in the EV charging rates and, consequently, quicker gains in SOC for the linked EVs. However, as shown in Fig. 3.5, the maximum charging rate for individual EVs decreases as their SOC levels rise. Therefore, the power absorption potential of the combined EV population diminishes not only when some EV batteries are completely charged but also as they reach higher SOC levels.

The limitations and issues discussed in the previous paragraph can be attributed partly to the work's oversimplification of keeping the grid connection limit constant

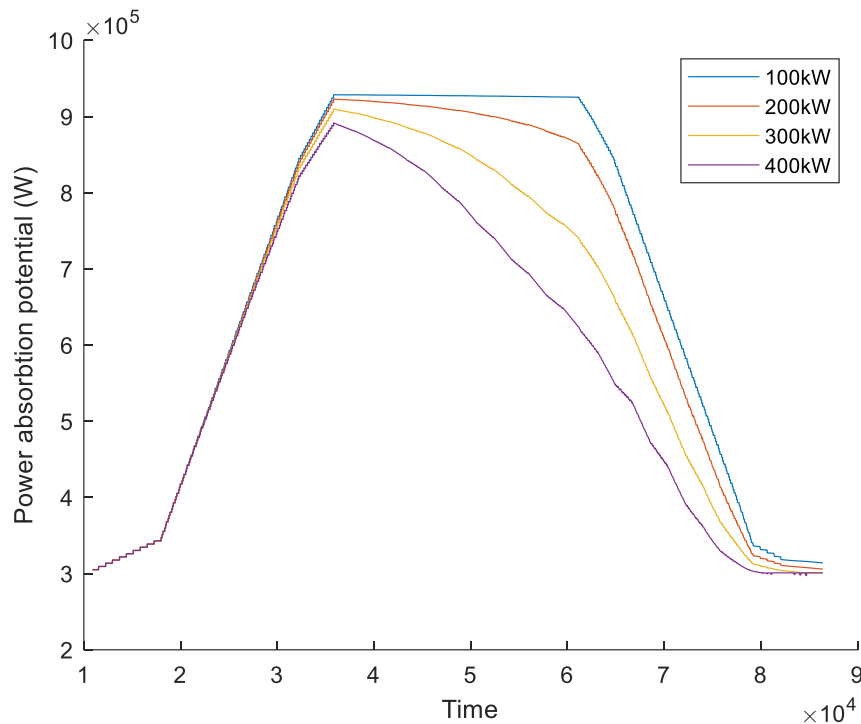
throughout the day. By implementing more sophisticated scheduling rules that adjust this parameter to the number of connected EVs, a decrease in power absorption potential can be prevented. However, any measures that restrict EV charging rates must be carefully considered in terms of user acceptance, since the V2G network heavily depends on the willingness of EV owners to participate. Therefore, determining charging rate limitations that are acceptable to EV owners may require insights from social and behavioral science, which are outside the scope of this study.



a) 75 EVs



b) 100 EVs



c) 150EVs

Figure 3.23: Total power absorption potential at varying grid connection limits over 24 h (6kW+HESS)

### 3.5.4 HESS (Battery and Supercapacitor)

In a HESS, the complementary capabilities of high-power supercapacitors and high-energy-density batteries can be used to satisfy the power requirements for acceleration and traction mode as well as the characteristics of regenerative braking energy. The HESS discharges when the high-speed train load is higher than 0. In order to keep the supercapacitors with enough capacity to store energy when the next regenerative braking energy comes, the supercapacitors are first given precedence through fast discharging.

The battery is begun to discharge energy and then the battery of EVs is discharged to meet the power demand when the supercapacitors' discharging power is insufficient to match the power of the system load. The supercapacitors' SOC comparison diagram when only supercapacitors are used to recover braking energy is shown in Figure 3.24. The SOC curve and supercapacitor utilization rate are very low, as can be seen from the figure, as the majority of the supercapacitors are not completely charged or discharged.

Although there are instances where supercapacitors are not completely charged or discharged in partly recycled situations, their utilization rate has significantly increased.

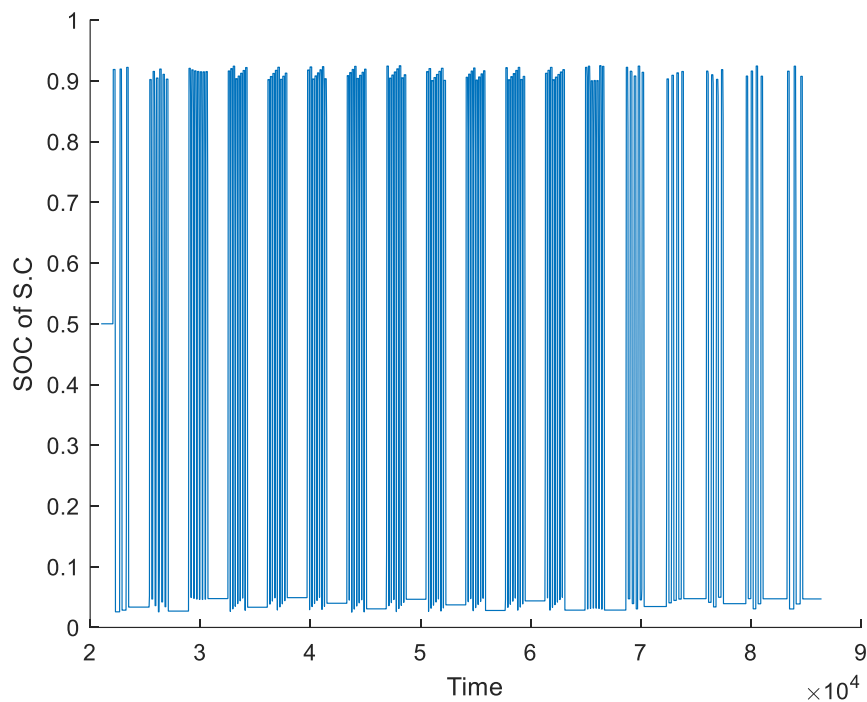


Figure 3.24: SOC of the supercapacitor

On the other hand, the other part of the HESS is the battery. The charging and discharging trend of battery is different from supercapacitors. Based on the Fig. 3.24 charge and discharge of the supercapacitor is done quickly because the charging rate is high and the its capacity is not so high. Therefore, in the short time the supercapacitor is filled or emptied. Unlike the super capacitor, battery has the low charging rate and its capacity is huge. Thus, the trend of the charging and discharging is dramatically different in comparison with supercapacitor.

Similarity, the number of the EV and the rate of the grid connection are the two main factor have effects on the charging and discharging trend. Fig. 3.25 shows the effect of the number of the EV on the SOC of the battery with HESS. As seen in this fig, whatever the number of the EV increase the SOC of the battery of the HESS reduce because the more contribution of grid connection power in the first step is injected to the EVs battery and the less remain power is store in the battery. Thus, the charging rate of battery of HESS reduces.

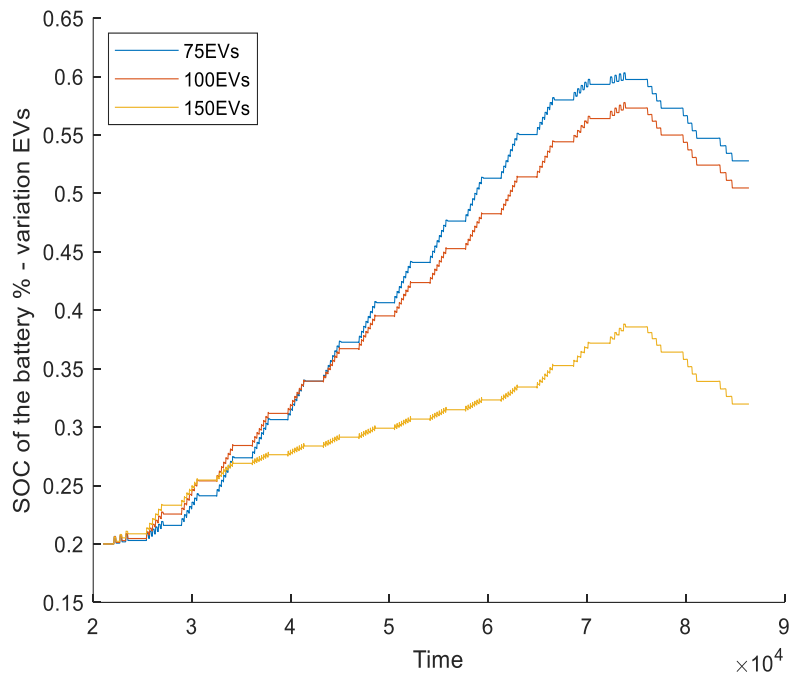
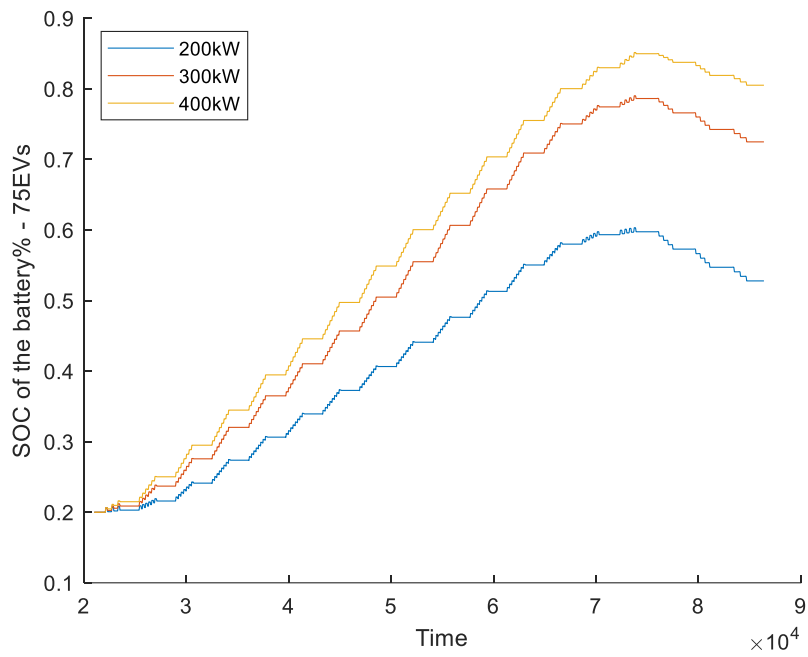
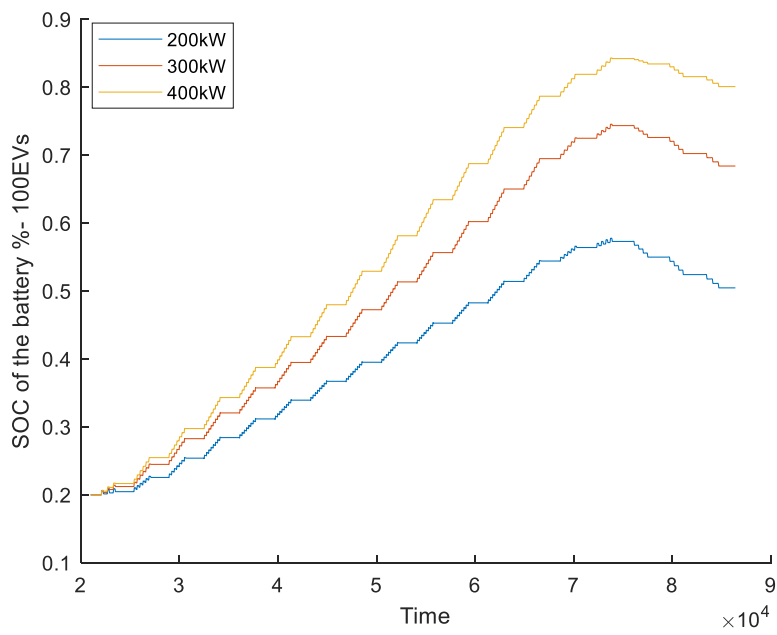


Figure 3.25: SOC of the battery in variation of EV

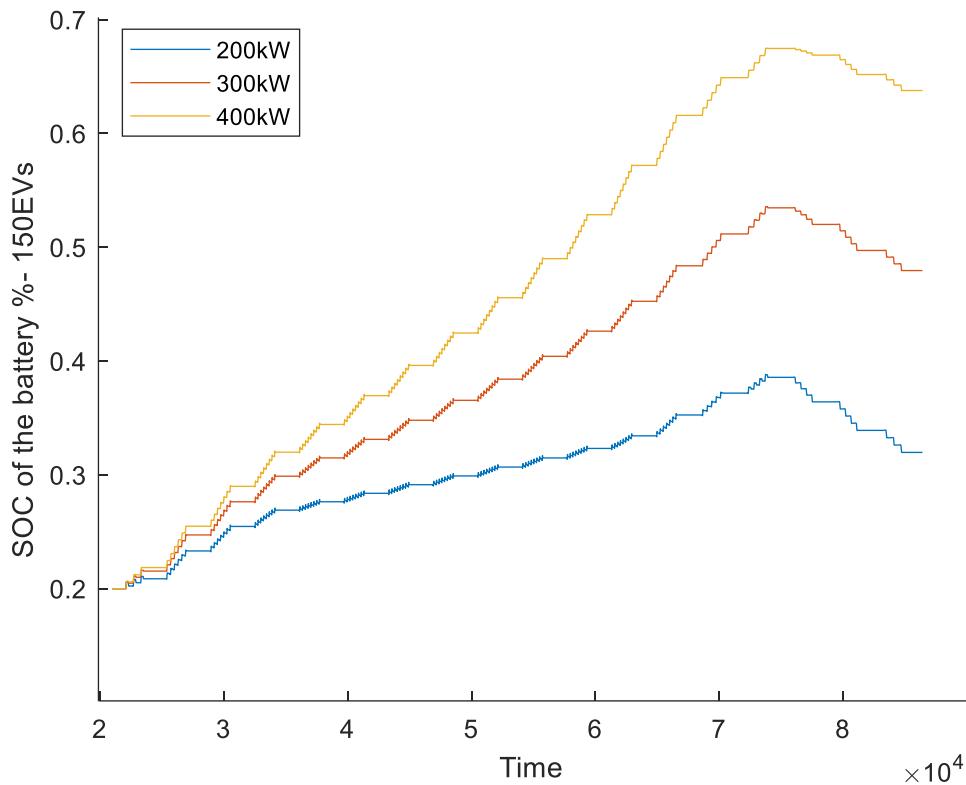
The other factor which has effect on the SOC of the battery of the HESS is the grid connection power. Fig. 3.26 shows the effect of the variation of the grid connection power in three scenarios for 75EVs, 100EVs and 150EVs. Based on this fig. the relation between SOC of the battery and grid connection is direct. Whatever the rate of the grid connection would increase, the rate of the charging increase. The main reason raised. Therefore, it is important to considered the optimum rate of the grid connection to avoid fulling the capacity of the battery.



a) 75EVs



b) 100EVs



c) 150EVs

Figure 3.26: SOC of the battery a, b, c

### 3.6 Discussion and Comparison

In the last part of this report, the results of the three scenario are compared in terms of the four technical issues such as Maximum Provision Power, Maximum absorption power, Maximum peak demand from the grid and Minimum number of required EVs.

In the first scenario (20 kW) as the fast charging rate is considered, the maximum power provision is significant high and is equal to 3000 kW for the 150 EV. In addition, even if number of the EV would be lower (75EV), there is not any concerning in providing the traction power for the acceleration mode. The second scenario (6 kW) cannot provide totally the traction power even in the maximum number of the EV (150). But in the modified scenario which is third scenario this problem is solved and it can supply the traction power completely.

The maximum absorption power in the first scenario is 2000 kW and it shows that the possibility for storing the power is dramatically high and we can absorb totally regenerative power and wasted energy is zero. But in the second scenario in the maximum number of the EV the system can only absorb the 620 kW and the remain

power is wasted. About the third scenario the store is the same but the wasted energy is not zero but is little (200kW).

One of the important technical issue is the peak power demand because the aim of the system mitigates the stress and tension on the power grid. Therefore, whatever the peak power demand would be lower, the performance of the proposed system is more reliable. With notice to this point, the third scenario (6 kW + HESS) is the best performance in comparison with the other scenario.

However, the main drawback of this method is the lack of the enough number of the EVs in park & ride. From this technical issue, the third and first scenario have the acceptable performance with reasonable number of the EV.

Overall, with comparing these scenarios and their result, the third scenario has the best performance in terms of four technical issues. In addition, the third scenario has the lower cost investment and lower cost of the implementation. In comparison with the other scenario.

Table 3.4: Technical performance of every scenario

Charging mode	Maximum Provision Power	Maximum absorption power	Maximum peak shaving	Minimum number of required EVs
20 kW	3000 kW	2000 kW	750 kW	75
6 kW	900 kW	620 kW	400 kW	200
6 kW + HESS	1350 kW	950 kW	700 kW	100

## 4. Conclusion and future development

The growing concern for decreasing our reliance on fossil fuels and lessening the environmental effects in personal transportation has caused a substantial rise in the amount of electric vehicles (EVs) used recently. Since the transportation sector is a significant contributor to global energy consumption, the automotive industry worldwide is making significant investments in EV technology with the aim of expanding their market share. Although considered as a favorable advancement, the electrification process poses significant obstacles for power grids on a global scale. The transition from fossil fuels in personal transportation results in a rise in electricity consumption due to the charging of EV batteries, which can cause power demand surges if the charging process is not adequately managed.

Even though electric vehicles (EVs) have an impact on public transportation, particularly with electric buses, the primary method of electrifying mass transportation is through railway electrification. To address these challenges, a significant amount of effort has been invested in the area of EV smart charging.

The V2G concept aims to transform electric vehicles (EVs) from being just a heavy demand on power grids to becoming a beneficial resource. This involves utilizing EV battery packs as a form of energy storage that is distributed across the grid. An aggregator typically manages the power flow, balancing the requirements of the EVs with those of the grid. This ensures that there is a net energy flow towards the EV battery packs, recharging them for driving purposes. For a V2G network to be effective, it must adequately meet the needs of both the grid and the connected EVs. This entails fulfilling the designated grid service requirements and also addressing

potential concerns of EV owners, such as range anxiety, to encourage their participation in V2G schemes.

To control the power flow between an electric vehicle (EV) and the power grid, the aggregator needs to access information about the current condition of the EV's battery pack. The basic information necessary includes the State-of-Charge (SOC) and the total capacity of the battery, as well as the potential rate at which it can be charged or discharged. The V2G system makes use of pre-existing storage that would otherwise remain inactive, namely the batteries of parked electric vehicles (EVs). Rather than creating and managing separate energy storage systems for electric rail systems, the batteries of existing EVs are repurposed to serve a secondary function. With the aid of intelligent charging technologies, EVs can be transformed from a liability to the power grid into a beneficial tool for sustaining grid stability. Furthermore, the V2G concept offers the possibility of system response times that could be as short as a few seconds, or even less than a second, but certain difficulties associated with vehicle management, communication, and decision-making must be resolved.

To tackle the difficulties associated with the intermittent supply of electricity, energy storage technologies are often employed. In the case of electric rail systems, which consume a significant amount of power, energy storage can be utilized as a method of demand-side management. In this context, energy storage can help ease the pressure of peak power demand on the electricity grid that results from the power requirements of electric trains, particularly during acceleration when traction power needs can reach several megawatts, depending on the rail system.

Conversely, energy storage could prove advantageous for the recovery of train brake energy. Typically, the electricity generated through regenerative braking can be transmitted back to the power grid with minimal loss of energy. However, the practice of converting brake energy into power and feeding it back into the grid is not yet prevalent, and the rail networks' power supply may benefit from the implementation of energy storage, which could facilitate efficient regenerative braking.

Different forms of energy storage, like batteries and supercapacitors, have been suggested as options for receiving power from regenerative braking. These storage solutions can either be located on-board the train or installed along the track lines. Storing this energy allows it to be used later during acceleration. While on-board solutions have the added benefit of providing some degree of independence from the track's power infrastructure, which enables electric rail vehicles to operate on non-electrified track sections, they come with some drawbacks, including increased vehicle weight, additional maintenance needs, and higher per-unit costs.

The primary drawback of vehicle-to-grid (V2G) technology, in contrast to other energy storage options, is that it depends on a sufficient number of electric vehicles being available and the charging rate of each EV being inadequate to meet the power

demand. Therefore, it's necessary to supplement EV parking with a hybrid energy storage system (HESS). This study aims to examine the estimated size of the electric vehicle population required to meet the necessary energy demands.

Since a hybrid energy storage system (HESS) consists of both batteries and supercapacitors, determining the appropriate ratio between these two components is crucial. For this reason, an optimization technique is utilized to identify the optimal proportion of batteries and supercapacitors. This method seeks to identify the best balance between storage capacity for energy and cost-effectiveness.

The utilization of energy storage technology can prove beneficial in recapturing the brake energy of electric train systems. This recovered energy can be stored in a dedicated storage device and later used to power the vehicle. The adoption of regenerative braking in electric rail networks and vehicles has resulted in significant improvements in energy efficiency and has helped to reduce operational expenses.

An alternative strategy for energy storage is proposed: implementing a V2G network near an electric rail system and coupling it with a hybrid energy storage system (HESS). V2G technology refers to a method of energy storage that combines the battery packs of stationary electric vehicles to provide various grid services through charging or discharging them.

Compared to other energy storage solutions, V2G technology stands out because it leverages existing energy storage that would otherwise go unused, namely, the batteries of parked electric vehicles. However, given the limited availability of EVs and their slow charging rate, a hybrid energy storage system is often used in conjunction with V2G to supplement the storage capacity.

In this research, the combination method is proposed to employ the advantages of both methods and remove the disadvantages of them. The plan is that renewable energy sources such as PV and wind turbine is inserted to this program to mitigate the grid connection power and increase the efficiency.

## Bibliography

- [1] International Energy Agency, 2019a. Energy Efficiency Indicators 2019. IEA publications, pp. 5–8. <https://www.iea.org/reports/energy-efficiency-indicators-2019>. (Accessed 3 May 2020).
- [2] H. Krueger, D. Fletcher and A. Cruden. “Vehicle-to-Grid (V2G) as line-side energy storage for support of DC-powered electric railway systems” *Journal of Rail Transport Planning & Management*. vol. 19, September 2021.
- [3] Mahdiyeh Khodaparastan, Ahmed A. Mohamed and Werner Brandauer, “Recuperation of Regenerative Braking Energy in Electric Rail Transit Systems” *IEEE Transactions on Intelligent Transportation Systems*, vol. 20, issue 8, pp. 2831-2847, August 2019.
- [4] Nasri, A., Moghadam, M.F. and Mokhtari, H., 2010, June. Timetable optimization for maximum usage of regenerative energy of braking in electrical railway systems. In *SPEEDAM 2010* (pp. 1218-1221). IEEE.
- [5] Albrecht, T., 2004. Reducing power peaks and energy consumption in rail transit systems by simultaneous train running time control, *Computers in Railways IX*. WIT Press, 885, p.894.
- [6] Fournier, D., Fages, F. and Mulard, D., 2014, April. A greedy heuristic for optimizing metro regenerative energy usage. In *Railways 2014*.
- [7] Yang, X., Li, X., Ning, B. and Tang, T., 2015. A survey on energy-efficient train operation for urban rail transit. *IEEE Transactions on Intelligent Transportation Systems*, 17(1), pp.2-13.
- [8] Kim, K.M., 2011. A Model and Approaches for Synchronized Energy Saving in Timetable. *Proceedings of WCRR 2011*.
- [9] Peña-Alcaraz, M., Fernández, A., Cucala, A.P., Ramos, A. and Pecharromán, R.R., 2012. Optimal underground timetable design based on power flow for maximizing the use of regenerative-braking energy. *Proceedings of the Institution of Mechanical Engineers, Part F: Journal of Rail and Rapid Transit*, 226(4), pp.397-408.

- [10] Chang, C.S., Phoa, Y.H., Wang, W. and Thia, B.S., 1996. Economy/regularity fuzzy-logic control of DC railway systems using event-driven approach. IEE Proceedings-Electric Power Applications, 143(1), pp.9-17.
- [11] Yang, X., Li, X., Gao, Z., Wang, H. and Tang, T., 2012. A cooperative scheduling model for timetable optimization in subway systems. IEEE Transactions on Intelligent Transportation Systems, 14(1), pp.438-447.
- [12] Ramos, A., Pena, M.T., Fernández, A. and Cucala, P., 2008. Mathematical programming approach to underground timetabling problem for maximizing time synchronization. Dirección y Organización, (35), pp.88-95.
- [13] Zhao, L., Li, K. and Su, S., 2014. A multi-objective timetable optimization model for subway systems. In Proceedings of the 2013 International Conference on Electrical and Information Technologies for Rail Transportation (EITRT2013)-Volume I (pp. 557-565). Springer Berlin Heidelberg.
- [14] Miyatake, M. and Ko, H., 2007, September. Numerical analyses of minimum energy operation of multiple trains under DC power feeding circuit. In 2007 european conference on power electronics and applications (pp. 1-10). IEEE.
- [15] Holmes, K., 2008. Smart grids and wayside energy storage: opportunities for transit. Passenger Transport, 66(40).
- [16] Bhargava, B., 1999, July. Railway electrification systems and configurations. In 1999 IEEE Power Engineering Society Summer Meeting. Conference Proceedings (Cat. No. 99CH36364) (Vol. 1, pp. 445-450). IEEE.
- [17] Steiner, M. and Scholten, J., 2004, June. Energy storage on board of DC fed railway vehicles PESC 2004 conference in Aachen, Germany. In 2004 IEEE 35th Annual Power Electronics Specialists Conference (IEEE Cat. No. 04CH37551) (Vol. 1, pp. 666-671). IEEE.
- [18] Gelman, V., 2013. Energy storage that may be too good to be true: Comparison between wayside storage and reversible thyristor-controlled rectifiers for heavy rail. IEEE Vehicular Technology Magazine, 8(4), pp.70-80.
- [19] Teshima, M. and Takahashi, H., 2014, May. Lithium-ion battery application in traction power supply system. In 2014 International Power Electronics Conference (IPEC-Hiroshima 2014-ECCE ASIA) (pp. 1068-1072). IEEE.
- [20] Liu, X. and Li, K., 2020. Energy storage devices in electrified railway systems: A review. Transportation safety and environment, 2(3), pp.183-201.

- [21] Faraji, F., Majazi, A. and Al-Haddad, K., 2017. A comprehensive review of flywheel energy storage system technology. *Renewable and Sustainable Energy Reviews*, 67, pp.477-490.
- [22] Bolund, B., Bernhoff, H. and Leijon, M., 2007. Flywheel energy and power storage systems. *Renewable and Sustainable Energy Reviews*, 11(2), pp.235-258.
- [23] Arnold, S.M., Saleeb, A.F. and Al-Zoubi, N.R., 2002. Deformation and life analysis of composite flywheel disk systems. *Composites part B: engineering*, 33(6), pp.433-459.
- [24] Jiang, L., Zhang, W., Ma, G.J. and Wu, C.W., 2017. Shape optimization of energy storage flywheel rotor. *Structural and multidisciplinary optimization*, 55, pp.739-750.
- [24] Kale, V. and Secanell, M., 2018. A comparative study between optimal metal and composite rotors for flywheel energy storage systems. *Energy Reports*, 4, pp.576-585.
- [26] Genta, G., 2014. *Kinetic energy storage: theory and practice of advanced flywheel systems*. Butterworth-Heinemann.
- [27] Tzeng, J., Emerson, R. and Moy, P., 2006. Composite flywheels for energy storage. *Composites Science and Technology*, 66(14), pp.2520-2527.
- [28] Patil, S.S. and Bhalerao, Y.J., 2017, February. Selection of levels of dressing process parameters by using TOPSIS technique for surface roughness of en-31 work piece in CNC cylindrical grinding machine. In *IOP Conference Series: Materials Science and Engineering* (Vol. 178, No. 1, p. 012033). IOP Publishing.
- [29] Asodariya, H., Patel, H.V., Babariya, D. and Maniya, K.D., 2018. Application of multi criteria decision making method to select and validate the material of a flywheel design. *Materials Today: Proceedings*, 5(9), pp.17147-17155.
- [30] Pena-Alzola, R., Sebastián, R., Quesada, J. and Colmenar, A., 2011, May. Review of flywheel-based energy storage systems. In *2011 International Conference on Power Engineering, Energy and Electrical Drives* (pp. 1-6). IEEE.
- [31] H. Bangcheng, Z. Shiqiang, W. Xi and Y. Qian, "Integral Design and Analysis of Passive Magnetic Bearing and Active Radial Magnetic Bearing for Agile Satellite Application," in *IEEE Transactions on Magnetics*, vol. 48, no. 6, pp. 1959-1966, June 2012, doi: 10.1109/TMAG.2011.2180731.
- [32] Filatov, A.V. and Maslen, E.H., 2001. Passive magnetic bearing for flywheel energy storage systems. *IEEE Transactions on Magnetics*, 37(6), pp.3913-3924.
- [33] Paden, B., Groom, N. and Antaki, J.F., 2003. Design formulas for permanent-magnet bearings. *J. Mech. Des.*, 125(4), pp.734-738.

- [34] Bassani, R., 2006. Earnshaw (1805–1888) and passive magnetic levitation. *Meccanica*, 41, pp.375-389.
- [35] Pillay, P. and Krishnan, R., 1989. Modeling, simulation, and analysis of permanent-magnet motor drives. I. The permanent-magnet synchronous motor drive. *IEEE Transactions on industry applications*, 25(2), pp.265-273.
- [36] Daoud, M.I., Abdel-Khalik, A.S., Massoud, A., Ahmed, S. and Abbasy, N.H., 2012, September. On the development of flywheel storage systems for power system applications: a survey. In 2012 XXth International Conference on Electrical Machines (pp. 2119-2125). IEEE.
- [37] Ratniyomchai, T., Hillmanssen, S. and Tricoli, P., 2014. Recent developments and applications of energy storage devices in electrified railways. *IET Electrical Systems in Transportation*, 4(1), pp.9-20.
- [38] Wang, G., Zhang, L. and Zhang, J., 2012. A review of electrode materials for electrochemical supercapacitors. *Chemical Society Reviews*, 41(2), pp.797-828.
- [39] Zhang, L.L. and Zhao, X.S., 2009. Carbon-based materials as supercapacitor electrodes. *Chemical Society Reviews*, 38(9), pp.2520-2531.
- [40] González, A., Goikolea, E., Barrena, J.A. and Mysyk, R., 2016. Review on supercapacitors: Technologies and materials. *Renewable and sustainable energy reviews*, 58, pp.1189-1206.
- [41] Simon, P. and Burke, A., 2008. Nanostructured carbons: double-layer capacitance and more. *The electrochemical society interface*, 17(1), p.38.
- [42] Chmiola, J., Yushin, G., Gogotsi, Y., Portet, C., Simon, P. and Taberna, P.L., 2006. Anomalous increase in carbon capacitance at pore sizes less than 1 nanometer. *science*, 313(5794), pp.1760-1763.
- [43] Gu, W. and Yushin, G., 2014. Review of nanostructured carbon materials for electrochemical capacitor applications: advantages and limitations of activated carbon, carbide-derived carbon, zeolite-templated carbon, carbon aerogels, carbon nanotubes, onion-like carbon, and graphene. *Wiley Interdisciplinary Reviews: Energy and Environment*, 3(5), pp.424-473.
- [44] Pumera, M., 2010. Graphene-based nanomaterials and their electrochemistry. *Chemical Society Reviews*, 39(11), pp.4146-4157.
- [45] Meyers, R.A., 2012. *Encyclopedia of sustainability science and technology* (pp. 529-564). New York: Springer.

- [46] Hemmati, R. and Saboori, H., 2016. Emergence of hybrid energy storage systems in renewable energy and transport applications—A review. *Renewable and Sustainable Energy Reviews*, 65, pp.11-23.
- [47] A. Khaligh and Z. Li, "Battery, Ultracapacitor, Fuel Cell, and Hybrid Energy Storage Systems for Electric, Hybrid Electric, Fuel Cell, and Plug-In Hybrid Electric Vehicles: State of the Art," in *IEEE Transactions on Vehicular Technology*, vol. 59, no. 6, pp. 2806-2814, July 2010, doi: 10.1109/TVT.2010.2047877.
- [48] V. Gelman, "Energy Storage That May Be Too Good to Be True: Comparison Between Wayside Storage and Reversible Thyristor Controlled Rectifiers for Heavy Rail," in *IEEE Vehicular Technology Magazine*, vol. 8, no. 4, pp. 70-80, Dec. 2013, doi: 10.1109/MVT.2013.2283350.
- [49] V. Gelman, "Energy Storage That May Be Too Good to Be True: Comparison Between Wayside Storage and Reversible Thyristor Controlled Rectifiers for Heavy Rail," in *IEEE Vehicular Technology Magazine*, vol. 8, no. 4, pp. 70-80, Dec. 2013, doi: 10.1109/MVT.2013.2283350.
- [50] Gelman, V., 2009. Braking energy recuperation. *IEEE Vehicular Technology Magazine*, 4(3), pp.82-89.
- [51] Yi, T.F., Yang, S.Y. and Xie, Y., 2015. Recent advances of  $\text{Li}_4\text{Ti}_5\text{O}_{12}$  as a promising next generation anode material for high power lithium-ion batteries. *Journal of Materials Chemistry A*, 3(11), pp.5750-5777.
- [52] Schipper, F., Erickson, E.M., Erk, C., Shin, J.Y., Chesneau, F.F. and Aurbach, D., 2016. Recent advances and remaining challenges for lithium ion battery cathodes. *Journal of The Electrochemical Society*, 164(1), p.A6220.
- [53] Xia, H., Chen, H., Yang, Z., Lin, F. and Wang, B., 2015. Optimal energy management, location and size for stationary energy storage system in a metro line based on genetic algorithm. *Energies*, 8(10), pp.11618-11640.
- [54] S. de la Torre, A. J. Sánchez-Racero, J. A. Aguado, M. Reyes and O. Martínez, "Optimal Sizing of Energy Storage for Regenerative Braking in Electric Railway Systems," in *IEEE Transactions on Power Systems*, vol. 30, no. 3, pp. 1492-1500, May 2015, doi: 10.1109/TPWRS.2014.2340911.
- [55] Herrera, V., Milo, A., Gaztañaga, H., Etxeberria-Otadui, I., Villarreal, I. and Camblong, H., 2016. Adaptive energy management strategy and optimal sizing applied on a battery-supercapacitor based tramway. *Applied Energy*, 169, pp.831-845.

- [56] Lencwe, M.J., Chowdhury, S.P.D. and Olwal, T.O., 2022. Hybrid energy storage system topology approaches for use in transport vehicles: A review. *Energy Science & Engineering*, 10(4), pp.1449-1477.
- [57] S. de la Torre, A. J. Sánchez-Racero, J. A. Aguado, M. Reyes and O. Martínez, "Optimal Sizing of Energy Storage for Regenerative Braking in Electric Railway Systems," in *IEEE Transactions on Power Systems*, vol. 30, no. 3, pp. 1492-1500, May 2015, doi: 10.1109/TPWRS.2014.2340911.
- [58] Brenna, M., Foadelli, F., Tironi, E. and Zaninelli, D., 2007, May. Ultracapacitors application for energy saving in subway transportation systems. In 2007 International Conference on Clean Electrical Power (pp. 69-73). IEEE.
- [59] Qu, K. and Yuan, J., 2021. Optimization research on hybrid energy storage system of high-speed railway. *IET Generation, Transmission & Distribution*, 15(20), pp.2835-2846.
- [60] Tang, S., Huang, X., Li, Q., Yang, N., Liao, Q. and Sun, K., 2021. Optimal sizing and energy management of hybrid energy storage system for high-speed railway traction substation. *Journal of Electrical Engineering & Technology*, 16, pp.1743-1754.
- [61] Li, Q., Liu, W., Shu, Z., Xie, S. and Zhou, F., 2014, May. Co-phase power supply system for HSR. In 2014 International Power Electronics Conference (IPEC-Hiroshima 2014-ECCE ASIA) (pp. 1050-1053). IEEE.
- [62] Wu, C., Lu, S., Xue, F., Jiang, L. and Chen, M., 2020. Optimal sizing of onboard energy storage devices for electrified railway systems. *IEEE Transactions on Transportation Electrification*, 6(3), pp.1301-1311.
- [63] İ. Şengör, H. C. Kılıçkiran, H. Akdemir, B. Kekezoğlu, O. Erdinç and J. P. S. Catalão, "Energy Management of a Smart Railway Station Considering Regenerative Braking and Stochastic Behaviour of ESS and PV Generation," in *IEEE Transactions on Sustainable Energy*, vol. 9, no. 3, pp. 1041-1050, July 2018, doi: 10.1109/TSTE.2017.2759105.
- [64] Kim, K.M., 2011. A Model and Approaches for Synchronized Energy Saving in Timetable. Proceedings of WCRR 2011.
- [65] Peña-Alcaraz, M., Fernández, A., Cucala, A.P., Ramos, A. and Pecharromán, R.R., 2012. Optimal underground timetable design based on power flow for maximizing the use of regenerative-braking energy. Proceedings of the Institution of Mechanical Engineers, Part F: Journal of Rail and Rapid Transit, 226(4), pp.397-408.
- [66] Miyatake, M. and Ko, H., 2007, September. Numerical analyses of minimum energy operation of multiple trains under DC power feeding circuit. In 2007 European conference on power electronics and applications (pp. 1-10). IEEE.

- [67] Chang, C.S., Phoa, Y.H., Wang, W. and Thia, B.S., 1996. Economy/regularity fuzzy-logic control of DC railway systems using event-driven approach. *IEEE Proceedings-Electric Power Applications*, 143(1), pp.9-17.
- [68] Ratniyomchai, T., Hillmanssen, S. and Tricoli, P., 2014. Recent developments and applications of energy storage devices in electrified railways. *IET Electrical Systems in Transportation*, 4(1), pp.9-20.
- [69] Jafari Kaleybar, H., Brenna, M., Foiadelli, F. and Castelli Dezza, F., 2023. Sustainable Electrified Transportation Systems Integration of EV and E-bus Charging Infrastructures to Electric Railway Systems. In *Electric Transportation Systems in Smart Power Grids* (pp. 237-267). CRC Press.
- [70] M. Brenna, F. Foiadelli and H. J. Kaleybar, "The Evolution of Railway Power Supply Systems Toward Smart Microgrids: The concept of the energy hub and integration of distributed energy resources," in *IEEE Electrification Magazine*, vol. 8, no. 1, pp. 12-23, March 2020, doi: 10.1109/MELE.2019.2962886.
- [71] L. S. Ashkezari, H. J. Kaleybar, M. Brenna and D. Zaninelli, "E-bus Opportunity Charging System Supplied by Tramway Line: A Real Case Study," *2022 IEEE International Conference on Environment and Electrical Engineering and 2022 IEEE Industrial and Commercial Power Systems Europe (EEEIC / I&CPS Europe)*, Prague, Czech Republic, 2022, pp. 1-6, doi: 10.1109/EEEIC/ICPSEurope54979.2022.9854598.
- [72] L. S. Ashkezari, H. Jafari Kaleybar and M. Brenna, "Integration of E-bus Opportunity Chargers to the Voltage-Stabilized DC Railway Grid," *2022 13th Power Electronics, Drive Systems, and Technologies Conference (PEDSTC)*, Tehran, Iran, Islamic Republic of, 2022, pp. 561-566, doi: 10.1109/PEDSTC53976.2022.9767260.
- [73] H. J. Kaleybar, M. Brenna and F. Foiadelli, "EV Charging Station Integrated with Electric Railway System Powering by Train Regenerative Braking Energy," *2020 IEEE Vehicle Power and Propulsion Conference (VPPC)*, Gijon, Spain, 2020, pp. 1-6, doi: 10.1109/VPPC49601.2020.9330920.
- [74] M. Ahmadi, H. J. Kaleybar, M. Brenna, F. Castelli-Dezza and M. S. Carmeli, "DC Railway Micro Grid Adopting Renewable Energy and EV Fast Charging Station," *2021 IEEE International Conference on Environment and Electrical Engineering and 2021 IEEE Industrial and Commercial Power Systems Europe (EEEIC / I&CPS Europe)*, Bari, Italy, 2021, pp. 1-6, doi: 10.1109/EEEIC/ICPSEurope51590.2021.9584729.
- [75] Miad Ahmadi, Hamed Jafari Kaleybar, Morris Brenna, Francesco Castelli-Dezza, Maria Stefania Carmeli "Implementation of DC Micro Grid Tied PV-Storage Based EV Fast Charging Station" *2021 IEEE International Conference on Environment and*

*Electrical Engineering and 2021 IEEE Industrial and Commercial Power Systems Europe (EEEIC / I&CPS Europe)*, Sep. 2021.

[76] Ahmadi, M., Jafari Kaleybar, H., Brenna, M., Castelli-Dezza, F. and Carmeli, M.S., 2021. Integration of Distributed Energy Resources and EV Fast-Charging Infrastructure in High-Speed Railway Systems. *Electronics*, 10(20), p.2555.

[77] H. J. Kaleybar, M. Brenna, F. Castelli-Dezza and D. Zaninelli, "Sustainable MVDC Railway System Integrated with Renewable Energy Sources and EV Charging Station," *2022 IEEE Vehicle Power and Propulsion Conference (VPPC)*, Merced, CA, USA, 2022, pp. 1-6, doi: 10.1109/VPPC55846.2022.10003272.

[78] Alper Çiçek, Ibrahim Sengör, Sıtkı Güner, Furkan Karakuş, Graduate Student, Ayşe Kübra Erenoglu, Ozan Erdiñç, Miadreza Shafie-Khah and João P. S. Catalão, "Integrated Rail System and EV Parking Lot Operation With Regenerative Braking Energy, Energy Storage System and PV Availability" *IEEE Transactions on Smart Grid*, vol. 13, issue 4, March 2022, pp. 3049-3058.

## List of Figures

Figure 1.1: schematic diagram of an FESS [19].....	6
Figure 1.2: Block diagram of a reversible substation [2].....	11
Figure 1.3: Hybrid energy storage system sizing methods [55] .....	13
Figure 1.4: Ultracapacitors/batteries/converters connection scheme [56] .....	15
Figure 1.5: Energy management flow chart of HESS [58] .....	17
Figure 1.6: Optimization flow chart [58] .....	18
Figure 1.7: Traction power supply system with HESS structure [59].....	19
Figure 1.8: Feeder traction load power curve [59] .....	20
Figure 2.1: Scheme of meantime integration between ERSs and EVCI [69].....	26
Figure 2.2: Scheme of ESS-based integration between ERSs and EVCI [69] .....	27
Figure 2.3: Integration configurations two-stage charging station [69] .....	28
Figure 2.4: Integration configurations single-stage charging station [69].....	29
Figure 2.5: T2V/V2T integration architecture in LVDC ERSs [69].....	30
Figure 2.6: T2V/V2T integration architecture in MVDC ERSs [69] .....	31
Figure 2.7: T2V/V2T integration architecture in hybrid ERSs [69].....	32
Figure 2.8: PV/wind/storage hybrid system general architecture[74] .....	33
Figure 2.9: Microgrid general architecture [75].....	34
Figure 2.10: Smart DC catenary system architecture [76].....	35

Figure 2.11: System overview and power flows [2] ..... 37

Figure 3.1: System overview and power flows [78] ..... 40

Figure 3.2: a) Assumed speed profile of simulated train (based on GPS data captured during real-life train journey); (b) Resulting train traction power demand (as experienced by the substation) during acceleration and regen power output during deceleration [2]..... 42

Figure 3.3: Assumed car park occupancy rate and number of train arrival/departure events over 24 simulation period [2] ..... 43

Figure 3.4: Proposed integration system in park & ride area. .... 45

Figure 3.5 Assumed maximum charging rate against SOC for simulated EV population. .... 48

Figure 3.6: Flowchart of the proposed algorithm ..... 50

Figure 3.7: Total power provision potential of EV populations of varying size over 24 h..... 53

Figure 3.8: (a) Power draw from substation for rail system traction power without connected V2G network over 24 h; (b) Power draw from substation for the rail system and EV population power demands with connected V2G network over 24 h – 75EVs..... 54

Figure 3.9: (a) Power draw from substation for rail system traction power without connected V2G network over 24 h; (b) Power draw from substation for the rail system and EV population power demands with connected V2G network over 24 h – 100EVs..... 54

Figure 3.10: (a) Power draw from substation for rail system traction power without connected V2G network over 24 h; (b) Power draw from substation for the rail system and EV population power demands with connected V2G network over 24 h – 150EVs..... 55

Figure 3.11: Total power absorption potential of EV populations of varying size over 24 h..... 56

Figure 3.12: changes in SOC over time of three control EVs..... 57

Figure 3.13: Total power absorption potential at varying grid connection limits over 24 h. a)75 b)100 c)150..... 59

Figure 3.14: Total power provision potential of EV populations of varying size over 24 h..... 60

Figure 3.15: Power draw from substation for the rail system and EV population power demands with connected V2G network over 24 h. a)75 b)100 c)150..... 61

Figure 3.16: Total power absorption potential of EV populations of varying size over 24 h. 6 kW ..... 62

Figure 3.17: Changes in SOC over time of the three control EVs within EV populations of varying size..... 63

Figure 3.18: Total power absorption potential at varying grid connection limits over 24 h..... 66

Figure 3.19: Total power provision potential of EV populations of varying size over 24 h with HESS ..... 67

Figure 3.20: Total power provision potential of EV populations of varying size over 24 h with HESS ..... 69

Figure 3.21: Total power absorption potential of EV populations of varying size over 24..... 70

Figure 3.22: Changes in SOC over time of the three control EVs within EV populations of varying size..... 71

Figure 3.23: Total power absorption potential at varying grid connection limits over 24 h..... 74

Figure 3.24: SOC of the supercapacitor ..... 75

Figure 3.25: SOC of the supercapacitor ..... 76

Figure 3.26: SOC of the battery a, b, c..... 78



## List of Tables

Table 1.1: Comparison of energy and power densities of ESS systems [19].....	12
Table 3.1: Parameters of the proposed system.....	51
Table 3.2: Comparison of Control EV battery pack SOC at departure time for EV populations of varying sizes (20kW).....	58
Table 3.3: Comparison of Control EV battery pack SOC at departure time for EV populations (6kW).....	63
Table 3.4: Technical performance of every scenario.....	79

## 5. Acknowledge

Dear Dr., Hamed Jafari Kaleybar and Prof. Morris Brenna

I am writing to express my deep gratitude for your guidance and support throughout my thesis project. Your expertise, feedback, and encouragement were invaluable in helping me complete this important milestone in my academic journey.

I would also like to thank my family for their unwavering support, love, and encouragement throughout this process. Their belief in me gave me the strength and motivation to persevere during challenging times.

Your feedback and constructive criticism helped me to improve my work and challenged me to think more critically and creatively. Your dedication to your students and your passion for your field have inspired me to pursue my own academic and professional goals with greater enthusiasm and determination.

I feel truly privileged to have had you as my professor and mentor, and I am grateful for the time and effort you invested in my research. Your guidance and support have been instrumental in helping me to achieve my academic goals, and I will always be grateful for the impact you have had on my life.

Once again, thank you for everything you have done for me. I could not have completed this thesis without your help, and I am honored to have had the opportunity to learn from you.

